Regulation of FasL expression, and delineation of differentiation states of cytotoxic lymphocytes

by

Shih Wei Wayne Juang

A thesis submitted in partial fulfillment of the requirements for the degree of

Doctor of Philosophy

in

IMMUNOLOGY

Department of Medical Microbiology and Immunology
University of Alberta

Abstract

$CD8^+$ T cells are vital cytotoxic lymphocytes against intracellular pathogens and tumor cells. $CD8^+$ T cells utilize a fast-acting degranulation of granzyme/perforin and slow-acting receptor:ligand, FasL:Fas, pathway of inducing target cell lysis. The importance of degranulation based target cell killing by $CD8^+$ T cells has been well established while the FasL:Fas based mechanism of killing has been far less characterized. Additionally, it remains unclear as to the purpose of possessing the slow-acting FasL:Fas mechanism of killing in $CD8^+$ T cells. In this thesis, I investigated the differential expression patterns of intracellular FasL and GrB in stimulated $CD8^+$ T cells to further delineate the roles between degranulation and FasL. Interestingly, while I found GrB expression in $CD8^+$ T cells to be proportional to the level of stimulation, weak stimulation is more favorable for FasL expression. In *ex vivo* stimulated $CD8^+$ T cells, while strong stimulation induced expression of intracellular FasL, only weakly stimulated cells were able to sustain FasL expression over an extended period of time. Using allogeneic tumors, I further demonstrated that high antigen availability stimulates $CD8^+$ T cells to express GrB and FasL while low antigen availability favors intracellular expression of FasL expression. Collectively, these results suggest two strategies of effector molecule expression: a low antigen level strategy favoring FasL expression and high antigen level strategy of GrB and FasL expression.

In addition to $CD8^+$ T cells, NK cells are also potent cytotoxic lymphocytes. As part of the innate immune system, NK cells were not believed to possess adaptive immune cell features. However, recent studies have demonstrated that following stimulation, NK cells may possess a number of memory cell-like features such as longevity, antigen specificity and enhanced secondary responses. While no definitive memory marker(s) have been found for memory NK cells, Ly-6C, a memory marker for $CD8^+$ T cells, is a promising candidate. In my study, I first demonstrated that Ly-6C positive NK cells are mature NK cells based on effector function and phenotype. Additionally, based on Ly-6C staining with monoclonal AL-21 and iMAP antibodies, two subsets of Ly-6C positive NK cells are visible, an AL-21 only reactive subset, Ly-$6C^{AL\text{-}21}$, and an AL-21/iMAP reactive subset, Ly-$6C^{AL\text{-}21/iMAP}$. I further demonstrated that Ly-6C positive NK cells develop from Ly-6C negative NK cells and that Ly-$6C^{AL\text{-}21/iMAP}$ NK cells develop from Ly-$6C^{AL\text{-}21}$ NK cells. In long term studies, this progression of Ly-6C expression suggests that Ly-$6C^{AL\text{-}21/iMAP}$ NK cells may represent a previously undescribed differentiation state of long-lived NK cells. Collectively, AL-21 and iMAP co-reactivity towards Ly-6C may further define the population of memory NK cells.

PREFACE

Data from chapter 4 was a collaborative work. Table 4-1 and Figures 4-1 and 4-2 were previously generated by former graduate student Dr. Chew Shun Chang. Figure 4-3 was previously generated by former graduate student Dr. Andy I. Kokaji.

Table of Contents

CHAPTER 1: General Introduction

List of Tables

List of Figures

List of Abbreviations

AIRE	Autoimmune regulator
A-LAK	Adherent lymphokine-activated killer cells
AP-1	Activator protein 1
APC	Antigen presenting cell
Bcl10	B-cell lymphoma 10
BCR	B cell receptor
BD	Becton Dickinson
BFA	Brefeldin A
^{o}C	Celsius
CARMA1	CARD-containing MAGUK protein-1
CCM	Complete culture media
CCR	CC chemokine receptor
CD	Cluster of differentiation
CFSE	5-(and 6-)carboxyfluoresceinsuccinimidyl ester
CHS	Contact hypersensativity
CLP	Common lymphoid progenitor
CXCL	CXC chemokine ligand
DC	Dendritic cells
dCS	Defined calf serum
DISC	Death-inducing signaling complex
DMEM	Dulbecco's modified Eagle's medium
DN	Double negative
DNFB	2,4-dinitro-1-fluorobenzene
DP	Double positive
EDTA	Ethylenediaminetetraacetic acid
EGTA	Ethyleneglycoltetraacetic acid
ELISA	Enzyme-linked immunosorbent assay
ELISPOT	Enzyme-linked immunospot
ER	Endoplasmic reticulum
FADD	Fas-associated death domain protein
FasL	Fas ligand
FCS	Fetal calf serum
FITC	Fluorescein isothiocyanate
G	Needle gauge

g	Gravity (ie. 200 x g)
g	Grams (ie. 0.03μg)
gp	Glycoprotein
GPI	Glycophosphatidyl-inositol
GrB	Granzyme B
Grb2	Growth factor receptor-bound protein 2
Gy	Gray
H-2	Murine major histocompatibility complex
HBSS	Hank's balanced salt solution
HEPES	N-2-hydroxyethylpiperazine-N'-2-ethansulfonic acid
hi	High
HIV	Human immunodeficiency virus
HSV2	Herpes simplex virus 2
ICAM-1	Intercellular adhesion molecule-1
IFN	Interferon
Ig	Immunoglobulin
IL	Interleukin
iNK	Immature NK cell
int	Intermediate
ip	Intraperitoneal
ITAM	Immunereceptor tyrosine-based activating motif
ITIM	Immunereceptor tyrosine-based inhibitory motif
L	Ligand
LCMV	Lymphocytic choriomeningitis virus
LFA-1	Lymphocyte function-associated antigen-1
lo	Low
LPS	Lipopolysaccharide
KLRG1	Killer cell lectin-like receptor G1
M	Molar
m	Milli-
μ	Mirco-
MALT1	Mucosa-associated lymphoid tissue lymphoma translocation 1
MAPK	Mitogen-activated protein kinase
MCMV	Murine cytomegalovirus
MHC	Major histocompatibility complex
MPEC	Memory precursor effector cell

mRNA	Messenger ribonucleic acid
Neg	Negative
NFAT	Nuclear factor of activated T cells
NF-κB	Nuclear factor-kappa B
NK	Natural killer
NKG2D	Natural-killer group2, member D
NKP	NK cell precursor
NP	Nucleoprotein
OD	Optical density
Oxazalone	4-ethoxymethylene-2-penyl-3oxazlin-5-one
PBS	Phosphate buffered saline
PEL	Peritoneal-exudate lymphocytes
PFU	Plaque forming units
pMHCI	Peptide MHC class I complex
PI3K	Phosphoinositide-3 kinase
PIP2	Phosphatidylinositol biphosphate
PIP3	Phosphatidylinositol triphosphate
PRR	Pattern recognition receptors
RAG	Recombination-activating genes
RPMI	Roswell Park Memorial Institute formulation 1640
RSV	Respiratory syncytial virus
SEM	Standard error of mean
SLEC	Short lived effector cell
SP	Single positive
Syk	Spleen tyrosine kinase
TCR	T cell receptor
T_{eff}	T effector
TNF	Tumor necrosis factor
TNFR	Tumor necrosis factor receptor
TP	Trans-presentation
U	Units
VSV	Vesicular stomatitis virus
VV	Vaccinia virus
WT	Wild type
ZAP-70	Zeta-associated protein-70

Chapter 1: General Introduction

The immune system

The immune system is tasked with sensing and eradicating potentially hazardous biological threats to a host. Jawed vertebrates have two main systems to combat potentially deadly intracellular and intercellular infections; the innate immune system and the adaptive immune system (1). Classically, the distinction between the innate and adaptive immune system is well defined. Innate immune cells are short lived cells that do not generate memory lineage cells and response from the innate immune system, following any repeated intrusion, is not enhanced due to prior activation or stimulation. The pathogen sensory system of innate immune cells rely on simple but reliable receptor:ligand pairs with limited diversity. In contrast, adaptive immune cells are able to generate highly precise epitope specific long lived memory cells following an infection and, collectively, display an enhanced response upon a subsequent infection (Figure 1-1).

With an array of germline encoded pattern recognition receptors (PRR), such as Toll-like receptors, immunoglobulin (Ig)-like receptors and lectin-like receptors, the innate immune system is the first line of defense against viral and microbial insults to a host (2, 3). Members of the innate immune system include cells such as neutrophils, monocytes, dendritic cells (DCs) and natural killer (NK) cells. A vital function of the innate immune system is the rapid containment of an invading pathogen, if not the elimination of the infection, while assisting in the development of long-lasting pathogen-specific responses by the adaptive immune system (4).

The adaptive immune system itself is further divided into humoral-mediated immunity, provided by B cells, and cellular-mediated immunity, provided by $CD4^+$ and $CD8^+$ T cells. In contrast to the innate immune system, a hallmark of both B and T cells of the adaptive immune system is the ability to recognize intruding pathogens with a high degree of specificity, however, full activation typically requires several days. It is believed that B and T cells are able to recognize up to ~$3x10^6$ different

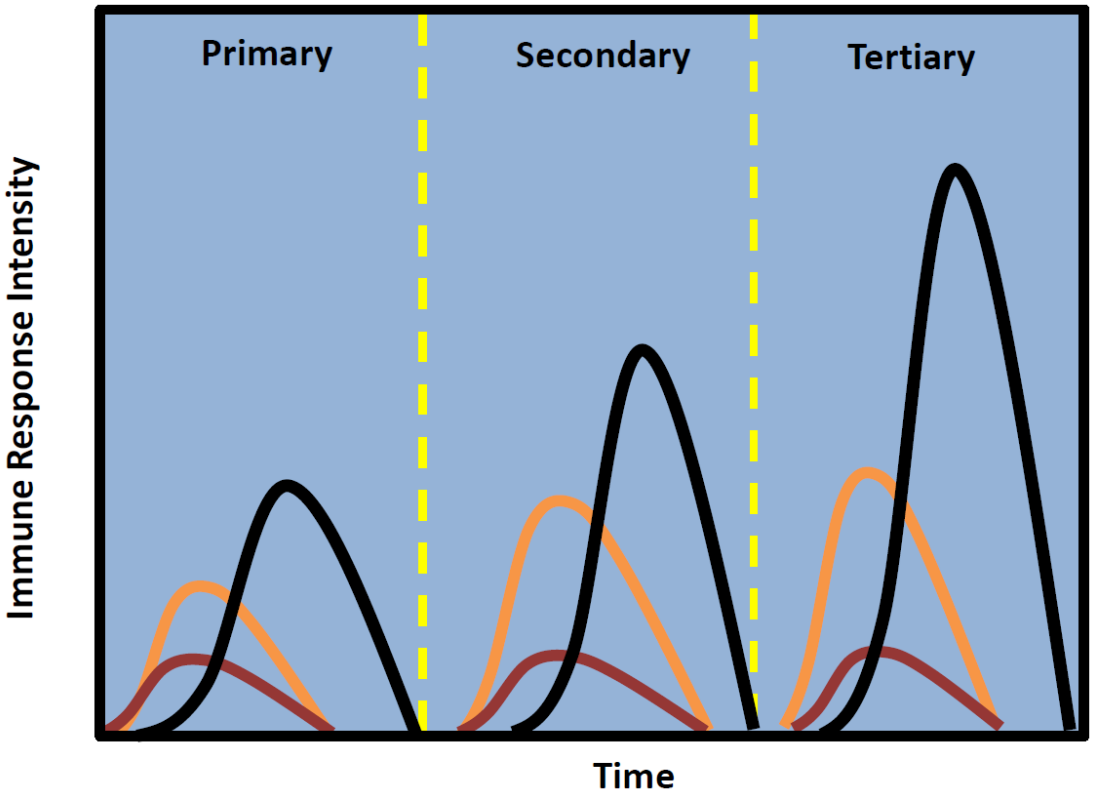

Figure 1-1: Immune response intensity by the immune system.
A representative immune response by classical innate (red), classical adaptive (black) immune system and memory NK cells (orange) following a primary, subsequent secondary and tertiary infection. A traditional view of innate immune response predicts an equivalent response to all three infections (red), while the adaptive immune system can provide increasing immune responses following each subsequent stimulus (black). Recent studies have demonstrated enhanced NK cell response to a secondary stimulation, compared to a primary stimulation, therefore mimicking responses of the adaptive immune system (black and orange). However, one study has found that NK cell responses following a tertiary stimulus do not differ in intensity compared to the secondary stimulus response (orange) (5).

pathogenic antigen variations through cell surface expression of B cell receptors (BCR) and T cell receptors (TCR), respectively (Kuby Immunology 5th edition 2003) . This remarkable diversity is driven recombination-activating genes (RAG) performing somatic gene rearrangements of the BCR and TCR genes during B and T cell development, respectively (6). Experimentally, deletion of RAG genes in mice result in the complete abolishment of mature B and T cells (7, 8). Furthermore, another trademark of the adaptive immune system is the generation of immunological memory against previous invading pathogens. Antigen specific memory B and T cells are able to respond more efficiently and effectively to a second infection by a pathogen of the host than naïve B and T cells, leading to an enhanced control and clearance of the pathogen upon a subsequent exposure (9, 10).

NK cells and $CD8^+$ T cells represent the cell mediated cytotoxic arm of the innate and adaptive immune system, respectively. Both NK cells and $CD8^+$ T cells express perforin and granzymes within cytoplasmic granules as well as death receptor ligand FasL (11). Upon activation and engagement of a target cell, stimulated NK and $CD8^+$ T cells degranulate releasing perforin and granzyme-containing granules and engage Fas expressed by target cells through FasL, ultimately inducing apoptosis of the engaged target cell. Utilizing degranulation and receptor mediated mechanisms of effector function, NK cells and $CD8^+$ T cells are vital in the host defense of invading intracellular pathogens and surveillance of tumor progression.

T cell development

T cells develop in the thymus from migrating T cell precursors exiting the bone marrow. Once in the thymus, developing thymocytes express RAG genes and undergo gene rearrangement events that produce a functioning TCR. Positive and negative selection processes then ensure T cell recognition of host major histocompatibility complex (MHC) and deletion of auto-reactive T cells, respectively (12-14). In conventional $CD4^+$ and $CD8^+$ T cells, the TCR is composed of an α chain and a β chain. Initially T cell progenitors in the thymus do not express CD4 or CD8

co-receptors and are termed double negative (DN) thymocytes. In the DN stages of T cell development, RAG genes are activated and first rearrange the variable (V), diversity (D), and joining (J) gene regions for the TCR β chain. Once complete, the TCR β chain is paired with an invariant pre-TCR α chain forming a pre-TCR that is expressed on the surface of the developing thymocyte. Formation of a pre-TCR allows for further differentiation of DN thymocytes into $CD4^+$ and $CD8^+$ expressing double positive (DP) thymocytes. During this transition, RAG genes rearrange the V and J gene segments of the TCR α chain generating a functioning TCR α chain that heterodimerizes with the existing TCR β chain (14). At the DP stage, thymocytes uniquely express both CD4 and CD8 co-receptors and a fully assembled TCR complex. At this point, DP thymocytes undergo positive selection by engaging MHC expressed by thymic epithelial cells to ensure TCR recognition of MHC and also selection of a CD4 or CD8 co-receptor. While a number of models have been suggested for CD4/CD8 lineage determination, current understanding is best described by the kinetic signaling model. During positive selection, DP thymocytes terminate CD8 gene expression to become an intermediate $CD4^+/CD8^{low}$ expressing DP thymocyte. In the kinetic signaling model, if TCR-pMHC engagement is maintained, $CD4^+/CD8^{low}$ thymocytes are believed to further develop into $CD4^+$ single positive (SP) thymocytes and MHC class II restricted $CD4^+$ T cells. In contrast, if TCR-pMHC recognition is lost, following the down regulation of CD8 expression, the developing thymocytes undergo co-receptor reversal. These developing thymocytes then re-engage CD8 gene transcription and terminate CD4 gene transcription. It has been suggested that γc cytokines may also contribute to the silencing of CD4 expression and re-initiation of CD8 expression. The thymocytes that proceed through co-receptor reversal then develop into a $CD8^+$ SP thymocyte and MHC class I (MHCI) restricted $CD8^+$ T cells (13). To prevent the generation of large quantities of potentially auto-reactive cells, DP and SP T cells undergo a process call negative selection. During this progression, thymocytes with high affinity for self-antigen bearing MHC complexes on thymic epithelial cells, and are therefore

potentially auto-reactive, are eliminated through apoptosis while low-reactive SP thymocytes are allowed to develop into mature $CD4^+$ or $CD8^+$ T cells (13, 15). Key transcription factors, such as AIRE, promote ectopic expression of peripheral tissue-restricted antigens in thymic epithelial cells that would not normally be expressed in the thymus (16, 17). These transcription factors allow for negative selection of auto reactive T cells to host peripheral antigens.

$CD8^+$ T cell activation

After $CD8^+$ T cells mature from the thymus, they circulate between the blood and secondary lymphoid organs. Receptors such as CD62L and CCR7 facilitate trafficking of naïve $CD8^+$ T cells to lymph nodes where they await stimulation by antigen-presenting cells (APC) (18). Upon infection, stimulated and matured APCs travel to secondary lymphoid organs to activate naïve $CD8^+$ T cells. Optimal stimulation of $CD8^+$ T cells are believed to require three signals: TCR recognition of MHCI-peptide complex on APCs, where the peptide is of foreign origin (signal 1), co-stimulation by co-stimulator ligands expressed on the mature APCs (signal 2) and a signal from pro-inflammatory cytokines, such as IL-12 or type I IFNs (signal 3) (19). In addition to signal 1 and 2, DC maturation resulting from PRR recognition of pathogen derived products or through $CD4^+$ T cell help via CD40L ligation, induces production of IL-12 and/or type I IFNs (19, 20). Additionally, *in vitro* studies have suggested that $CD4^+$ T cells can help $CD8^+$ T cell activation through IL-2 production (21, 22). IL-2 has been suggested to be important during primary infection for programming $CD8^+$ T cells for a full secondary response (23). $CD4^+$ T cells have also been shown to be vital for the generation of functioning memory $CD8^+$ T cell following an acute infection (24, 25).

Following stimulation, antigen-specific naïve $CD8^+$ T cells are able to undergo multiple rounds of cell proliferation and expansion and increase in population size by ~10^4 to 10^5 fold in as little as eight days (10, 26-28). While signal 1 and 2 were recognized early on as vital for $CD8^+$ T cell expansion, naïve $CD8^+$ T

cells stimulated without the presence of pro-inflammatory cytokines were found to be defective in effector function potential (19, 27, 29). Past studies have demonstrated that without pro-inflammatory cytokine signal 3, stimulated $CD8^+$ T cells have reduced lytic potential of target cells and reduced capacity for cytokine production (27, 30). Interestingly, *ex vivo* stimulated naïve $CD8^+$ T cells in the absence of IL-12 were unable to lyse target cells despite being able to degranulate as indicated by degranulation marker CD107a expression (29). Additionally, the nature of the infection may determine the specific requirements for signal 3. For instance, antigen-specific $CD8^+$ T cells following lymphocytic choriomeningitis virus (LCMV) infections are critically dependent upon type I interferons, while IL-12 is vital for $CD8^+$ T cell mediated protective immunity against vaccinia virus (VV) (31, 32).

The role of co-stimulation in $CD8^+$ T cell activation

The discovery of co-stimulatory molecules provided evidence for a 'signal two' requirement during T cell activation. T cell co-stimulation is defined as an engagement of cell surface receptors on the T cell surface, distinct from the TCR, that provides a supportive second signal for T cell activation (33). As a means of peripheral tolerance, co-stimulatory molecules are initiated following microbial insult. Accordingly, T cells require TCR and co-stimulatory signals from APCs for effective activation and over the years, a large number of additional co-stimulator molecules have been discovered (34, 35). Most co-stimulatory molecules can be classified into the CD28/B7 family or the tumor necrosis factor receptor (TNFR/TNF) family. Broadly defined, co-stimulatory molecule pairs function to synergize with TCR signaling to enhance T cell proliferation, survival, production of effector molecules and even memory generation (36). The TNFR/TNF family of co-stimulator molecules contains multiple extracellular cysteine repeats to form disulfide bridges (36). Functionally, TNFR/TNF co-stimulatory molecules are expressed as trimers on T cells and APCs (37). Intracellullarly, TNFRs signal through TNFR-associated factor (TRAF) adaptor proteins. The recruitment of TRAF proteins are able to initiate NF-

κB, MAPK and NFAT signaling cascades to promote cell proliferation, survival and enhanced cytokine production (38). The CD28/B7 family of molecules, on the other hand, are characterized as proteins with an Ig-like extracellular domain and a short intracellular cytoplasmic tail for signaling (36). Members of the CD28/B7 family of co-stimulators are predominantly type I transmembrane proteins that contain disulfide links in the stalk region to form functioning homodimer receptors (39). Among the CD28 family, the effects of CD28/B7 co-stimulation on $CD8^+$ T cell activation are most well characterized and studied.

CD28/B7 co-stimulation in $CD8^+$ T cell activation

CD28 is expressed on nearly all $CD8^+$ T cells in mice with increased expression levels shortly after TCR stimulation (40). Following TCR-pMHCI recognition, engagement of CD28/B7 augments $CD8^+$ T cells production of IL-2 and induction of anti-apoptotic proteins, which result in enhanced T cell proliferation and survival (38). Initial studies into CD28/B7 requirements for $CD8^+$ T cell activation were controversial. Following acute LCMV infections, negligible differences in the expansion and response of WT and CD28 deficient $CD8^+$ T cell were observed (41, 42). $CD8^+$ T cells from CD28 knock-out mice were able to generate LCMV specificity and killed LCMV target cells comparable to $CD8^+$ T isolated from wild-type virus infected mice (42). In contrast, blocking of B7 during influenza infections greatly diminished $CD8^+$ T cells IFNγ responses and *ex vivo* cytolysis capabilities (43). *In vivo* studies using vesicular stomatitis virus (VSV), murine gammaherpesvirus-68 and influenza indicated that CD28/B7 co-stimulation was necessary for primary responses by $CD8^+$ T cells as well as long-term survival of virus specific $CD8^+$ T cells and secondary memory $CD8^+$ T cell responses (44-46). Additionally, deficiency in CD28 or disruption of co-stimulation provided by B7-CD28 was also shown to reduce $CD8^+$ T cell responses to a number of influenza virus epitopes (47, 48). Interestingly, the discrepancy in CD28 signaling requirements came from differences in TCR signal duration between the different viral infections (36).

Viruses with high replicative rates, such as the case with LCMV, are able to provide a stronger and longer lasting TCR signal from APCs and thus may overcome the absolute requirement for CD28 co-stimulation (49). Conversely, CD28 co-stimulation may help lower the activation threshold for easier optimum T cell stimulation, particularly for sub-dominant epitopes (50). Additionally, not only is CD28 co-stimulation required for $CD8^+$ T cell activation during a primary infection, it is also required for maximum memory $CD8^+$ T cell responses against influenza and Herpes simplex virus-1 (51).

While CD28 lacks intrinsic catalytic functions, it is able to recruit a number of signaling proteins. Tyrosine phosphorylation of the YMNM sequence motif initiates CD28 signaling and leads to the recruitment of PI3K and Grb2 (34, 52). Recruitment of PI3K initiates production of PIP2 and PIP3 which in turn activates AKT and increases T cell survival, proliferation and cellular metabolism (53). Additionally, signaling through Grb2 is able to induce IL-2 production through the activation of the NFAT/AP-1 signaling pathways (53, 54). Finally, CD28 can also activate NF-κB through a three protein complex; CARMA1, Bcl10 and MALT1 (34, 53).

LFA-1/ICAM-1 co-stimulation in $CD8^+$ T cell activation

Lymphocyte function-associated antigen-1 (LFA-1) expressed on T cells bind to intercellular adhesion molecule-1 (ICAM-1) expressed by APCs. Formed by non-covalently linked α- and β- subunits, LFA-1 is best known for its function as an adhesion molecule and responsible for stabilizing T cell and APC interactions during T cell activation (55). However, LFA-1 has also been suggested to provide T cell activation signals in a capacity similar to functions performed by co-stimulatory molecules. LFA-1 co-stimulation has previously been shown to influence AP-1, PI3K, Ras and Erk 1/2 signaling in $CD8^+$ T cells (56-59). Additionally, LFA-1 also enhances IL-2 production by stabilizing IL-2 mRNA in an actin polymerization dependent mechanism, distinct from CD28 mediated IL-2 mRNA stability (58, 60, 61). Also, while both $CD4^+$ and $CD8^+$ T cells express LFA-1, LFA-1 signaling has

been suggested to be able to synergize with B7 for IL-2 induction in $CD8^+$ T cells (62). Additionally, LFA-1 enhancement of $CD4^+$ T cell proliferation cannot be compensated for by high density presentation of TCR ligands, suggesting a role for LFA-1 beyond simple adhesion mediated increase in TCR signal strength (63). Nonetheless, deficiency in ICAM-1 expression by APCs significantly reduced the duration of contact between $CD8^+$ T cells and DCs during stimulation and resulted in greatly inhibited memory cell formation (64). Collectively, these studies suggest that LFA-1/ICAM-1 interactions may mediate more than adhesion during T cell activation and, in a broader sense, provide co-stimulatory signals for $CD8^+$ T cell during stimulation.

$CD8^+$ T cell memory generation

Following clearance of an acute infection, $CD8^+$ T cells undergo a massive contraction phase reducing the numbers of activated $CD8^+$ T cells by as much as 90~95% (10). This process is believed to be driven by intrinsic and extrinsic mechanisms involving the balance of pro- and anti-apoptotic protein activity and death receptor ligations, such as Fas-FasL, respectively (65). The remaining previously stimulated $CD8^+$ T cells remain in the host as antigen-specific memory $CD8^+$ T cells capable of heightened responses and protection upon a subsequent infection of the host (10) (Figure 1-2). This functional difference may be a result of, in part, epigenetic modifications of key effector genes in memory T cells compared to naïve T cells (66, 67).While the existence and functional properties of memory $CD8^+$ T cells have been well documented, how memory $CD8^+$ T cell development occurs following a primary infection still remains unresolved. Currently, there are a number of proposed models for memory $CD8^+$ T cell generation; decreasing potential model, fixed lineage model and fate commitment with progressive differentiation model (68) (Figure 1-3).

The decreasing potential model suggests that effector T cells initially all have equal memory potential. However, as effector T cells encounter increased or

prolonged stimuli, they progressively lose memory potential and become short lived effector cells (SLEC) (10). In the fixed lineage model, memory lineage and effector lineage T cells represent distinct branches of T cell activation and are determined early following antigen stimulation, perhaps as early as the first round of cell division. In this model, all effector T cells are destined for cell death during the contraction phase while stimulated T cells destined for memory development do not progress through an intermediary effector stage (10). This model is supported by findings demonstrating asymmetric division of daughter $CD8^+$ T cells at the first division (69). Chang *et al.* observed that one daughter cell preferentially adopted a memory cell phenotype whereas the other an effector cell phenotype (69). Finally, the fate commitment with progressive differentiation model is a combination of the previous described models. In this model, high signal strength generate SLECs with high effector potential whereas reduced signal strength allows for the generation of memory precursor effector cells (MPEC). Cells destined for memory development, MPECs, display some effector properties and are not required to become memory cells. In fact, during the course of the infection, if MPECs encounter further or prolonged activation signals, they may progress to become SLECs. While the MPEC memory cell lineage is not fixed, SLEC cells are fixed and cannot become memory cells (10) (Figure 1-3).

Early days of natural killer cell discovery and characterization

The "natural killing" ability of NK cells was initially identified as a functional observation of splenic lymphocytes rather than an effector function of a specific cell type. Isolated splenocytes were found to be able to lyse certain tumor cell lines *ex vivo* without the need for prior sensitization; an effector function uncharacteristic of cells of the adaptive immune system (68, 70). The "natural killing" activity was also observed in isolated splenocytes depleted of both B and T cells resulting in a population of cells roughly 1~5% of original splenic lymphocyte population (71). By

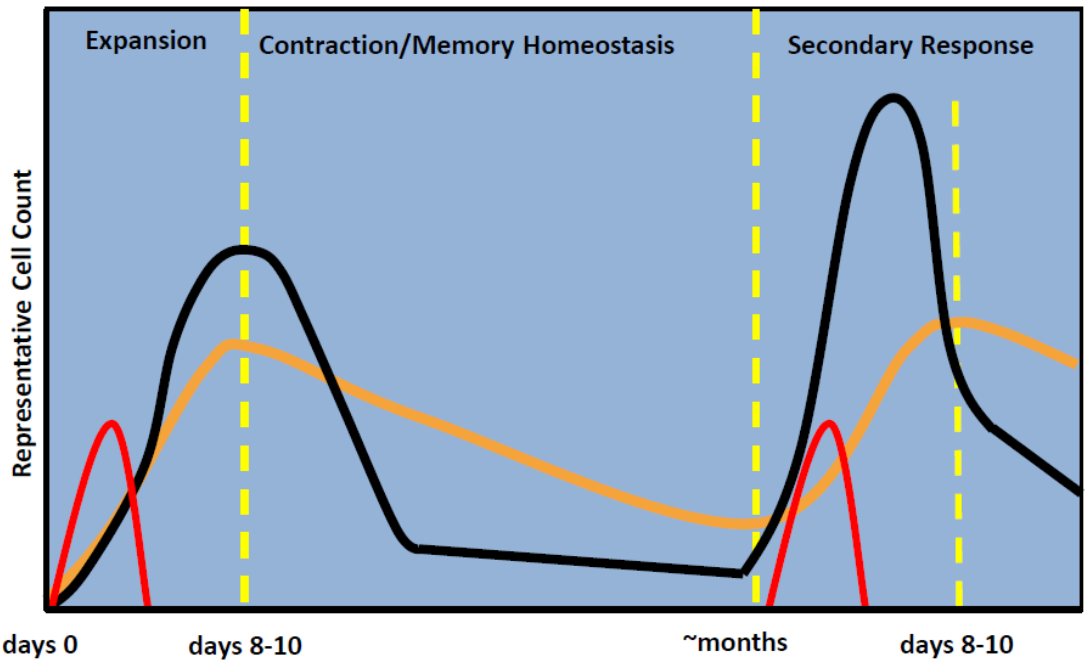

Figure 1-2: $CD8^+$ T cell and NK cell kinetics following infection.
The graph shows total antigen-specific $CD8^+$ T cell (black) and NK cell numbers (orange) following a primary and secondary infection (red). The primary expansion, contraction/memory homeostasis and secondary response phases are depicted. Notably, while $CD8^+$ T cells have a rapid and dramatic contraction phase, NK cell contraction is more gradual and prolonged, reminiscent of $CD4^+$ T cell contraction. Additionally, while epitope specific $CD8^+$ T cells are estimated to be between 10^2-10^3 cells/spleen, following acute LCMV strain infection, antigen specific $CD8^+$ T cells expand nearly 2000 fold. Following clearance, memory $CD8^+$ T cells maintain a population between 10^5-10^6 cells/spleen (28). Upon re-stimulation, memory $CD8^+$ T cells have nearly a six fold enhancement in their proliferative capacity over naive $CD8^+$ T cells (72). Comparatively, MCMV reactive $Ly49H^+$ NK cells represent roughly 50% of all NK cells in the spleen of a naive mouse and expand 100 fold in numbers following MCMV infection. However, when normalized, naive and memory NK cells have comparable proliferative capabilities (73).

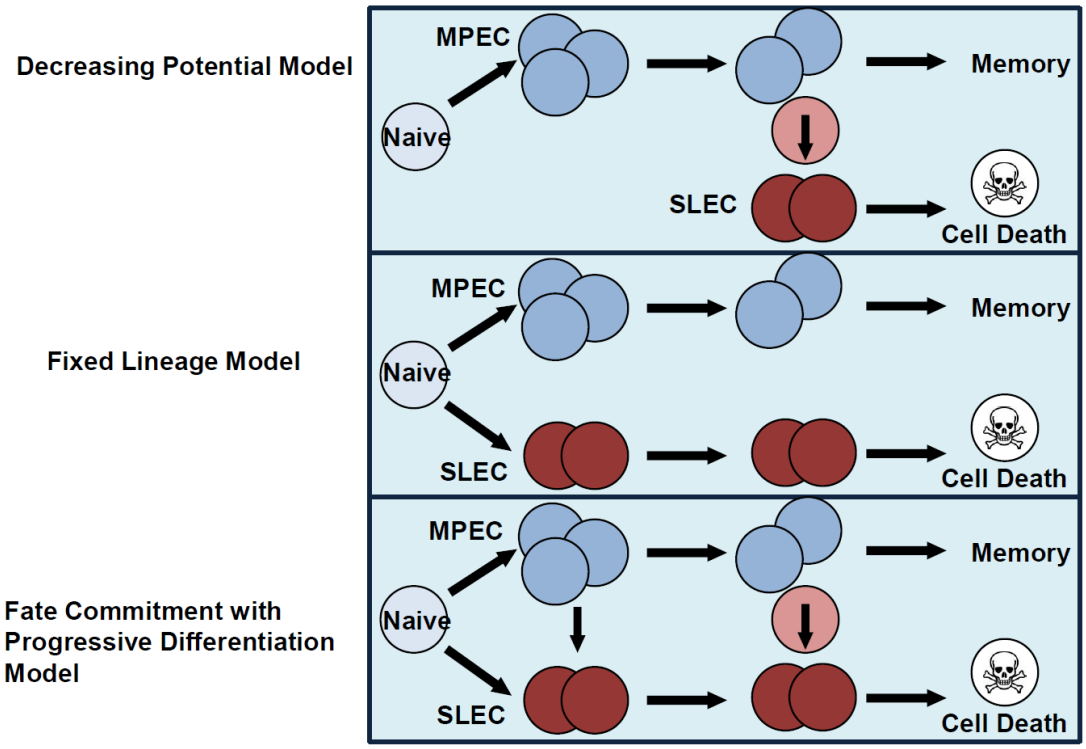

Figure 1-3: Models of CD8$^+$ T cell memory development.
Currently there are three models of memory CD8$^+$ T cell development.
Decreasing Potential Model: All stimulated naïve CD8$^+$ T cells have the potential to become long-lived memory cells through the MPEC stage. However, as MPECs acquire stronger/more sustained activation signals, they may lose memory potential to become SLECs and are then destined for high effector function and cell death during the contraction phase.
Fixed Lineage Model: Following naïve CD8$^+$ T cell stimulation, memory lineage and effector lineages are determined and fix early on, perhaps even after the first cell division. MPEC cells are destined to become long-lived memory cells whereas SLEC are destined for high effector function and cell death.
Fate Commitment with Progressive Differentiation Model: This model is a combination of the Decreasing Potential and Fixed Lineage Models. Following naïve CD8$^+$ T cell stimulation, activated T cells can become either MPECs or SLECs. As in previous models, SLECs are destined for high effector function and cell death while MPECs lineage cells have the potential for memory. However, if MPECs encounter further stimulation, they may differentiate into SLECs.

the mid 1980's, the identification of the NK1.1 marker proved instrumental in characterizing NK cells in C57BL/6 mice (74). NK cells were later found to preferentially kill MHCI deficient tumor cell lines while sparing MHCI expressing parental cell lines *in vivo* and *ex vivo* (75). Additional studies using β_2-microglobulin mutant cells further confirmed the importance of MHCI expression on a target as an inhibitor of NK cell killing (76, 77). Collectively, these studies suggested that, in stark contrast to $CD8^+$ T cells, NK cell mediated immune surveillance may function through the detection of the loss of MHCI, "missing self" by surrounding cells. Later studies would reveal that NK cells use a combination of inhibitory and activating receptors to recognize healthy "self" cells from transformed or infected cells.

NK cell development

In the bone marrow, common lymphoid progenitors (CLP) are precursor cells to all lymphocyte subsets including NK, T and B cells, but have lost the potential for myeloid cell development (78, 79). One of the early steps of NK cell development is the commitment of CLPs to NK cell precursors (NKP). Expression of IL-15 receptor β chain has been demonstrated on NKPs and responsiveness to IL-15 is an important differentiation step downstream of CLPs (79). *In* vivo, deficiencies in IL-15 result in marked reduction in NK cell development while overexpression of IL-15 in mice results in early expansion of NK cells numbers (80-82). In addition to cytokine requirements, the transcriptional repressor, Id2, has also been shown to be vital for NK cell development from the bone marrow (83, 84). For NK cell development, Id2 has been reported to suppress a number of E proteins, which are essential for commitment of B cell progenitors from CLPs (84, 85). As NKPs develop, they acquire a number of NK cell receptors including DX5 and NK1.1 in C57BL/6 mice and become immature NK cells (iNK) (85). It is also at this stage that iNK cells acquire expression of MHCI recognition receptors, such as inhibitory Ly49 receptors, and initiate the education process for NK cells (85). Further maturation of NK cells can be identified by surface expression of CD11b and CD27 (86, 87). In the spleen,

four subsets of NK cells based on CD11b and CD27 are present; $CD11b^{-}CD27^{-}$, $CD11b^{-}CD27^{+}$, $CD11b^{+}CD27^{+}$ and $CD11b^{+}CD27^{-}$ (88). Chiossone *et al.* demonstrated that there is a clear NK cell developmental progression from $CD11b^{-}CD27^{-}$ to $CD11b^{-}CD27^{+}$ to $CD11b^{+}CD27^{+}$ and finally $CD11b^{+}CD27^{-}$ (88). Additionally, while $CD11b^{-}$ NK cells are often regarded as 'immature', these NK cells are able to exert cytotoxic and cytokine effector function (86). It has also been suggested that fully differentiated NK cells express the inhibitory receptor KLRG1. In accordance with this notion, KLRG1 has only been reported on $CD11b^{+}CD27^{-}$ NK cells (87, 89).

NK cell education

The missing "self" MHCI concept and its related ideas has been the guiding principle of our understanding of NK cell functions. During development, NK cells undergo an education process that renders NK cells capable of recognizing "self" MHCI molecules with inhibitory receptors a full range of effector functions, including cytotoxicity and cytokine production (90). To educate NK cells to recognize self, and therefore not become auto-reactive, one hypothesis is that NK cells are instinctually endowed to be hyporesponsive. In this model, NK cell inhibitory receptor engagement of MHCI during development "arms" or "licenses" NK cells to be responsive to activating signals. Therefore, only NK cells capable of being inhibited by self MHCI expressing cells will be functional. Alternatively, in the "disarming" hypothesis, NK cells are initially responsive. However, if NK cells do not encounter MHCI inhibitory signals, and are therefore chronically stimulated, the NK cells become anergic or "disarmed" (90, 91). While these two classical NK cell education models are not mutually exclusive, more recently, a third "tuning" or "rheostat" model of NK cell education has also been proposed (91).

In C57BL/6 mice, there are two main inhibitory Ly49 receptors, Ly49 C and I, that recognize self MHCI $H\text{-}2K^{b}$ and a third inhibitory receptor, CD94/NKG2A, that recognizes the non-classical MHCI molecule Qa1b presenting peptide derived from

the H-2D^b leader sequence (92, 93). In C57BL/6 mice, individual NK cells have been found to express between zero, one, two or all three of the three inhibitory receptors (94, 95). Previous studies have approximated that 85% of splenic NK cells express at least one inhibitory receptor and accordingly, roughly 15% of NK cells do not express any of three aforementioned inhibitory receptors (90, 95). It was found that NK cells that express higher numbers of different inhibitory receptors were increasingly more responsive upon stimulation (94, 95). Conversely, NK cells that do not express any inhibitory receptors responded poorly to many *ex vivo* stimuli, even to MHCI deficient tumor cells (94). Collectively, a strong net stimulation of NK cells during development, possibly due to low expression of inhibitory receptors, drives a reduced state of responsiveness. In contrast, a weak net stimulus, resulting from the balance of activating and inhibitory receptor signals, directs a highly responsive NK cell. These recent studies challenge previously held assumptions that all NK cells expressed at least one inhibitory receptor specific for self MHCI. Additionally, these studies also suggest that during NK cell education, NK cell responsiveness may be determined in a rheostat-like fashion and not simply as either a responsive and hyporesponsive NK cell state (90).

NK cell activating and inhibitory receptors

Unlike T cells, initiation of NK cell effector function is determined through a balance between signals from activating and inhibitory receptors. In mice, a number of inhibitory receptors, such as Ly49C and I, that engage classical MHCI expressed by target cells have been described (96). When engaged, inhibitory receptors signal through intracellular immunoreceptor tyrosine-based inhibitory motifs (ITIMs) located on the cytoplasmic tail of the receptors. While the specific mechanism of how ITIM signals interfere with NK cell activation remains to be fully characterized, it is believed that a key aspect of ITIM signaling is the downstream phosphorylation and dephosphorylation of various cellular components (96, 97). Upon engagement, ITIMs are tyrosine-phosphorylated and recruit tyrosine phosphatases such as Src homology

2 (SH2) domain containing phosphatases (SHP1 or 2) (96, 98). It is believed that SHP-1 recruitment to ITIM motifs dephosphorylates a guanine nucleotide exchange factor, Vav-1 (90, 96). Stebbins *et al.* suggested that engagement of NK cell inhibitory receptors recruit and localize SHP-1 where SHP-1 is then able to selectively dephosphorylate Vav1, thus disrupting actin polymerization (99). Vav-1 has been proposed as a common point of intersection between activating and inhibitory signals in NK cells (96, 100). Additionally, Peterson and Long previously demonstrated that engagement of inhibitory receptors on NK cells also induced tyrosine phosphorylation of adaptor protein Crk (97). Furthermore, inhibitory signals can override degranulation signals provided by activating receptors (100). As such inhibitory receptors are considered more dominant to NK cells than activating receptors. The outcome of mixed activating/inhibitory signals therefore typically favor the inhibition of NK cell activation (101).

In contrast to inhibitory receptors, NK cell activating receptors recognize cell stress related proteins, such as NKG2D recognition of Rae-1, Mult-1 and H60, or viral products such as Ly49H recognition of murine cytomegalovirus (MCMV) viral product m157 (96). Additionally, NK cell activating receptors signal through immunoreceptor tyrosine-based activating motifs (ITAMs). While these motifs are not expressed on the cytoplasmic tail of activating receptors, they are expressed by adaptor molecules non-covalently associated with activating receptors (96). When engaged, NK cell activating receptors such as NKG2D and Ly49H associate with ITAM containing DAP-12 molecules through a negatively charged residue in the transmembrane domain to initiate NK cell activation (96, 102). Following aggregation, the tyrosine residue in the ITAM motif is phosphorylated and SH2 domain containing kinases such as Syk and ZAP-70 are recruited, both expressed by NK cells (103, 104). Since no significant functional defects were detected from Syk or ZAP-70 deficient NK cells in mice, Syk and ZAP-70 may exhibit a level of redundancy in transmitting ITAM activating signals in NK cells (105, 106). Alternatively, activating receptors such as NKG2D may also signal through

association with DAP-10, another signaling adapter protein (96). The cytoplasmic tail of DAP-10 contains a SH2 domain-binding site that is able to recruit p85 and signal through PI3K (96, 107). While NKG2D is able to associate with DAP-10 and DAP-12, the functional outcome of signaling through both adaptor molecules differ. DAP-10 signaling results in only cytotoxicity of an engaged target cell whereas DAP-12 signaling induce both cytokine production and cytotoxicity (108).

NK cell activation by cytokines

In addition to specific activation of NK cells through activating receptors, NK cells can also be activated through pro-inflammatory cytokines, a mechanism independent of activating ligands for specific activating ligands or foreign products. In a viral infection, such as MCMV, NK cells from C57BL/6 mice have been shown to demonstrate two stages of activation; an early stage mediated non-specifically through pro-inflammatory cytokines and a later stage mediated by Ly49H specific stimulation by MCMV viral product m157 (109, 110). During the first two days of MCMV infection, there are no distinguishable differences in response from m157 specific Ly49H positive and m157 non-specific Ly49H negative NK cells, however, by day six, there is a preferential proliferation of Ly49H positive NK cells (110). The early stage of NK cell activation has previously been attributed to pro-inflammatory cytokines such as IL-12, IL-18 and IL-15 (111-113). Additionally, while each of these cytokines are able to augment NK cell activation, synergistic effects of these cytokines on NK cells have also been demonstrated (114, 115). In addition to viral infections, NK cells pre-activated with IL-12, IL-18 and IL-15 have demonstrated sustained effector functions against established tumors *in vivo* (116).

Role of IL-15 in NK cell function

IL-15 is a member of the γc family of cytokines. The IL-15 receptor is composed of three subunits; a common γ chain shared with other γc cytokines, such as IL-2, IL-7 and IL-21, a common β chain shared with the IL-2 receptor and a unique

IL-15 high affinity α chain (115). As a vital cytokine for NK cell development and survival, deficiency in IL-15 results in the absence of mature NK cells (80, 115, 117). Interestingly, the IL-15 high affinity α receptor functions to present IL-15 from an IL-15 producing cell to an adjacent cell expressing the IL-15 receptor β and common γ chains in a process called trans-presentation (TP) (118, 119). The mechanism of IL-15 TP explains previous puzzling findings that NK cells do not require the expression of the unique IL-15 receptor α chain, but rather, α chain expression is required on neighboring cells for NK cell homeostatic maintenance. Instead, only the β and common γ chains are required to be expressed by NK cells (120-122). Furthermore, when APCs are stimulated, such as the case with LPS stimulated DCs, the DCs are able to prime NK cells by IL-15 TP (119, 123). IL-15 TP-primed NK cells produce higher quantities of IFNγ and have higher cytolytic abilities (123, 124). Additionally, the effects of IL-15 TP can synergize with IL-12 to augment NK cells stimulation (123, 124).

Role of IL-12 in NK cell function

IL-12 was first characterized for its ability to induce IFNγ, cytotoxic activity and proliferation in NK cells *in vitro* (115, 125, 126). IL-12 is formed by a disulfide linked IL-12p40 and p70 subunit and was initially called the "NK cell stimulating factor" (115, 126). Indeed, a major role of IL-12 on NK cells *in vivo* is the induction of IFNγ following viral infections, such as MCMV (112, 127). IL-12 has also been shown to augment NK cell IFNγ response to antibody-coated tumor cells *ex vivo* and is critical for optimal memory NK cell development *in vivo* (125, 128, 129). In IL-12 deficient mice, NK cells have significantly decreased IFNγ production capabilities while cytotoxicity functions remain intact (112). Much like IL-15, IL-12 is produced by antigen presenting cells, such as DCs, and is produced early after viral infections *in vivo* (113, 130, 131). As a positive feedback loop, IL-12p40 subunit production has also been shown to be augmented by NK cell derived IFNγ during a *Toxoplasma gondii* infection (132). Interestingly, the delivery of IL-12 produced by DCs to NK

cells is contact dependent and involves the formation of an immunological synapse (133). In addition to synergistic effects of IL-12 with IL-15, as mentioned above, IL-12 and IL-18 have been reported to cooperatively induce optimal NK cell expansion (134). IL-12 and IL-18 have also been suggested to be capable of inducing NK cell responses in mice deficient of IL-15 (135, 136).

Role of IL-18 in NK cell function

Similar to IL-12, IL-18 was also initially recognized as an IFNγ inducing factor capable of enhancing NK cell effector function (115). In accordance, deficiency in IL-18 has been shown to result in reduced NK cell responses (137, 138). NK cell production of IFNγ from IL-18 signaling is critical for a number of bacterial, fungal, parasitic and viral infections with IL-18 being constitutively expressed in an inactive precursor state as proIL-18 (113, 115, 139). Following infection, proIL-18 must be cleaved by proteases, most commonly caspase 1, to become biologically active (115, 139). Similar to IL-15 and IL-12, effective IL-18 mediated induction of IFNγ in NK cells by IL-18 expressing DCs requires cell-to-cell contact (140). Indeed, during priming of NK cells, DCs polarize IL-18 to the immunological synapse between DCs and NK cells (141). The polarization is a Ca^{2+}-dependent and tubulin mediated process that allows for directed secretion of IL-18 to the engaged NK cells (141). Recently, IL-12, IL-18 and IL-15 stimulated NK cells have been demonstrated to enhance anti-tumor capabilities by retarding tumor expansion *in vivo* (116). Additionally, cytokine stimulated NK cells have also recently been shown to possess adaptive immune features such as longevity and enhanced effector cell functions (142-144).

NK cell memory

While NK cells have traditionally been viewed as the cytotoxic lymphocyte population of the innate immune system, recent findings are now challenging this concept. Recently, a number of model systems have been utilized to study memory

NK cells or 'memory-like' features of NK cells; a liver restricted memory NK cell model, a MCMV induced memory NK cell model and a cytokine induced 'memory-like' NK cell model (145, 146) (Figure 1-4). In these studies, similar to the cells of the adaptive immune system, memory NK cells are long-lived cells capable of enhanced effector function such as cytotoxicity against target cells and IFNγ production, as compared to naïve NK cells, and in some circumstances, are able to recognize target cells in an antigen-specific manner (146, 147). Additional studies have also demonstrated co-stimulatory and cytokine requirements for memory NK cell generation (129, 148). Collectively, these studies are drawing new parallels between NK cells and $CD8^+$ T cells (149) (Figure 1-5).

Liver restricted memory NK cell model

The first descriptions of memory NK cells in mice were generated using classical hapten based contact hypersensitivity (CHS) models with chemical irritants 2,4-dinitro-1-fluorobenzene (DNFB) and 4-ethoxymethylene-2-penyl-3oxazlin-5-one (oxazalone) (147). Using Rag2 deficient mice, which lack mature T and B cells, hapten sensitized mice displayed an enhanced hypersensitivity response upon a secondary hapten challenge (150). Similar to recall responses of the adaptive immune system, for enhanced NK cell secondary response, the same chemical hapten was required for the primary and secondary stimulations (150). However, NK cell mediated CHS responses were not found to increase with repeated hapten stimulations beyond a second challenge (5). O'Leary *et al.* further demonstrated that enhanced hapten sensitivity in Rag deficient mice was transferable to an unstimulated mouse through adoptive transfer of hepatic NK cells, but not splenic NK cells (150). Later, hepatic NK cells from Rag deficient mice were shown to be able to generate antigen-specific memory against influenza, HIV, VSV virus-like particles and to VV (151, 152). Expression of CXCR6, a chemokine receptor, on hepatic NK cells was found to be critical for memory NK cell mediated CHS responses (151). CXCR6 has a single known ligand, CXCL16, which is constitutively expressed by the liver

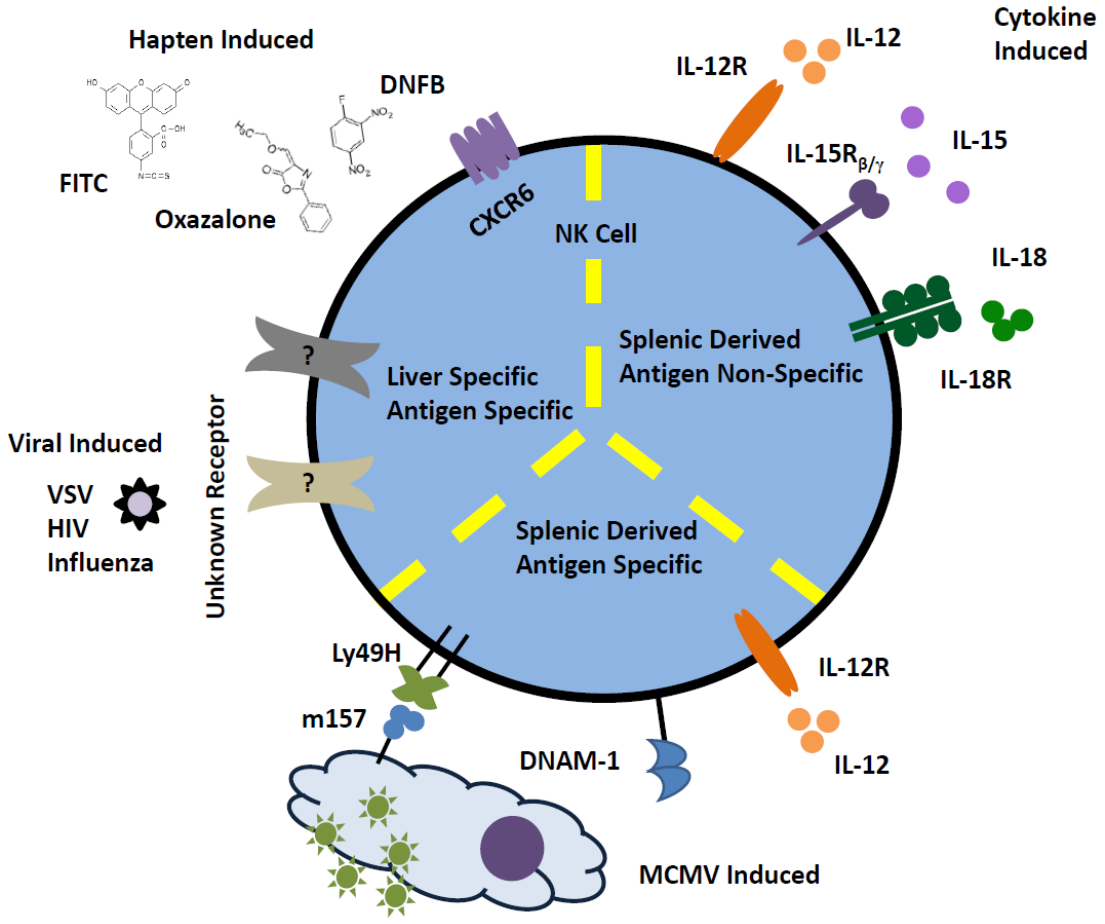

Figure 1-4: Memory and 'memory-like' NK cell systems in mice.
A variety of factors and systems have been used to study adaptive immune features in NK cells. Using chemical haptens and viral infections or virus-like particle immunizations, hepatic NK cells have been shown to mediate chemical specific and viral specific secondary responses. While the receptor for this specificity in hepatic NK cells is currently unknown, surface expression of CXCR6 on NK cells is vital to hepatic memory NK cell generation. In contrast, splenic NK cells have been shown to mediate MCMV specific memory via Ly49H-m157 interactions. Studies using the MCMV model have suggested that co-stimulation and cytokine stimulation are vital for optimal memory NK cell development through DNAM-1 and IL-12, respectively. Additionally, 'memory-like' NK cells can be generated through cytokine stimulation with IL-12, IL-18 and IL-15. 'Memory-like' NK cells are non-antigen specific.

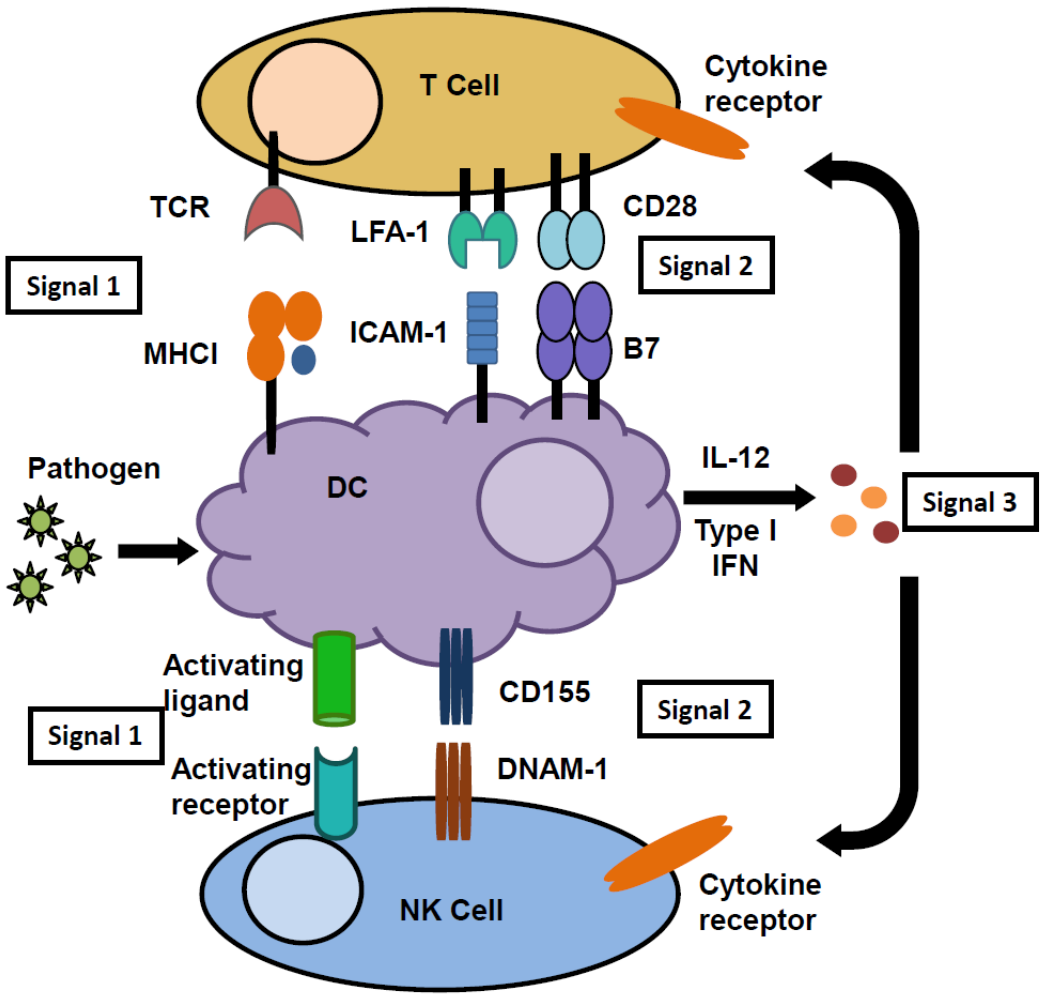

Figure 1-5: Parallels between $CD8^+$ T cell and NK cell activation.
It is well documented that $CD8^+$ T cells require three signals from mature DC for optimal activation; 1) a TCR-pMHCI signal, 2) co-stimulation signal, classically provided by CD28-B7, and 3) pro-inflammatory cytokine signal from IL-12 and/or Type I IFNs. NK cell activation and priming by DCs follow a similar three signal requirement. Signal 1 is provided by engagement of activating receptors/ligands, signal 2 is a co-stimulatory signal, perhaps DNAM-1-CD155, and lastly, a pro-inflammatory cytokine signal provided by IL-12.

sinusoidal endothelium (153, 154). Using fluorescein isothiocyanate (FITC) as a chemical hapten, Peng *et al.* later demonstrated that sensitization of mouse skin with FITC resulted in FITC-laden cells in the liver but not the spleen (155). Using parabiotic mice, where the circulatory system of two mice are conjoined, Peng *et al.* also demonstrated that hepatic memory NK cells remained stationary in the liver of the sensitized mouse and did not circulate in the blood or to the adjoining unsensitized mouse (155). From these studies, hepatic memory NK cells were also found to express Thy1, CD49a and, lack DX5, a traditional splenic NK cell marker (150, 152, 155). Currently, how liver derived memory NK cells are able to generate such specificity to virus-like particles and chemical irritants is still unknown. However, antigen/chemical specific hepatic memory NK cells may have these capabilities due to intrinsic properties of hepatic NK cells or through the influence of the microenvironment in the liver.

MCMV induced memory NK cell model

In C57BL/6 mice, roughly 50% of all NK cells express Ly49H, which recognizes the MCMV viral product m157 and is vital in mediating C57BL/6 mice resistance to MCMV infections (145, 147). After MCMV infections, there is an expansion of $Ly49H^+$ NK cells followed by a contraction phase and establishment of a long-lived pool of memory Ly49H expressing NK cells (73). This pool of memory NK cells was able to undergo a secondary expansion phase, enhanced IFNγ production and degranulation through *ex vivo* anti-NK1.1 stimulation and increased protection of naïve neonatal mice against MCMV infections compared to naïve NK cells (73). The expansion and development of $Ly49H^+$ memory NK cells are dependent on Ly49H stimulation, as m157 deficient MCMV infections do not induce the expansion and establishment of a $Ly49H^+$ memory NK cell pool (73). This study identified a number of key adaptive immune features in NK cells; expansion/contraction phases, enhanced secondary protection and viral product dependent recognition (Figure 1-2 and 1-4). While NK cells functionally possess

hallmarks of a cytotoxic lymphocyte, like $CD8^+$ T cells, the kinetics of $Ly49H^+$ NK cell contraction is reminiscent of the more prolonged and gradual kinetics seen for $CD4^+$ T cells contraction (73, 156). Furthermore, optimal generation of $Ly49H^+$ memory NK cells also requires signaling through pro-inflammatory cytokine and co-stimulatory molecule such as IL-12 and DNAM-1, respectively (129, 148). In contrast to the CHS models, $Ly49H^+$ memory NK cells can be generated from splenic as well as hepatic origins (73, 129, 148, 149). In parallel, splenic NK cells also generate memory against vaginal immunization with herpes simplex virus type-2 (HSV2) in mice (157). Abdul-Careem *et al.* showed that NK cells from a prior immunization with HSV-2 exhibited enhanced IFNγ production up to 60 days post-immunization and reduced HSV-2 induced genital lesions up to three weeks post-immunization (157).

Cytokine induced memory NK cell model

While expansion of $Ly49H^+$ NK cells is well documented from MCMV infections, during the early stages of infection, there is an expansion of NK cells that is independent of Ly49H expression (109, 110). This early phase of NK cell expansion seems to be driven by cytokine stimulation soon after infection (111, 112). Recently, work from the Yokoyama laboratory demonstrated that NK cells activated with IL-12 and IL-18 imprint long-lasting effects on NK cell activity (142). In their study, adoptively transferred IL-12, IL-18 and IL-15 activated splenic NK cells from Rag deficient mice were capable of enhanced IFNγ production up to three weeks post-transfer compared to non-activated NK cells upon a secondary *ex vivo* stimulation (142). These NK cells were designated as 'memory-like' as their stimulation was not dependent upon a specific ligand interaction or foreign antigen specificity (142). In a later study, Keppel *et al.* demonstrated that the enhanced IFNγ responses of 'memory-like' NK cells are maintained following subsequent homeostatic proliferations *in vivo* (143). Additionally, IL-12, IL-18 and IL-15 were shown to enhance NK cell mediated suppression and clearance of tumor growth *in*

vivo with a detectable population of 'memory-like' NK cells in the spleen, liver, blood and lungs up to 90 days after adoptive transfer (116). In parallel, human 'memory-like' NK cells have also been described to possess enhanced IFNγ production capabilities *ex vivo* (141).

Killing pathways of cytotoxic lymphocytes

Activated $CD8^+$ T cells and NK cells are able to eliminate transformed and intracellular pathogen infected cells. The lysis of target cells is mediated by 1) a degranulation mechanism of lytic molecules and is extracellular Ca^{2+} dependent and 2) a receptor:ligand dependent mechanism whereby FasL expressing effector cells induce apoptosis of Fas expressing target cells (11). Early studies demonstrated that these two mechanism account for most of the cytolytic function in $CD8^+$ T cells and NK cells (158). Initially, studies in human cell lines suggested that FasL is stored in lytic granule compartments together with perforin/granzyme in effector cells (159, 160). However, recent studies have suggested that FasL and granzyme storage are independently compartmentalized in distinct vesicular compartments (161, 162) (Figure 1-6). Functionally, FasL mediated protection was thought to only be relevant in the absence of degranulation mediated immunity (163). In contrast, recent studies have uncovered vital roles for FasL in tumor surveillance and viral immunity (164-170). Additionally, FasL is expressed in activated cytotoxic lymphocytes in a biphasic manner, resulting from an early and late wave of FasL expression (160, 171).

Mechanism of degranulation mediated killing

Perforin, a membrane pore forming protein, is exclusively found in cytolytic granules of cytotoxic lymphocytes such as $CD8^+$ T and NK cells (11). Perforin expression is an integral part of cytotoxic lymphocyte immunity as perforin-knockout mice are more susceptible to tumor progression and infections (172, 173). While perforin is essential, it alone is unable to fully mediate degranulation dependent

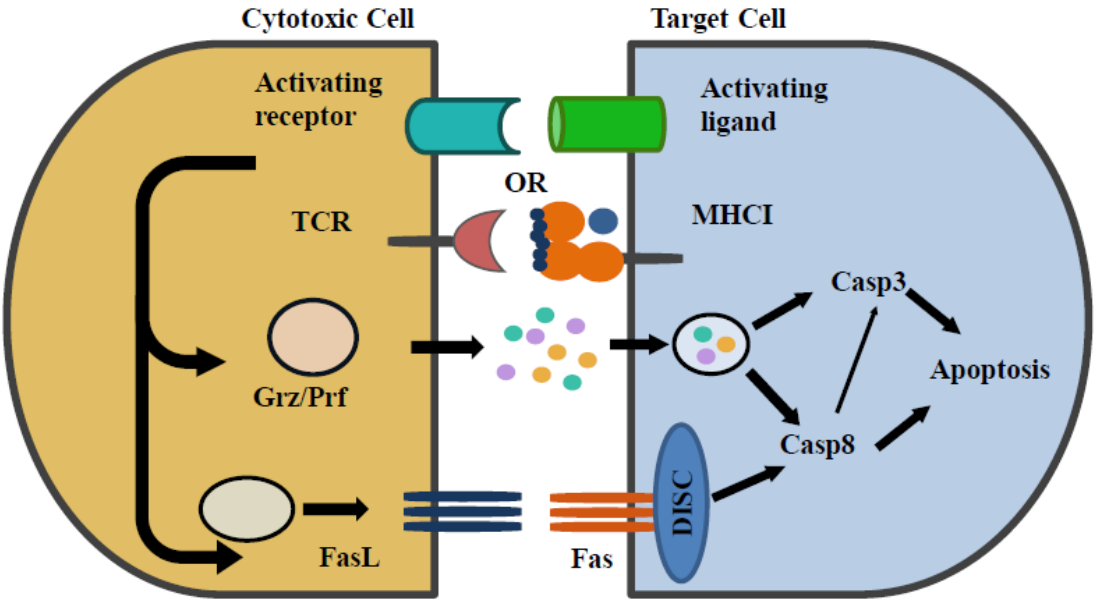

Figure 1-6: Killing mechanisms of cytotoxic cells.
Cytotoxic cells, such as $CD8^+$ T cells and NK cells utilize two main killing mechanisms; 1) a degranulation based mechanism employing perforin and granzymes and 2) a receptor-ligand mediated mechanism, mainly FasL-Fas. Following recognition of the target cell, either through TCR-pMHCI recognition by $CD8^+$ T cells or activating receptors/ligands by NK cells, secretory granules containing perforin and granzymes are released in a targeted fashion towards the target cell. Once in the cytosol, the proteolytic activity of granzymes activate caspases resulting in target cell apoptosis. In parallel, FasL, which is stored in distinct granule vesicles than perforin/granzymes, are translocated to the surface where they engage Fas receptors expressed on the target cell. Following engagement, the death-inducing signaling complex (DISC), is recruited and activates caspase 8 which, in turn, can induce target cell apoptosis or also activate caspase 3.

killing by $CD8^+$ T cells and NK cells. Instead, perforin works cooperatively with granzymes, one of the most characterized being granzyme B (GrB). How perforin and GrB navigate entry into the target cell is still not fully understood. However, there are currently two working theories centered around the pore forming properties of perforin (174, 175). In the first model, after the granular contents are released from the cytotoxic lymphocyte, perforin forms pores in the cell membrane of the target cell and, through diffusion, GrB enters the target cell (174, 175). In the alternative hypothesis, perforin and GrB first bind to the cell surface of the target cell. GrB binding may be accomplished through either receptors expressed by target cells, such as a receptor for mannose-6-phosphate, or through electrostatic properties; positively charged free GrB molecules interacting with negatively charged surface structures on the cell surface of the target cell in a non-specific manner (176-178). Subsequently, perforin and GrB are both endocytosed whereby perforin then disrupts the endocytic vesicle, releasing GrB into the cytoplasm (174, 175). Once free, GrB is then able to cleave and activate pro-caspase 3 directly or indirectly through activation of caspase 8, and ultimately inducing target cell apoptosis (11) (Figure 1-6).

Fas:FasL death receptor pair

Ligation of Fas induces the rapid assembly of the intracellular "death-inducing signaling complex" (DISC). Composed of Fas, the adaptor protein FADD (Fas-associated death domain protein) and caspase 8, DISC assembly is able to induce cell apoptosis (179). As a tetrameric complex, four FADD bind four Fas molecules through interactions between the "death domains" of Fas and FADD (180). Recruitment of FADD promotes dimerization and conformational change of pro-caspase 8 to initiate auto-proteolytic activation of caspase 8. Active caspase 8 is then released from the DISC to trigger apoptosis or activate additional apoptotic elements, such as caspase 3 (179) (Figure 1-6).

In vivo, tumor cells have been found to enhance Fas expression compared to *ex vivo* culture conditions (181). Additionally, a number of pro-inflammatory

cytokines have been shown to increase Fas expression on tumor cells, including IL-12, IFNγ and TNFα (166, 168, 182). In contrast, factors and signals that enhance FasL expression on cytotoxic lymphocytes have been less defined. In humans, IFNγ and IL-2 have been reported to only slightly increase FasL expression on $CD4^+$ T cells and NK cells, respectively (183, 184). Additionally, stimulation through CD28 and CD44 have also been reported to up-regulate FasL expression in human T cells (185, 186). In mice, however, IL-2 has been reported to stabilize FasL mRNA in T cells and both $CD4^+$ and $CD8^+$ T cells from mice infected with respiratory syncytial virus (RSV) co-expressing IL-4 have enhanced FasL compared to T cells from animals infected with RSV that do not express IL-4 (187, 188). However, recent reports have found that IL-2, IL-12, IL-15, IL-18, IFNγ, IFNα and TNFα all had minimal effects on FasL protein expression in $CD8^+$ T cells (168, 189). Of note, surface staining of FasL, which is most often used to determine FasL expression, is difficult to detect as FasL may be expressed in a membrane bound form or cleaved from the cell surface by metalloproteases forming soluble FasL (179). Nonetheless, only membrane bound form of FasL, but not soluble FasL, is important for Fas mediated apoptosis (190). Currently, no reports have closely examined the effects of co-stimulatory signals on FasL expression in murine $CD8^+$ T cells.

Ly-6C

Expression of Ly-6 family of molecules has proven invaluable for the characterization and identification of immune cells in mice. Ly-6 genes are encoded on murine chromosome 15 and are membrane bound molecules expressed on the cell surface by a C-terminal GPI anchor (191). While there are multiple members in the Ly-6 family, genomic studies have confirmed two alleles for many of the Ly-6 genes in mice. The Ly-6.1 haplotype strains include BALB/c, CBA and C3H/J mice, whereas Ly-6.2 haplotype strains include C57BL/6, 129/J, AKR/J and DBA/2 mice (191). A few of the more notable Ly-6 members include Ly-6A/E (more commonly referred to as Sca-1), Ly-6G and Ly-6C have been used widely as markers to

differentiate between different cell types. Sca-1 has been shown to be expressed on CD4 and CD8 DN thymocytes with increased expression later on mature $CD4^+$ and $CD8^+$ T cells (192). Ly-6G (also known as Gr-1) has been particularly useful as a granulocyte-differentiation marker present on neutrophils but absent on monocytes, macrophages and lymphocytes (191, 192). Lastly, among lymphocytes, expression of Ly-6C has been found on $CD8^+$ T cells, NK cells and, depending on mouse strain, $CD4^+$ T cells (191-193).

In the past, Ly-6C has been used as a memory $CD8^+$ T cell marker in conjunction with other memory markers such as CD44 (194-196). The core element of Ly-6C is an 89 amino acid long LU domain. The LU domain is present as a three finger-fold structure and contains five disulfide bonds. Despite the absence of a cytoplasmic tail, Ly-6C may initiate signaling cascades due to its association with lipid rafts (191). Ly-6C expression has also been suggested to mediate endothelial adhesion for $CD8^+$ T cell homing into lymph nodes, specifically, central memory $CD8^+$ T cells (197, 198). In accordance with this, Ly-6C stimulation has also been shown to induce LFA-1 clustering on $CD8^+$ T cells (199). While the specific ligand for Ly-6C has not be identified, CD22 expressed on B cells has been suggested as a possible ligand (200). However, in the same report, chimeras of Ly-6E and Ly-6I displayed much stronger binding than Ly-6C chimeras to CD22 (200). Additionally, recent studies suggested Ly-6C expression may identify terminally differentiated immune cells. Ly-6C expression has been found to identify terminally differentiated plasma cells from other B cell subsets, differentiated high effector function memory $CD4^+$ T cells, and memory NK cells from MCMV infected mice (73, 201, 202).

Project overview and Hypotheses

$CD8^+$ T cells are an integral component of the mammalian immune system. As part of the cytolytic function of $CD8^+$ T cells, previous studies have identified the importance in FasL mediated host protection under low antigen availability conditions. I hypothesize that FasL may have a distinct role from GrB in $CD8^+$ T cell

immunity and is not simply a redundant lytic mechanism to degranulation. However, how co-stimulator ligands affect FasL protein expression in $CD8^+$ T cells has not been well characterized. Additionally, kinetic studies of intracellular FasL expression were limited to mRNA expression. The kinetic expression of FasL on the protein level and its relation to antigen dose remains to be defined. To address these questions, I examined the expression kinetics of intracellular FasL over time following co-stimulation by CD28-B7.1 and LFA-1-ICAM-1 pairs and in *in vivo* stimulated $CD8^+$ T cells following injection of allogeneic tumors.

Among the innate immune system, NK cells have recently been shown to possess adaptive immune cell features, such as longevity. While NK cell maturation markers such as CD27, CD11b and KLRG1 have been well defined, markers identifying long-lived NK cells remain elusive. One potential candidate marker is Ly-6C. I hypothesize that Ly-6C expression may provide a means to further characterize and differentiate mature NK cell stages of differentiation. To further characterize the relationship between Ly-6C expression and NK cell longevity, I closely examined phenotypic changes to Ly-6C expression in purified NK cells subsets following adoptive transfer into congenic hosts.

Study objectives

1) Determine the role of co-stimulator ligands in intracellular FasL expression compared to GrB expression.

2) Examine whether antigen availability determines intracellular FasL expression compared to GrB expression.

3) Examine expression of Ly-6C epitopes on NK cells in different differentiation states.

4) Characterize long-lived NK cells for their expression of Ly-6C epitopes.

Chapter 2: Materials and Methods

Mice and Reagents

Six to eight week old female C57BL/6 mice and congenic CD45.1 C57BL/6 were purchased from Charles River and housed in conventional housing conditions. Recombinant mouse chimeric B7.1Fc and ICAM-1Fc proteins were purchased from R&D Systems and reconstituted as per the manufacturer's instructions. Anti-CD3ε cross-linking antibody (clone 145-2C11) was produced from hybridoma clones in our laboratory under sterile conditions. Fluorescently labeled anti-CD3ε (145-2C11), anti-CD8α (53-6.7), anti-CD44 (IM7), anti-CD62L (MEL-14), anti-CD4 (GK1.5), anti-Ly-6C (AL-21), anti-Ly-6A/E (D7), anti-Ly-6G (RB6-8C5), anti-CD45.1 (A20), anti-CD45.2 (104), anti-CD27 (LG.7F9), anti-CD11b (M1/70), anti-KLRG1 (2F1), anti-IFNγ (R4-6A2), anti-FasL (MFL3), anti-active caspase 3 (C92-605) and biotinylated anti-B7.1 (16-10A1) and anti-ICAM-1 (YN1/1.7.4) antibodies were purchased from eBiosciences or BD Biosciences. Anti-granzyme B (GB12), goat-anti-rabbit IgG secondary antibodies and CellTrace CFSE Cell Proliferation Kit and CellTrace Violet Cell Proliferation Kit were purchased from Life Technologies. Recombinant mouse IL-2 and anti-CD16/32 Fc blocking antibody (2.4G2) were produced in our laboratory. Mouse serum was isolated from blood of >six week old C57BL/6 mice purchased from Charles River. Recombinant mouse IL-12 and IL-15 were purchased from PeproTech and recombinant mouse IL-18 was purchased from Medical and Biological Laboratories Co.

Cell Line and Culture Conditions

The P815 mastocytoma (H-2^d) and L1210 leukemia (H-2^d) cells were maintained as single cell suspensions in DMEM media supplemented with 8% dCS. Fas transfected L1210 cells (Fas.L1210) were maintained in RPMI-1640 media supplemented with 5% FCS and 0.055mM 2-ME. EL4J lymphoma, HEK293T human kidney cell line, RF33.70 T-T hybriomas, RMA lymphoma and MDAY-D2

lymphoma cells were maintained in DMEM or RPMI-1640 containing 5% FBS, 2mM L-glutamine, 100U/ml of penicillin and 100μg/ml of streptomycin. Fas.L1210 cells were obtained from Dr. R.C. Bleackley (University of Alberta, AB, Canada). EL4J Ly-6 transfectants were kindly provided by Dr. T.R. Malek (University of Miami School of Medicine, FL). HEK293T cells were transfected with Ly-6A.2/E.1, Ly-6C2 or Ly-6I.2 plasmids kindly provided by Dr. A.L. Bothwell (Yale School of Medicine, New Haven, CT) using lipofectamine 2000 (Invitrogen) as per manufacturer's recommendations. RF33.70 cells were provided by Dr. K.L. Rock (University of Massachusetts, MA). MDAY-D2 cells were obtained from Dr. J.W. Dennis (Samuel Lunenfeld-Tanenbaum Research Institute, ON, Canada).

Anti-CD3ε and recombinant B7.1Fc or ICAM-1Fc coating of plates

Twenty-four well tissue culture treated plates from Corning were incubated at 4^{o}C overnight with 150μl PBS containing the desired concentration of stimulating anti-CD3ε antibody and/or recombinant B7.1Fc or ICAM-1Fc. The next day, excess unbound antibody and recombinant proteins were washed extensively with PBS. Unbound sites were blocked with 2% BSA in PBS at 37^{o}C for at least 30 minutes and again washed extensively with PBS. Quantification of immobilized antibody and protein was determined by ELISA.

ELISA determination of antibody and recombinant protein immobilization

Antibody and protein immobilized 24 well plates were stained with biotin conjugated anti-B7.1, anti-ICAM-1 or anti-Armenian hamster antibody for one hour at room temperature. Excess biotin conjugated antibody was washed extensively with 0.05% Tween-20 in PBS. Plates were then incubated with ExtrAvidin-Alkaline Phosphatase (Sigma) for two hours at room temperature and again washed extensively with 0.05% Tween-20 in PBS and lastly, phosphatase substrate (Sigma) was then added. Substrate reaction was determined by a Kinetic microplate reader (Molecular Devices) at the wave length of 405nm.

Isolation of CD44^{lo} CD8^{+} T cells for ex vivo stimulation

Mice were anesthetized with isofluorane (Pharmaceutical Partners of Canada Inc.) and euthanized via cervical dislocation. The spleens and lymph nodes (superfacial, axillary, brachial and inguinal) were removed, pooled and disrupted with a tissue homogenizer. CD44^{lo} naïve phenotype CD8^{+} T cells were isolated using EasySep Negative Selection Mouse CD8^{+} T cell Isolation Kit (Stemcell Technologies) with the addition of 0.03µg/1 x 10^{6} cells of anti-CD44 biotinylated antibody (IM7) from eBioscience during the antibody labeling isolation step. Typical CD44^{lo} naïve CD8^{+} T cells yields were between 7~10 x10^{6} cells per mouse with a purity of greater than 90%.

Plate bound ex vivo CD8^{+} T cell stimulation and preparation

Twenty-four well tissue culture treated plates were coated with 0.2µg/ml of anti-CD3ε antibody with or without 10nm, 20nm or 30nm of recombinant B7.1Fc or 2.5nm, 5nm or 10nm recombinant ICAM-1Fc protein overnight at 4^{o}C. The next day, unbound antibody or protein was removed by extensive washes with PBS and unbound sites in the wells were blocked with PBS containing 2% BSA for at least 30 minutes at 37^{o}C and washed extensively with PBS. Three-hundred thousand isolated CD44^{lo} naïve phenotype CD8^{+} T cells were plated in Complete Culture Media (CCM) (RPMI supplemented with 10% FCS, 2mM L-glutamine, 100µg/ml penicillin/streptomycin, 0.1mM non-essential amino acids, 1mM sodium pyruvate and 53nM β-mercaptoethanol). On day two, the CD8^{+} T cells were transferred to a new 24 well plate in CCM plus 5U/ml of recombinant IL-2. On the indicated days, intracellular expression of FasL and GrB in stimulated CD8^{+} T cell was determined by flow cytometry.

Intraperitoneal allogeneic P815 stimulation

Between $0.02x10^6$ to $25x10^6$ P815 (H-2^d) cells were injected intraperitoneally (ip) into C57BL/6 mice (H-2^b) of eight to twelve week old mice at a volume of 500µl in PBS. At the indicated days, peritoneal exudate lymphocytes (PELs) were recovered from tumor challenged mice. To do so, peritoneal cavities of mice were flushed twice with 4ml of PBS using a 23G needle.

Intracellular FasL and granzyme B cell staining and flow cytometry analysis

Isolated PELs were first treated for 20 minutes with 4% mouse serum from C57BL/6 mice in RPMI containing 2.5µg of 2.4G2 antibody per 100µl volume to block Fc receptors and then surface stained with anti-CD3ε, CD8α, CD44 and CD62L fluorescently labeled antibodies both at 4°C in the dark. Next, the cells were fixed in PBS containing 2% Formaldehyde, 2% FCS and 5mM EDTA for 15 minutes at room temperature in the dark. Cells were then permeabilized and stained in 0.2% saponin in PBS containing 2% FCS and 5mM EDTA for 30 minutes at 4°C in the dark. Data was acquired on a BD Fortessa flow cytometer and analyzed with FCS Express 3 software (De Novo Software).

Active caspase 3 killing assay

Active caspase 3 analysis by flow cytometry has previously been used to determine FasL mediated killing by cytotoxic T lymphocyte clones as an alternative to ^{51}Cr release assay (161). Effector PELs were isolated by peritoneal lavage with PBS as described above, and erythrocytes lysed with 0.15M NH_4Cl in Tris. To discriminate between target L1210 or Fas.L1210 cells and allo-antigen simulated effector PELs from >21 day P815 stimulation ip *in vivo*, effector cells were labeled with 0.5µM of CFSE for 20 minute at 37°C. The dye was then quenched with the addition of CCM of at least five times the labeling volume for 10 minutes at 37°C and washed twice with RPMI supplemented with 2% FCS. Additionally, L1210 and Fas.L1210 cells were pre-incubated with 4mM EGTA/3mM $MgCl_2$ in PBS containing 2% FCS or PBS containing 2% FCS for 30 minutes at 37°C before mixing

with the CFSE labeled effector PEL cells. Once mixed, effector and target cells were centrifuged at 200 x g for 3 minutes and incubated together for four hours at 37^{o}C. Following incubation, the cells were fixed, permeabilized and stained with primary anti-active caspase 3 antibody and fluorescently labeled secondary goat-anti-rabbit-IgG antibody. Data was acquired on a BD Fortessa flow cytometer and analyzed with FCS Express 3 software (De Novo software).

LCMV infections

More than 6 week old female C57BL/6 mice were infected ip with 2x10^{5} PFU of LCMV-Armstrong (gift from Dr. Pamela Ohashi) and housed in a level 2 bio-containment facility. At the indicated times splenic and lymph node T cells were isolated from the infected mice using EasySep T cell enrichment kits and cell surface markers were analyzed by flow cytometry.

IFNγ ELISPOT assay for LCMV specific memory CD8^{+} T cells

Splenic CD8^{+} T cells from C57BL/6 mice infected with LCMV >40 days were sorted into Ly-6C$^{iMAP(neg, lo, int or hi)}$ subsets. EL4 target cells were pulsed with either LCMV peptides (gp33-41, gp276-286, NP394-404) purchased from NeoMPS Inc. or influenza A/PR8 peptide (NP366-374) purchased from BIOpeptide Co., for one hour at 37^{o}C and washed extensively to remove excess unbound peptides. Purified CD8^{+} T cells were incubated with peptide pulsed EL4 cells at an effector:target ratio of 1:100 in a 96 well MultiScreen-HA plate from Millipore. The MultiScreen plates were coated with anti-IFNγ antibodies (AN-18) for five hours at 37^{o}C. Following incubation, the ELISPOT plate was washed and biotin-conjugated anti-IFNγ antibody (R4-6A2) was used to detect capture of IFNγ followed by HRP-conjugated streptavidin. Plates were subsequently developed using BCIP/NBT substrate and IFNγ spots enumerated with a Bioreader-4000 (Biosys.).

Isolation of splenic and intrahepatic lymphocytes

For isolation of splenic lymphocytes, spleens were retrieved from C57BL/6 mice and gently disrupted using a tissue homogenizer in PBS containing 2% FCS and 5mM EDTA. The cells were then strained through a 70µm cell strainer and erythrocytes depleted using 0.15M NH_4Cl solution. Lastly, the cells were washed extensively with RPMI containing 10% FCS, 2mM of L-glutamine 100U/ml of penicillin, 100µg/ml of streptomycin and 0.055mM 2-ME.

For isolation of intrahepatic lymphocytes, a modified mechanical isolation procedure from Blom *et al.* was utilized (203). Briefly, the inferior vena cava was first severed and the liver was perfused with 5ml of PBS via the hepatic portal vein until the liver became blanched. Next the liver was carefully removed from the mouse and the gall bladder excised. The liver was then minced and forced gently through a sterile 200µm-gauge stainless steel mesh using a sterile 10ml syringe plunger. The cell suspension was then re-suspended in 50ml of RPMI containing 10% FCS and 2mM of L-glutamine and centrifuged for 1 minute at 60 x g at room temperature with the brake-off setting. Next, the supernatant was recovered (~45ml volume) and the cells pelleted by centrifuging at 480 x g at room temperature for 8 minutes with a high-brake setting. The pelleted cells were then re-suspended in a 37.5% Percoll solution in HBSS containing 100U/ml of heparin and spun at 850 x g for 30 minutes at room temperature with the brake-off setting. The supernatant was discarded and the pellet re-suspended in 2ml of 0.15M NH_4Cl solution to lyse any remaining erythrocytes from the sample preparation. Lastly, the cells were washed extensively with RPMI containing 10% FCS, 2mM of L-glutamine 100U/ml of penicillin, 100µg/ml of streptomycin and 0.055mM 2-ME.

iMAP antibody generation

iMAP (mouse IgM) antibody was generated by immunizing BALB/c mice with C57BL/6 A-LAK cells, as previously described (204). iMAP was purified from protein free hybridoma media by $(NH_4)_2SO_4$ precipitation and dialyzed against PBS.

iMAP was fluorescently labeled with Alexa Flour 488 Protein Labeling Kit from Life Technologies as per manufacturer's instructions.

Surface Ly-6C and intracellular IFNγ staining of CD8$^+$ T and NK cells

Lymphocytes from C57BL/6 spleens or livers followed a three step antibody staining procedure. First, Fc receptors were blocked with 4% mouse serum with 2.5μg of anti-CD16/32 (2.4G2) antibody per 100ul in RPMI for 20 minutes at 4^{o}C in the dark. Following incubation, where indicated, fluorescently labeled anti-CD3ε, CD8α, NK1.1, CD45.1, CD45.2, CD11b, CD27 and KLRG1 antibodies and unless otherwise indicated, specified amounts of AL-21 were also added directly into the staining sample and further incubated for an additional 20 minutes at 4^{o}C in the dark. Lastly, indicated quantities of iMAP were added directly to the sample and the cells incubated for an additional 20 minutes at 4^{o}C in the dark. For some experiments, the order AL-21 and iMAP antibody addition may be reversed. Following this last incubation step, the cells were washed to remove any unbound antibodies with PBS containing 2% FCS plus 5mM EDTA. For samples requiring intracellular IFNγ detection, the cells were subsequently fixed with 2% formaldehyde in PBS containing 2% FCS with 5mM EDTA for 15 minutes at room temperature in the dark. The cells were then permeabilized and stained with fluorescently labeled anti-IFNγ antibody in 0.2% saponin in PBS containing 2% FCS and 5mM EDTA for 30 minutes at 4^{o}C in the dark. The cells were then washed extensively to remove any excess unbound antibody. Data was acquired on a BD Fortessa flow cytometer and analyzed with FCS Express 3 software (De Novo Software).

Hapten sensitization

Hapten sensitization of mice was performed as previously described (151). Briefly, abdomens of six to eight week old C57BL/6 mice were shaved using an animal hair clipper. On day zero and one, the shaved abdomen was sensitized with

50µl of 0.5% DNFB in acetone. On day four, hepatic NK cells were isolated and purified via cell sorting for adoptive transfer.

Cytokine stimulation

Cytokine stimulations of NK cells were performed as previously described with modifications (142). Briefly, purified splenic NK cells by cell sorting were stimulated with 10ng/ml of IL-12, 50ng/ml of IL-1 and 10ng/ml of IL-15 or as control, 10ng/ml of IL-15 alone overnight (13~15 hours). For short term stimulations, purified splenic NK cells were incubated with IL-12 and IL-15 for four hours with the addition of Brefeldin A (BFA) after the first hour of incubation.

NK cell Adoptive transfer and sub-lethal irradiation of recipient mice

Purified NK cells via cell sorting were washed extensively with PBS and loaded into a 26G needle syringe and adoptively transferred into recipient mice at a volume of <250µl via tail vein injection. The quantity of cells transferred ranged from $3x10^5$ to $1x10^6$ per mouse. Where indicated, recipient mice received total body sub-lethal irradiation (5Gy) using a Cesium-137 GC3000E irradiator, prior to NK cell adoptive transfer. For *in vivo* proliferation assays, stimulated NK cells were labeled with CellTrace Violet Cell Proliferation Kit per manufacturer's instructions (Life Technologies).

Cell sorting

Hepatic and splenic lymphocytes were labeled with indicated fluorescent antibodies and re-suspended in PBS containing 2%FCS, 5mM EDTA and 25mM HEPES at a concentration of roughly $100x10^6$ per ml. NK cells were sorted on a BD Aria III cell sorter at a rate of between 20,000 to 25,000 events/second. For increased recovery, NK cells were sorted into heat inactivated FCS serum for an approximate final serum concentration of >10% serum. Typically, approximately 300,000 hepatic

NK cells can be isolated per liver and roughly $1x10^6$ splenic NK cells per spleen. Final sort purity is generally greater than 95%.

Statistical analysis

Statistical analysis of results was done using unpaired Students *t* test with Prism software (Graphpad Software, La Jolla, California, USA.).

Chapter 3: Activation Signal Strength Dependent Expression of Intracellular FasL and Granzyme B in $CD8^+$ T Cells

Introduction

$CD8^+$ T cells are able to provide sterilizing immunity against tumor and intracellular pathogens. Activated effector $CD8^+$ T cells utilize two mechanisms of target cell lysis; a degranulation pathway consisting of granzyme/perforin cytolytic molecules and cell surface presentation of FasL against Fas expressing target cells (11). Upon T cell receptor recognition of appropriate peptide/MHCI complexes, secretory granules are transported to the immunological synapse with the target cell whereby granzyme/perforin molecules are released and FasL displayed to the target cell (205). The prevailing view had been that granzyme/perforin-mediated target cell killing was the dominant effector pathway over FasL-Fas mediated target cell lysis. In many regards, the FasL pathway had been suggested to only be essential for viral clearance in the absence of the degranulation pathway (163). Consequently, from these studies very little was understood regarding the role of FasL mediated immunity.

More recently, FasL has been shown to be important in a number of viral infections in various capacities. During influenza infection, FasL was shown to be a key contributor in limiting the emergence of influenza variants containing mutations in the immunodominant NP366-374 epitope recognized by $CD8^+$ T cells (170). FasL also contributed to reduced LCMV viral titers in the spleen following infection and reduced West Nile virus titers and host protection (164, 169). In addition to new findings regarding the importance of FasL during viral infections, FasL has also been shown to be essential for controlling tumor metastasis (166-168). In these studies, FasL contributed to the reduction in the numbers of metastasized pulmonary tumor nodes and enhanced survival of tumor challenged mice. While FasL-mediated target cell killing is slower than granzyme/perforin based degranulation killing (205-207), collectively, these studies illustrate a non-redundant role for FasL in $CD8^+$ T cell mediated immunity.

He *et al.* has previously shown that intracellular FasL is stored in separate and distinct vesicle compartments from granzyme/perforin containing lytic granules and cell surface presentation of intracellular stored FasL is extracellular Ca^{2+}-independent (171). This is in stark contrast to the Ca^{2+}-dependency of $CD8^+$ T cell degranulation (208, 209). Additionally, He *et al.* and others have also demonstrated a lower threshold of T cell receptor stimulation required for intracellular FasL expression and function in $CD8^+$ T cell compared to induction of degranulation (161, 210). These studies suggest differential mechanisms for controlling FasL and degranulation dependent granzyme/perforin molecule expression. In accordance with this notion, Meiraz *et al.* have recently shown that following allogeneic intraperitoneal (ip) tumor challenge in mice, responding $CD8^+$ T cells in the peritoneum cavity switch from utilizing both perforin and FasL early following tumor challenge to FasL only mechanisms of effector function over time (211). However, in their study, expression of FasL was inferred through examination of mRNA levels (211). Thus, expression of intracellular FasL at the protein level in activated $CD8^+$ T cells over time following T cell activation has not been characterized.

During $CD8^+$ T cell activation, co-stimulatory molecules augment $CD8^+$ T cell proliferation, survival and effector function (35). A recent study suggested that FasL is required for optimum $CD8^+$ T cell immune surveillance of spontaneous B cell lymphomas *in vivo* and dependent upon CD28 co-stimulation, the receptor ligand for the classical B7 co-stimulatory molecule (212). In addition, ICAM-1 has previously been shown to co-stimulate $CD8^+$ T cell activation, separate from B7 co-stimulation (58, 62). Our laboratory also demonstrated that ICAM-1 co-stimulation enhanced effector molecule expression and function in $CD8^+$ T cells in culture (Dr. Hockley Thesis). However, the specific role of B7 and ICAM-1 co-stimulation on FasL expression has not been fully addressed.

In this chapter, I quantitatively compared the expression patterns of intracellular FasL and GrB in *ex vivo* and *in vivo* activated $CD8^+$ T cells over a period of up to 11 days after plate bound culture with stimulating anti-CD3ε antibodies plus

recombinant B7.1 or ICAM-1 and up to 21 days after ip tumor challenge, respectively. I revealed distinct FasL and GrB expression patterns in activated $CD8^+$ T cells. My data indicates, in agreement with previous findings, a lower threshold of T cell activation requirement for FasL induction compared to GrB induction. I showed that while GrB expression is not maintained, FasL expression in activated $CD8^+$ T cells is sustained at least three weeks after allogeneic tumor challenge *in vivo*. During early responses to allogeneic tumor challenge, low quantity of antigen burden preferentially induces FasL expression over GrB expression in $CD8^+$ T cells. My results suggest that in activated $CD8^+$ T cells, expression of FasL and GrB may depend, at least partially, upon activation signal strength.

Results

Determining the amount of anti-CD3ε stimulating antibody for sub-optimum TCR stimulation

During T cell activation, co-stimulatory molecules enhance the activation signal provided through the TCR and determine the functional outcome of the activated T cell (35). To properly evaluate the contribution of co-stimulatory signal strength to intracellular FasL expression, I first needed to determine a sub-optimum level of anti-CD3ε antibody that would provide a sub-optimal TCR stimulation of naïve $CD44^{lo}$ $CD8^+$ T cells. Additionally, as my objective is not only to evaluate the role of co-stimulation on FasL expression, but also a comparison of intracellular FasL and GrB expression kinetics, the induction of GrB was used to determine the quantity of anti-CD3ε antibody required for sub-optimum TCR stimulation. A suitable level of sub-optimum TCR stimulation alone would induce a minimal proportion of GrB responding naïve $CD44^{lo}$ $CD8^+$ T cells with a strong augmentation of responding T cells in the presence of co-stimulatory molecules. Therefore, isolated naïve $CD44^{lo}$ $CD8^+$ T cells using commercially available negative isolation kits were stimulated in 24 well plates coated with varying concentrations of anti-CD3ε (0.1µg/ml ~0.5µg/ml)

alone or with 10nm of recombinant mouse ICAM-1 or B7.1. After two days of stimulation, which mimic previous findings of T-DC cell interactions in lymph nodes (213), the $CD8^+$ T cells were removed from the stimulating plate and allowed to rest in low level of recombinant IL-2, as a survival factor. The next day, intracellular expression of GrB was examined by flow cytometry.

Following stimulation and irrespective of the quantity of immobilized anti-CD3ε antibody, only 10~15% of stimulated $CD8^+$ T cells produced GrB and based on flow cytometry analysis, GrB production was very limited (Figure 3-1A). However, the addition of immobilized co-stimulatory molecule presentation strongly augmented GrB production in stimulated $CD8^+$ T cells. Co-immobilization of 10nm of ICAM-1 increased the percentage of GrB expressing $CD8^+$ T cells even at low TCR stimulation of 0.1μg/ml of anti-CD3ε antibody. Starting at 0.2μg/ml of anti-CD3ε levels, ICAM-1 co-stimulation enhanced GrB production in greater than 90% of stimulated $CD8^+$ T cells. Additionally, with higher TCR stimulation, ICAM-1 augmented not only the percentage of GrB expressing $CD8^+$ T cells, but also the quantity of GrB produced per cell as examined by flow cytometry (Figure 3-1 B). In contrast, B7.1 only weakly co-stimulated GrB production in $CD8^+$ T cells at lower levels of TCR stimulation and strongly at high levels of anti-CD3ε stimulation. An increasing trend of B7.1 co-stimulated GrB production and percent of GrB expressing $CD8^+$ T cells was observed with increasing TCR stimulation (Figure 3-1 C). The reduced production of GrB in B7.1 compared to ICAM-1 co-stimulated $CD8^+$ T cells, despite equimolar amounts of ICAM-1 and B7.1, suggests that ICAM-1 is a better co-stimulator of GrB expression. Since ICAM-1 was able to greatly enhance GrB production of 0.2μg/ml anti-CD3ε stimulated $CD8^+$ T cells, this concentration of TCR stimulating antibody was determined as the amount for sub-optimal TCR stimulation.

High levels of recombinant B7.1 and ICAM-1 do not reach saturating levels in 24 well plates

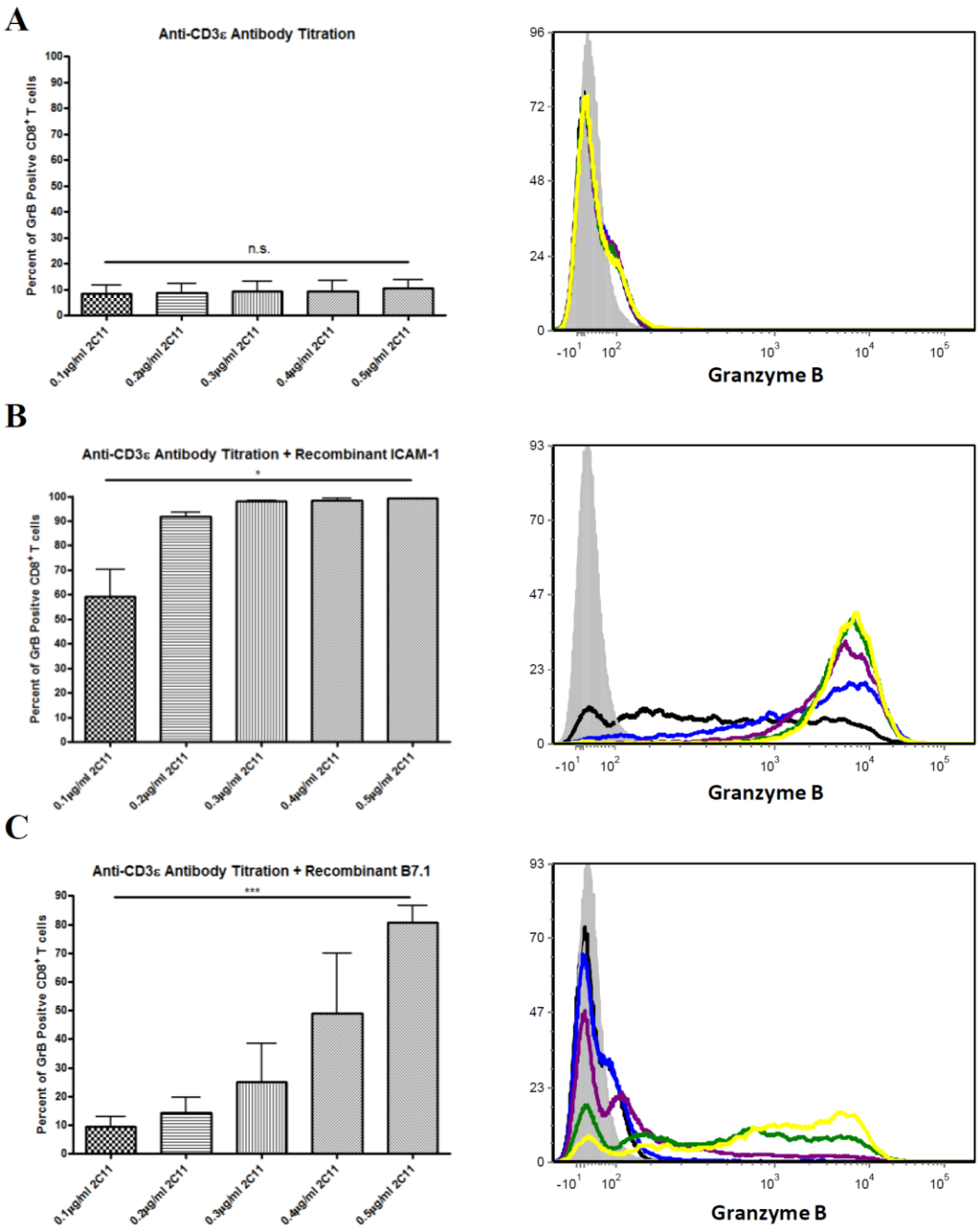

Figure 3-1: Determination of sub-optimum TCR stimulation.
Isolated naïve CD44^{lo} CD8^{+} T cells from spleen were stimulated in 24 well plates coated with 0.1µg/ml to 0.5 µg/ml of anti-CD3ε stimulating antibody (A) or plates coated with anti-CD3ε antibody plus 10nm of ICAM-1 (B) or B7.1 (C) for 48 hours.

On day two, the cells were transferred to a new 24 well plate with the addition of low levels of IL-2. The next day, GrB production was examined by flow cytometry. Histograms represent flow cytometry analysis of GrB production from cells stimulated with varying levels of anti-CD3ε stimulating antibody in the presence or absence of B7.1 or ICAM-1 co-stimulation: 0.1μg/ml (black), 0.2 μg/ml (blue), 0.3 μg/ml (purple), 0.4 μg/ml (green) and 0.5 μg/ml (yellow). Histograms represent one of three experiments. Statistical significance was determined using unpaired two-tailed t tests. Bar graph data represent mean ± SEM of three experiments.*$p<0.05$, ***$p<0.001$ and n.s. not significant.

Thus far, I have determined a suitable sub-optimum concentration of anti-CD3ε antibody (0.2μg/ml) for TCR stimulation of naïve $CD8^+$ T cells. To effectively evaluate the quantitative contributions of co-stimulatory molecules to intracellular FasL and GrB expression, varying levels of recombinant B7.1 or ICAM-1 were immobilized in the stimulating plates. Additionally, since ICAM-1 and B7.1 have differing levels of GrB co-stimulating effects (Figure 3-1), with ICAM-1 being a stronger co-stimulator of GrB production than B7.1, differing concentrations of low, medium and high levels of ICAM-1 (2.5nm, 5nm and 10nm) and B7.1 (10nm, 20nm and 30nm) were assessed. To ensure these concentrations do not exceed saturating binding levels and therefore potentially obscuring high level co-stimulatory effects to intracellular FasL and GrB production, the amounts of anti-CD3ε antibody, ICAM-1 and B7.1 coated 24 well plates with 2.5nm, 5nm or 10nm of ICAM-1, or 10nm, 20nm or 30nm of B7.1, plus 0.2μg/ml of anti-CD3ε antibody was determined by ELISA with ICAM-1 and B7.1 specific antibodies. Anti-hamster IgG was used to determine the level of anti-CD3ε binding also by ELISA.

The optical density (OD) values for low, medium and high levels of immobilized B7.1 and ICAM-1 co-stimulator ligands ranged from 1.0 to 2.0 and 0.3 to 0.7, respectively, with a continuous increase in the OD readings with increasing co-stimulator ligand concentration (Figure 3-2 A and B). Additionally, to ensure a consistent level of TCR stimulation, plate binding of anti-CD3ε stimulating antibody at the differing B7.1 and ICAM-1 co-stimulatory molecule concentrations was also assessed. Using anti-hamster IgG antibodies, I observed a relatively stable plate binding level of anti-CD3ε stimulating antibody at all concentrations of B7.1 and ICAM-1 with OD values between 0.5 to 0.6 (Figure 3-2 C and D). Collectively, these results demonstrate that B7.1 and ICAM-1 co-stimulatory molecule are immobilized in 24 well plates in a concentration dependent manner. Low, medium and high levels of B7.1 or ICAM-1 immobilization do not exceed saturating levels and presentation of TCR stimulating antibody remained relatively constant between all levels of B7.1 and ICAM-1 co-stimulation.

Low levels of B7.1 co-stimulation augment intracellular FasL expression

With sub-optimal TCR stimulating antibody and low, medium and high levels of B7.1 concentrations determined for GrB expression, I next sought to evaluate the quantitative effects of B7.1 co-stimulation on the kinetic expression of intracellular FasL compared to GrB in naïve $CD8^+$ T cells. Previous studies have suggested that CD28 co-stimulation of human $CD4^+$ T cells and mouse $CD8^+$ T cells, the T cell co-stimulatory partner of B7, may enhance FasL expression and apoptotic function (185, 212). However, neither of these studies examined the quantitative effects of B7.1 on the intracellular protein expression levels of FasL and GrB.

To investigate the contribution of B7.1 co-stimulation signal strength to intracellular FasL and GrB expression, I isolated naïve $CD44^{lo}$ $CD8^+$ T cells that were then activated with low, medium and high levels of B7.1 (10nm, 20nm and 30nm) in the presence of sub-optimum TCR stimulation for 48 hours, to allow for sufficient activation of $CD8^+$ T cells. On day two, stimulated $CD8^+$ T cells were removed from TCR and B7.1 co-stimulation and transferred to a new plate containing low level of IL-2, as a survival factor. Intracellular FasL and GrB expression in stimulated $CD8^+$ T cells were analyzed by flow cytometry starting on day three and every other day until day 11.

After transferring $CD8^+$ T cells from the stimulating plate, increases in the percent of GrB producing T cells was dependent on the quantity of B7.1 co-stimulation and time. With low levels of B7.1 co-stimulation, the percent of GrB expressing T cells steadily increased with 80% of the cultured $CD8^+$ T cells expressing GrB by day11. When co-stimulated with medium and high levels of B7.1, the percentage of GrB expressing T cells also increased over time, however, a more rapid increase was observed. Under medium and high levels of B7.1 co-stimulation, around 80% percent of $CD8^+$ T cells produced GrB by day seven and day five, respectively (Figure 3-3 A). At low levels of B7.1 co-stimulation, the percent of intracellular FasL expressing stimulated $CD8^+$ T cells increased steadily over time

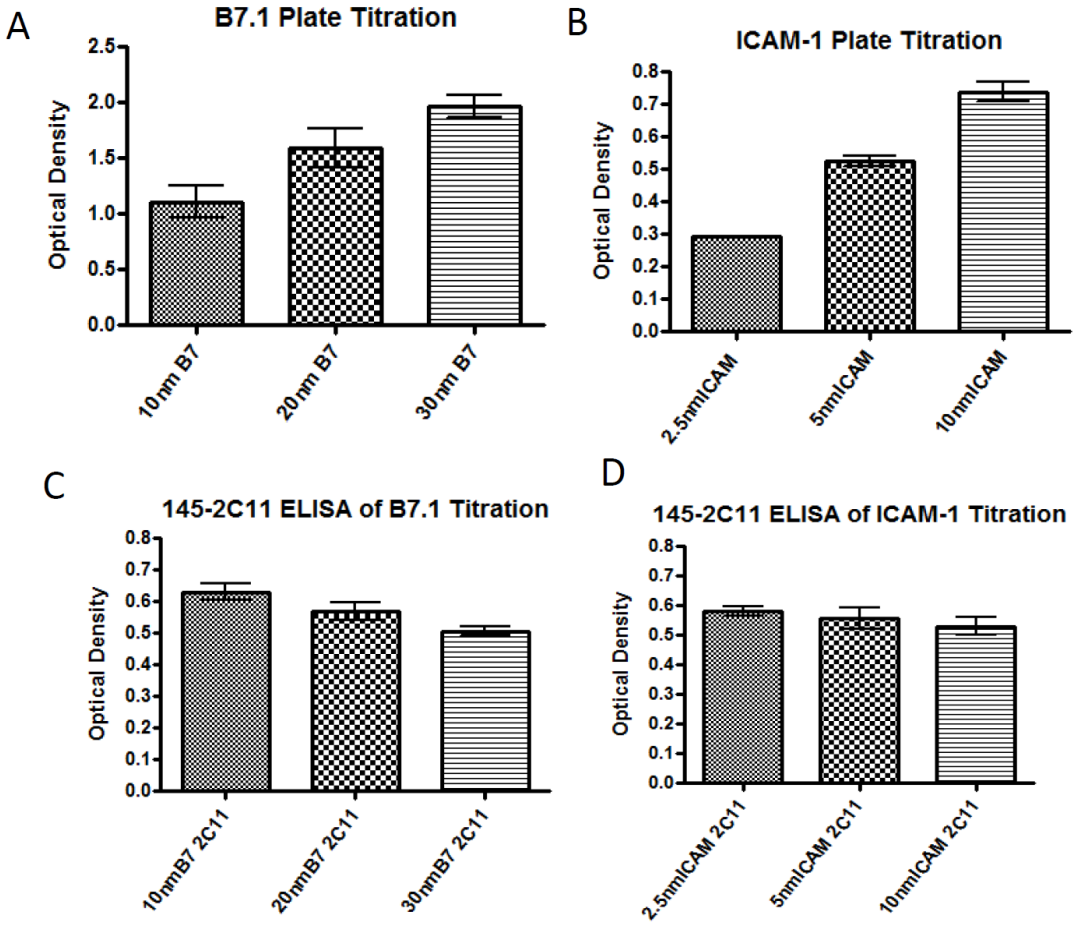

Figure 3-2: Recombinant B7.1 and ICAM-1 plate coating do not exceed plate binding saturation levels.

Twenty-four well plates were coated with 0.2 μg/ml of anti-CD3ε stimulating antibody plus 10nm, 20nm or 30nm of B7.1 or 2.5nm, 5nm or 10nm of ICAM-1 over night at 4^{o}C. The next day, excess unbound antibody and co-stimulatory molecules were washed out and unbound sites blocked with 2% BSA in PBS. The level of B7.1 (A) and ICAM-1 (B) presentation in the coated 24 well plates were determined by ELISA with antibodies that bind B7.1 and ICAM-1, respectively. Additionally, plate binding of anti-CD3ε antibody in the presence of 10nm, 20nm and 30nm of B7.1 (C) or 2.5nm, 5nm or 10nm ICAM-1 (D) in the 24 well plates was also measured by ELISA. Data represent average of two experiments. Error bars represent the OD value range of the two experiments.

from day three to day 11, similar to production of GrB (Figure 3-3 B). However, when co-stimulated with medium or high levels of B7.1, an initial increase in the percent of FasL expressing $CD8^+$ T cells was observed (Figure 3-3 B). On day five, I observed a peak in the percent of intracellular FasL expressing $CD8^+$ T cells which subsequently decreased steadily, after this time point (Figure 3-3 B). By day 11, over half of the $CD8^+$ T cells co-stimulated with low level of B7.1 were positive for intracellular FasL expression, whereby less than half of the medium and high B7.1 co-stimulated $CD8^+$ T cells expressed intracellular FasL (Figure 3-3 B). When examining intracellular FasL and GrB co-expression, under low level of B7.1 co-stimulation, I observed a steady increase in the proportion of intracellular FasL/GrB double expressing T cells through day 11. In contrast, when co-stimulated with medium and high levels of B7.1, on day seven, a substantial population of FasL/GrB double positive and GrB only expressing $CD8^+$ T cells were observed. The percentage of FasL/GrB expressing $CD8^+$ T cells, however, decreased gradually beyond day seven, resulting in the overall apparent loss of FasL expression in stimulated $CD8^+$ T cells (Figure 3-3 C). From these findings, it is possible that different B7.1 co-stimulatory signal strengths induce differential expression of intracellular FasL and GrB in $CD8^+$ T cells. Specifically, strong B7.1 co-stimulation favors a robust and sustained expression of GrB in stimulated $CD8^+$ T cells, whereas weaker B7.1 co-stimulation allow for a gradual and sustained expression of intracellular FasL and GrB in $CD8^+$ T cells.

Low levels of ICAM-1 co-stimulation sustain intracellular FasL expression

From the contrasting B7.1 co-stimulation results on FasL and GrB expression in $CD8^+$ T cells, I next wanted to examine the effects of another co-stimulatory molecule. ICAM-1 has previously been suggested to not only be an adhesion molecule during T cell activation, but also a co-stimulator ligand for $CD8^+$ T cell activation and also distinctly co-stimulates $CD8^+$ T cells independently of B7.1 (58, 62). Additionally, previous work in our laboratory has demonstrated that ICAM-1 is a

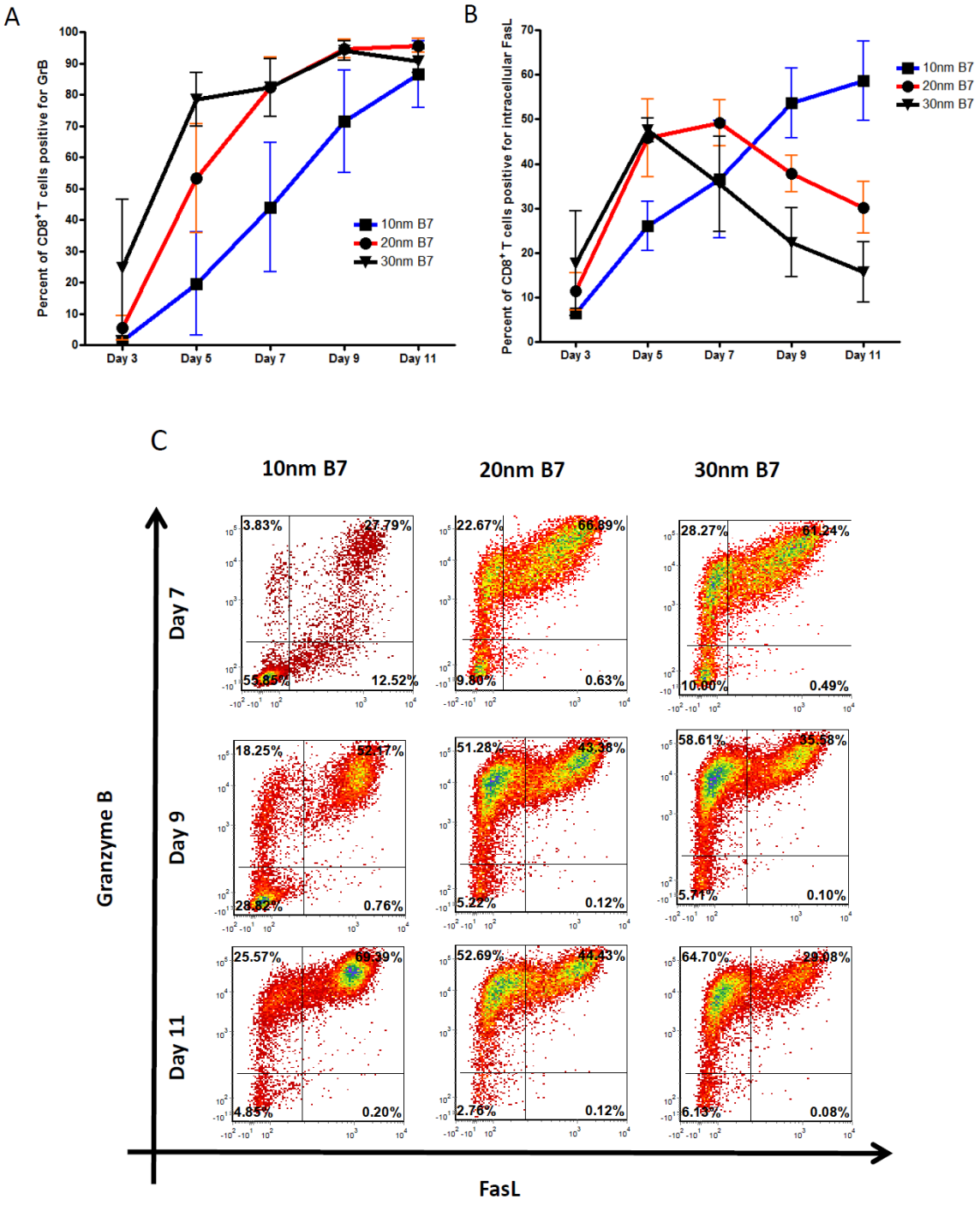

Figure 3-3: Differential production of granzyme B and intracellular FasL by activated CD8$^+$ T cells to increasing amounts of recombinant B7.1 co-stimulation. Isolated naïve CD44^{lo} CD8$^+$ T cells from spleen were stimulated in 24 well plates coated with 0.2µg/ml of anti-CD3ε antibody plus 10nm, 20nm or 30nm of recombinant B7.1 for 48 hours. On day two, the cells were transferred to a new plate

containing 5U/ml of IL-2. The percent of GrB positive $CD8^+$ T cells (A) or intracellular FasL positive $CD8^+$ T cells (B) was determined by flow cytometry on the indicated days. Data represent mean ± SEM of three experiments. A representative dot plot of three experiments of intracellular FasL and GrB staining of stimulated $CD8^+$ T cells on days 7, 9 and 11 is also shown (C).

more effective $CD44^{lo}$ $CD8^+$ T cell co-stimulator ligand than B7.1 in terms of cell proliferation and GrB induction (Dr. Hockley PhD thesis). Therefore, I next sought to examine the contributions of ICAM-1 to FasL and GrB production.

To investigate the role of ICAM-1 co-stimulatory signal strength to FasL and GrB expression, naive $CD44^{lo}$ $CD8^+$ T cells were co-stimulated with low, medium and high levels of plate bound ICAM-1 (2.5nm, 5nm or 10nm) in combination with sub-optimum amounts of immobilized anti-CD3ε crosslinking antibody for 48 hours. Following stimulation, the $CD8^+$ T cells were transferred to a new plate containing low levels of IL-2. Starting on day three, FasL and GrB expression was examined in the stimulated cells every other day until day 11. Under low level of ICAM-1 co-stimulation, similar to low level B7.1 co-stimulation, the percent of GrB expressing T cells increased continuously over time. By day 11, >80% of the cultured $CD8^+$ T cells expressed GrB. Comparatively, when co-stimulated with medium and high levels of ICAM-1, nearly all of the T cells expressed GrB by day five and, furthermore, the proportion of GrB positive T cells were maintained until day 11 (Figure 3-4 A). In contrast, over time, FasL production was not proportional to the amount of ICAM-1 available for co-stimulation. Similar to what I observed with B7.1 co-stimulation, low level of ICAM-1 stimulation induced and sustained FasL expression in roughly 40%~50% of stimulated $CD8^+$ T cells from day three to day 11. With medium and high levels of ICAM-1 co-stimulation, a maximum of between 40%~50% of stimulated $CD8^+$ T cells expressed FasL on day five. Beyond day five, the percent of FasL expressing T cells gradually decreased over time (Figure 3-4 B). When examined together, similar to what I observed with low level of B7.1 co-stimulation, low level of ICAM-1 co-stimulation augmented a sustained increase in FasL/GrB double expressing $CD8^+$ T cells. In contrast, a substantial population of T cells co-stimulated with medium and high levels of ICAM-1expressed FasL and GrB or GrB only by day seven. However, beyond day seven, FasL/GrB expressing $CD8^+$ T cells gradually lost expression of FasL resulting in an increase in the proportion of GrB only expressing $CD8^+$ T cells (Figure 3-4 C). Collectively, these results suggest that,

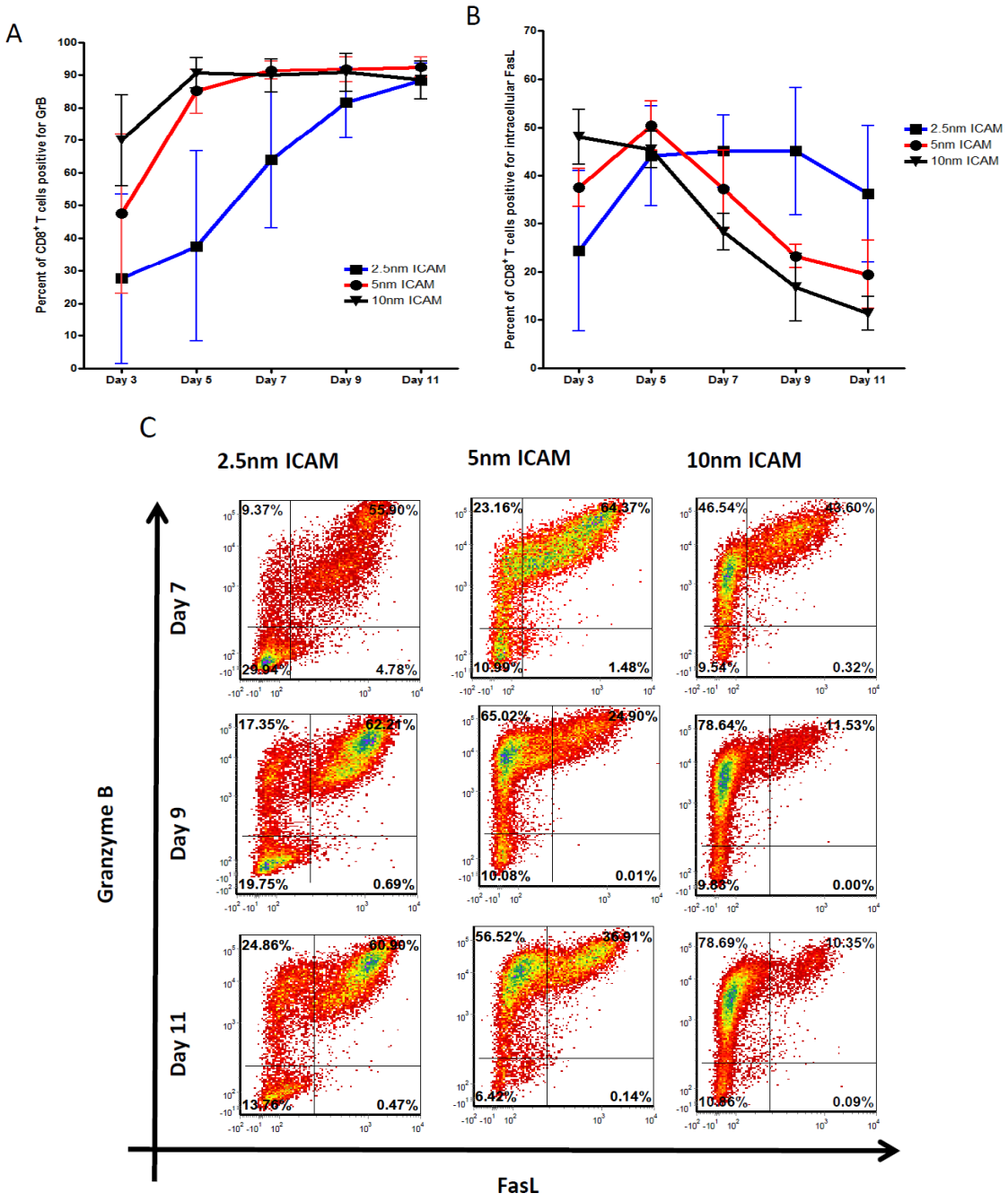

Figure 3-4: Differential production of granzyme B and intracellular FasL by activated CD8$^+$ T cells to increasing amounts of recombinant ICAM-1 co-stimulation.

Isolated CD44^{lo} CD8$^+$ T cells from spleen were stimulated in 24 well plates coated with 0.2ug/ml of anti-CD3ε antibody and 2.5nm, 5nm or 10nm recombinant

ICAM-1 for 48 hours. On day two, the cells were transferred to a new plate containing 5U/ml of IL-2. The percent of GrB positive $CD8^+$ T cells (A) or intracellular FasL positive $CD8^+$ T cells (B) was determined by flow cytometry on the indicated days. Data represent mean ± SEM of three experiments. A representative dot plot of three experiments of intracellular FasL and GrB on days 7, 9 and 11 is also shown (C).

much like what was observed with B7.1 co-stimulation, strong ICAM-1 co-stimulation augmented a rapid expression of FasL and GrB in stimulated $CD8^+$ T cells, however, only GrB expression was maintained over time. In contrast, weak ICAM-1 co-stimulation allowed for a more gradual increase in GrB complemented with a sustained expression of FasL.

Sustained T_{eff} $CD8^+$ T cell response to allogeneic tumor challenge

Thus far I have demonstrated differential FasL and GrB expression kinetics depending on the degree of B7.1 or ICAM-1 co-stimulation *in vitro*. Additionally, FasL mediated tumor responses have previously been suggested to be pivotal in tumor surveillance, clearance, controlling tumor metastasis and relapse (166, 167, 182, 212, 214). Additionally, a number of tumors have been shown to up-regulate Fas surface expression following pro-inflammatory cytokine stimulations such as IFNγ and upon *in vivo* injection (166, 168, 181, 182). From these studies, I utilized injections of allogeneic tumor cells to examine the expression kinetics of FasL and GrB in activated $CD8^+$ T cells *in vivo*. A similar system had previously been employed but was limited in that only mRNA levels of FasL was examined (211).

For allogeneic stimulations, C57BL/6 ($H\text{-}2^b$) mice were ip injected with $25x10^6$ P815 ($H\text{-}2^d$) mastocytoma cells, a quantity commonly used to examine T cell responses to tumor cell injections (181, 211, 215). Peritoneal-exudate lymphocytes (PEL) were then isolated by intraperitoneal lavage with PBS and $CD8^+$ T cells, as defined by $CD8^+$ $CD3^+$ cells, were examined by flow cytometry. To effectively determine the kinetic patterns of FasL and GrB expression in activated $CD8^+$ T cells, I first sought to characterize the $CD8^+$ T cell response in the peritoneum after tumor challenge. As the peak of $CD8^+$ T cell responses occur between eight to ten days after stimulation *in vivo* (156), I examined $CD8^+$ T cells in the peritoneal cavity from eight to 21 days post injection. The percentage, recovered numbers of $CD8^+$ T cells and percent of activated $CD8^+$ effector T cells (T_{eff}), characterized by a surface phenotype of $CD44^{hi}CD62L^{lo}$ (216), among the total $CD8^+$ T cell population were examined. As

early as day eight, both the percent and number of infiltrating $CD8^+$ T cells increased dramatically after tumor injection (Figure 3-5 A & B). $CD8^+$ T cells represented over half of the PEL population by day 11 and numbered over $10x10^6$ cells by day eight (Figure 3-5 A & B). By day 21, $CD8^+$ T cells still numbered roughly $1x\ 10^6$ cells and accounted for close to 35% of all PELs (Figure 3-5 A& B). While these represent a significant decrease in terms of cell numbers and representation among the PEL population from the peak observed on day eight and 11, these findings still represent a significant increase in overall $CD8^+$ T cell representation when compared to day zero (Figure 3-5 A & B). Additionally, nearly all $CD8^+$ T cells examined in the peritoneal cavity between day eight and day 21 post-injection were of an activated $CD44^{hi}$ $CD62L^{lo}$ T_{eff} phenotype (Figure 3-5 C). Importantly, there was no significant difference in the proportion of $CD8^+$ T_{eff} observed on day eight to day 21 (Figure 3-5 C). Collectively, my results suggest that $CD8^+$ T cells respond robustly to an allogeneic tumor challenge, demonstrated by an increased number of infiltrating $CD8^+$ T cells, representation and level of $CD8^+$ T_{eff}. Additionally, the $CD8^+$ T cells response to P815 is sustained over a period of three weeks. With this prolonged $CD8^+$ T cell response, injection of allogeneic tumor cells is ideal for evaluating the long term relationship between intracellular FasL and GrB expression in $CD8^+$ T_{eff} cells *in vivo*.

T_{eff} $CD8^+$ T cells express intracellular FasL and granzyme B early following injection but lose granzyme B expression over time

To induce $CD8^+$ T_{eff} cells *in vivo*, mice were ip injected with $25x10^6$ P815 cells, as previously described. Every other day starting eight days post-injection until day 21, PEL $CD8^+$ T_{eff} cells were identified as $CD44^{hi}CD62L^{lo}$ $CD8^+$ T cells. The expression kinetics of intracellular FasL and GrB in $CD8^+$ T_{eff} cells were then examined by flow cytometry.

On day eight post-P815 challenge, nearly all of the $CD8^+$ T_{eff} cells expressed GrB. However, beyond day eight, I observed a steady and consistent decrease in the

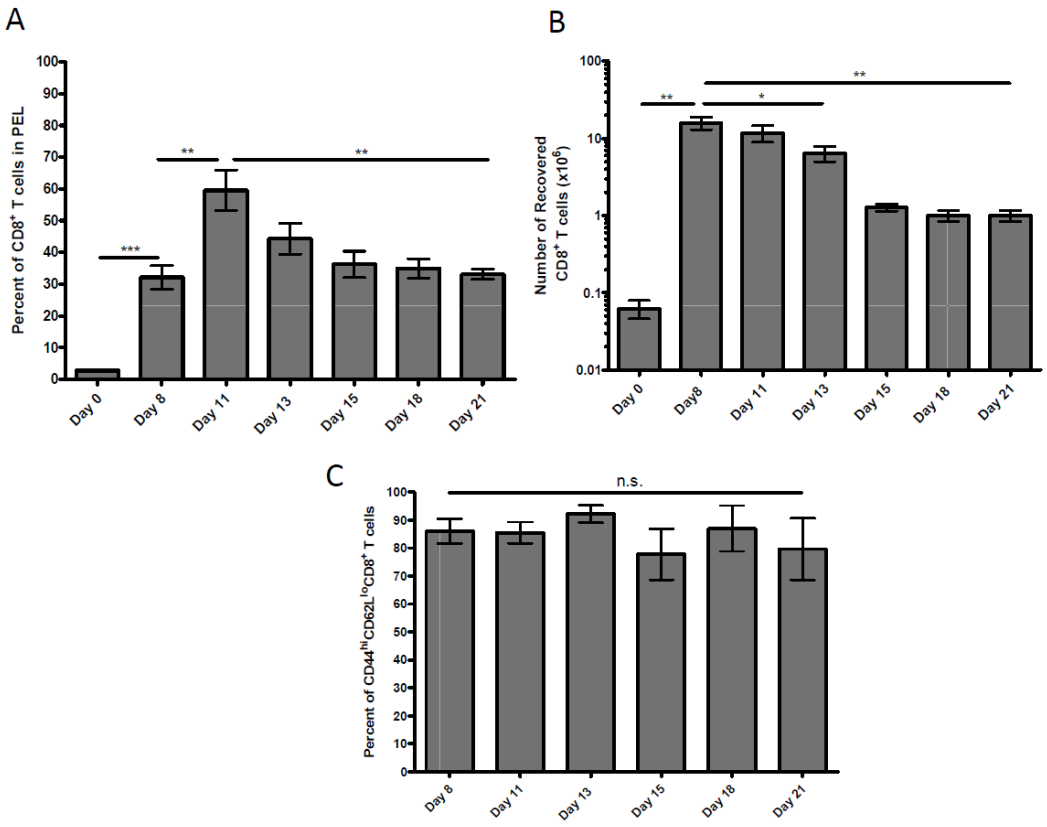

Figure 3-5: Sustained PEL CD8$^+$ T cell response to allogeneic P815 injection. C57BL/6 mice were ip injected with 25x10^6 P815 on day zero. On days 8, 11, 13, 15, 18 and 21 after injection, the percent of CD8$^+$ T cells in the total PEL population (A), total numbers of CD8$^+$ T cells (B) and percent of PEL CD8$^+$ T_{eff} cells (CD44^{hi}CD62L^{lo}) in peritoneum (C) were determined by flow cytometry. The total number of CD8$^+$ T cells in the peritoneum lavage was calculated based on hemocytometer cell counts and the percentage of CD8$^+$ T cells determined by flow cytometry. Bar graphs represent mean ± SEM of three experiments with at least three mice per indicated day. Statistical significance was determined using unpaired two-tailed t tests. *p<0.05, **p<0.01, ***p<0.001 and n.s. not significant.

percentage of GrB positive $CD8^+$ T_{eff} cells. By day 21, only 10% of $CD8^+$ T_{eff} cells expressed detectable levels of GrB (Figure 3-6 A). In contrast, about half of the $CD8^+$ T_{eff} cells present in the PEL expressed detectable levels of intracellular FasL on day eight, but this percentage of FasL expressing $CD8^+$ T_{eff} was maintained until day 21 (Figure 3-6 B).

When examined for co-expression of FasL and GrB, nearly all $CD8^+$ T_{eff} cells on day eight were positive for GrB, but only about half of these cells also expressed FasL (Figure 3-7 A). By day 13 distinct GrB positive and negative populations of $CD8^+$ T_{eff} cells were observed, and by day 21, the vast majority of recovered $CD8^+$ T_{eff} cells did not express detectable levels of GrB (Figure 3-7 A). Interestingly, expression level of FasL and the percentage of FasL positive PEL $CD8^+$ T_{eff} cells remained relatively elevated over the various post-injection time points (Figure 3-7 A). As the $CD8^+$ T_{eff} cells gradually lost expression of GrB, I observed a significant decrease in percentage of FasL/GrB double expressing and GrB only expressing $CD8^+$ T_{eff} cells (Figure 3-7 B and C). In contrast, the proportion of FasL only expressing $CD8^+$ T_{eff} cells increased significantly over the same three week time period (Figure 3-7 D).

Collectively, these findings suggest differential expression kinetics between FasL and GrB in *in vivo* T_{eff} $CD8^+$ T cells. My findings complement previous FasL mRNA studies that suggest *in vivo* $CD8^+$ T_{eff} cells switch from a degranulation/FasL dependent response during early stages to a FasL dependent late stage response following an allogeneic tumor cell challenge (211). Of note, my results demonstrated that FasL protein is expressed at relatively consistent levels during all time points examined, whereas GrB is only expressed in high percentages of $CD8^+$ T_{eff} cells during the early stages of the tumor cell challenge.

Ex vivo killing assay using day 21 peritoneal exudate lymphocytes

Thus far I have demonstrated a sustained $CD8^+$ T_{eff} cell response to ip injection of P815 tumor cells. Additionally, *in vivo* response of $CD8^+$ T_{eff} cells to the

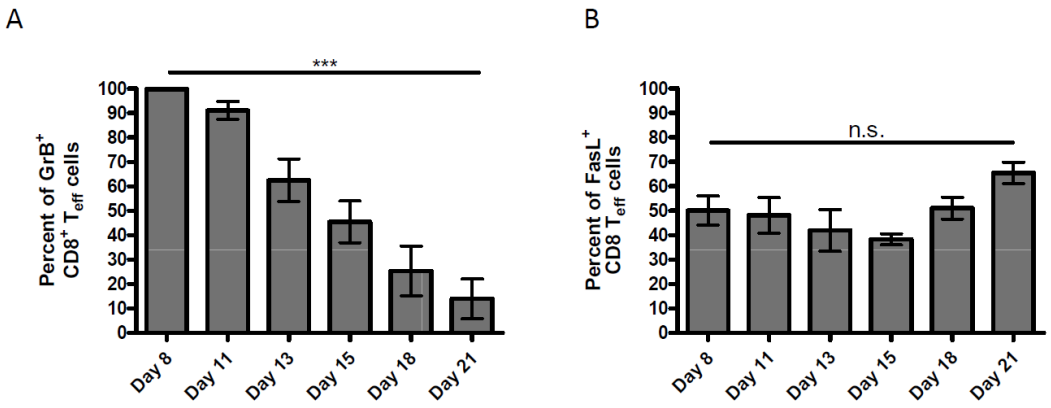

Figure 3-6: Sustained intracellular FasL expression in activated PEL CD8$^+$ T cells to P815 injection.
C57BL/6 mice were ip injected with 25x10^6 P815 on day zero. On days 8, 11, 13, 15, 18 and 21 after injection, the percent of GrB positive (A) and intracellular FasL positive (B) PEL CD8$^+$ T$_{eff}$ cells were determined by flow cytometry. Data represent mean ± SEM of three experiments with at least three mice per day. Statistical significance was determined using unpaired two-tailed t tests. ***p<0.001 and n.s. not significant.

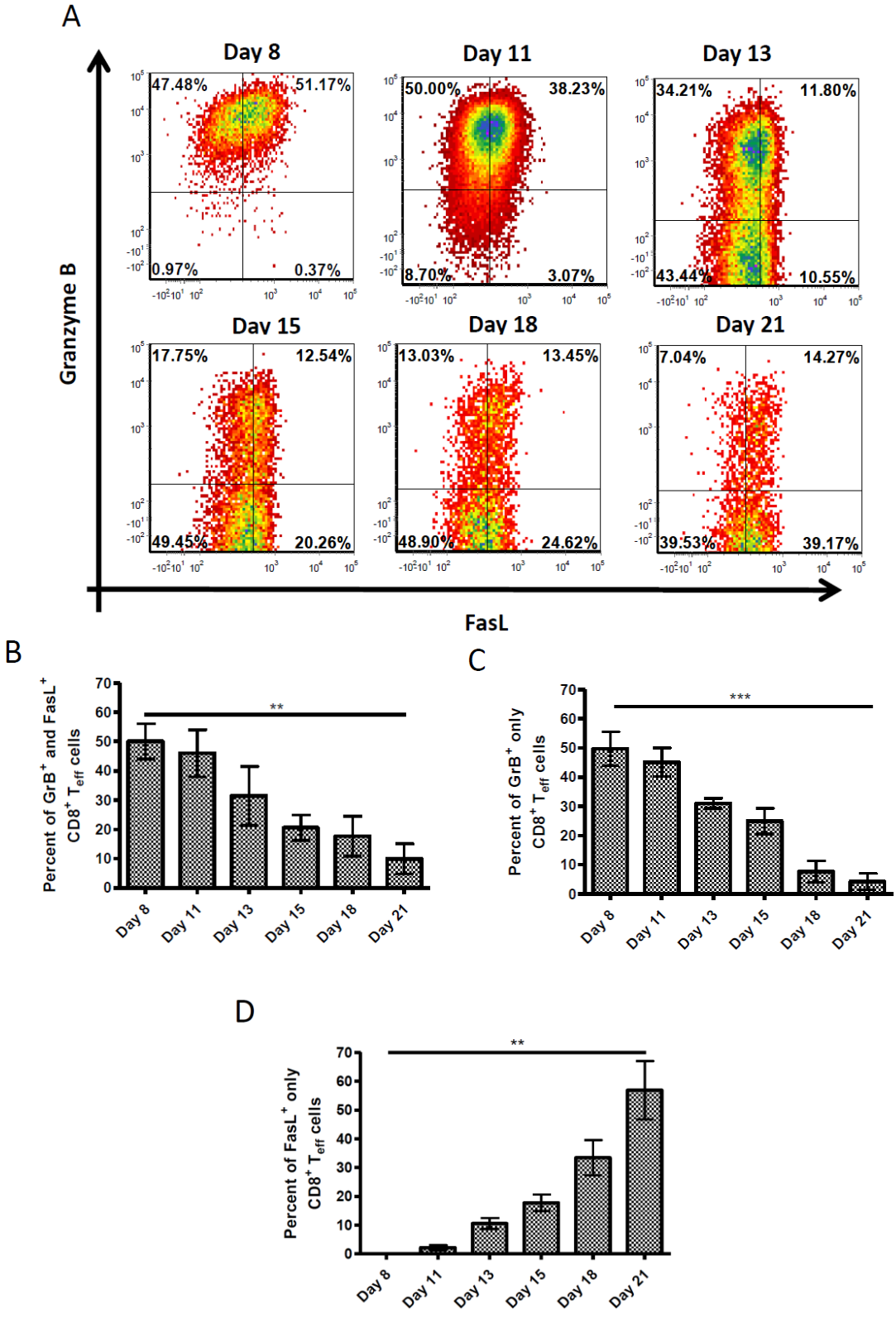
A
Day 8
47.48%
51.17%
0.97%
0.37%
Day 11
50.00%
38.23%
8.70%
3.07%
Day 13
34.21%
11.80%
43.44%
10.55%
Day 15
17.75%
12.54%
49.45%
20.26%
Day 18
13.03%
13.45%
48.90%
24.62%
Day 21
7.04%
14.27%
39.53%
39.17%
Granzyme B
FasL
B
Percent of GrB+ and FasL+ CD8+ Teff cells
**
Day 8
Day 11
Day 13
Day 15
Day 18
Day 21
C
Percent of GrB+ only CD8+ Teff cells
***
D
Percent of FasL+ only CD8+ Teff cells
**

Figure 3-7: Gradual loss of granzyme B in activated PEL CD8$^+$ T cells to P815 injection over time.
C57BL/6 mice were ip injected with 25x10^6 P815 on day zero. On days 8, 11, 13, 15, 18 and 21 after injection, PEL CD8$^+$ T_{eff} cells were analyzed for expression of intracellular FasL and GrB. A representative staining of intracellular FasL and GrB in CD8$^+$ T_{eff} cells on the indicated days is shown (A). The percent of T_{eff} CD8$^+$ T cells expressing both intracellular FasL and GrB (B), intracellular GrB only (C) or intracellular FasL only is also shown (D). Data represent mean ± SEM of three experiments with a total of at least three mice per day in B, C and D. Statistical significance was determined using unpaired two-tailed t tests. ** $p<0.01$ and ***$p<0.001$.

allogeneic tumor challenge can be observed for at least 21 days post-injection. Interestingly, after three weeks, the majority of $CD8^+$ T_{eff} cells did not have detectable levels of GrB, however, a considerable proportion of $CD8^+$ T_{eff} cells maintained detectable levels of FasL. From this finding, I next sought to evaluate the FasL dependent effector function capabilities of $CD8^+$ T_{eff} cells present during the later stages of an allogeneic response to tumor cells.

As previously described, $25x10^6$ P815 cells (H-2^d) were injected into C57BL/6 mice (H-2^b). On day 21, PELs were isolated and used as effector cells for an *ex vivo* killing assay. For target cells, I used L1210 and Fas transfected L1210 cells (Fas.L1210), both MHCI H-2^d haplotype tumor cells. L1210 cells do not naturally express Fas receptor, whereas Fas.L1210 cells have detectable levels of Fas receptor expression on the cell surface (Figure 3-8 A). To distinguish between effector PELs and target cells, effector cells were labeled with CFSE while target cells were not labeled. Additionally, effector PELs were incubated with or without EGTA/$MgCl_2$ in PBS for 30 minutes, to chelate extracellular Ca^{2+}, prior to culture with L1210 or Fas.L1210 target cells and during the four hour killing assay. The presence of extracellular Ca^{2+} has previously been demonstrated to be essential for degranulation but not intracellular pre-stored FasL mediated effector function of $CD8^+$ T cells (161, 208, 209). Delivery of the lethal hit of FasL by effector $CD8^+$ T cells on Fas expressing target cells activates caspase 3 (11). As such, to determine L1210 and Fas.L1210 killing, the presence of active caspase 3 in the target cells was examined by flow cytometry, as previously established (161, 217).

After a four hour incubation of target and PEL effector cells at an E:T ratio of 10:1, as expected, none of the L1210 target cells stained positive for active caspase 3, regardless of the presence or absence of EGTA/$MgCl_2$ (Figure 3-8 B). In contrast, a small but noticeable population of Fas.L1210 target cells stained positive for active caspase 3 when incubated with PEL effector cells, regardless of presence or absence of EGTA/$MgCl_2$ (Figure 3-8 B). Collectively, these findings suggest that while nearly all the $CD8^+$ T_{eff} cells three weeks after H-2^d allogeneic tumor challenge do not

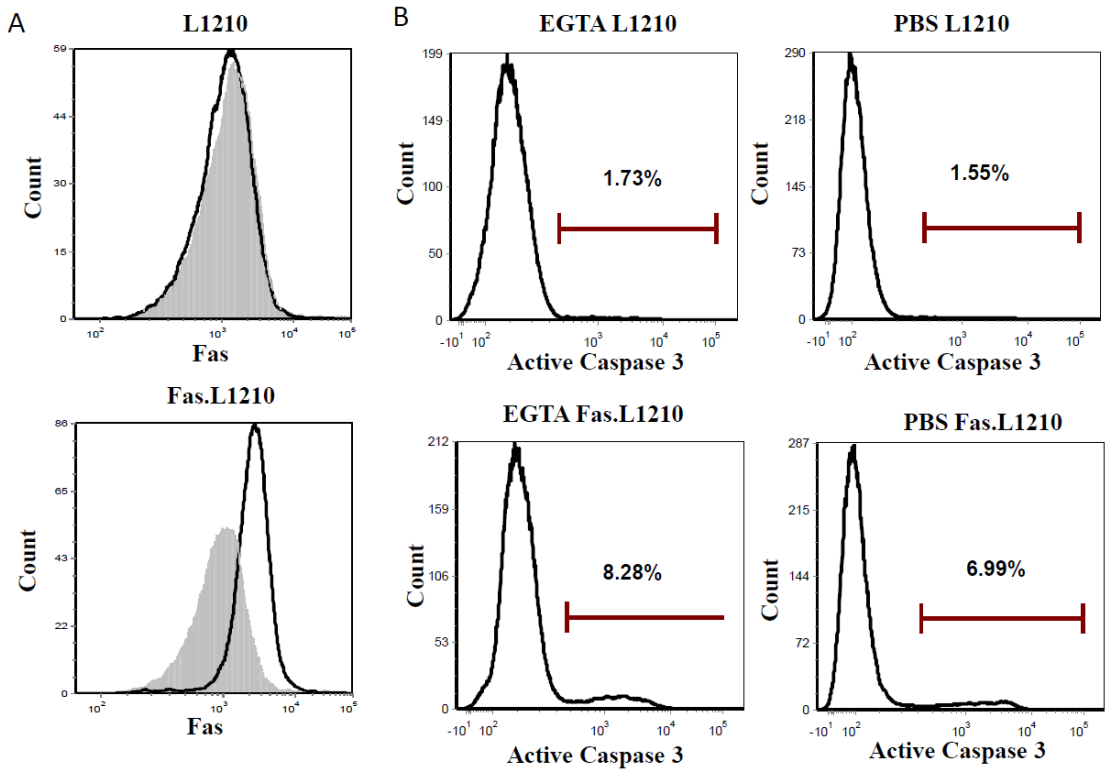

Figure 3-8: T_{eff} $CD8^+$ T cells three weeks post P815 injection kill *ex vivo* targets via FasL.

Mice were ip injected with $25x10^6$ P815 cells on day zero. On day 21, PEL were isolated and pre-incubated with PBS or PBS containing EGTA/Mg_2Cl for 30 minutes and labeled with CFSE and used as effector cells. L1210 and Fas.L1210 cells were used as target cells. Cell surface expression of Fas on L1210 and Fas.L1210 cells was examined by flow cytometry (A). Effector to target cells of 10:1 were incubated for 4 hours at 37°C in the presence or absence of EGTA/Mg_2Cl. Percentage killing of CFSE negative target cells was assessed via intracellular staining for active caspase 3 by flow cytometry (B). Histograms are representatives of one of two experiments. Shaded histograms represent isotype staining control.

express detectable levels of GrB, these $CD8^+$ T_{eff} cells are still able to lyse allogeneic Fas-expressing H-2^d target cells, albeit to a low degree. Furthermore, my results also suggest that the *ex vivo* killing of target cells was dependent on FasL expression by $CD8^+$ T_{eff} cells and not the degranulation pathway as killing was only seen in Fas.L1210 cells. As expected, *ex vivo* FasL mediated killing by activated $CD8^+$ T_{eff} cells was also found to be extracellular Ca^{2+} independent.

Reduced P815 tumor dose induces a sub-maximum $CD8^+$ T cell response

Thus far, I have demonstrated distinct FasL and GrB expression kinetics in *in vivo* $CD8^+$ T_{eff} cells following allogeneic tumor challenge. In accordance with previous findings, FasL and degranulation dependent effector molecules are expressed during early stages of $CD8^+$ T_{eff} cells response to an allogeneic tumor cell challenge, however, as the immune response progresses, $CD8^+$ T_{eff} cell shift to primarily FasL expression (211). This shift in effector molecule expression has been proposed to be driven by antigen availability, as lower levels of allogeneic antigen are expected during later, rather than early, stages of the tumor challenge (211). Several other groups have also suggested that FasL mediated immune response or surveillance is more pronounced under lower $CD8^+$ T cell stimulating conditions (171, 210, 212). Therefore, I next sought to further define the effect of antigen quantity on FasL and GrB expression. Specifically, how reduced allogeneic tumor cell injections influences the expression of FasL and GrB in $CD8^+$ T_{eff} cells. I hypothesized that with a lower P815 challenge dose, antigen availability will be limiting and result in sub-maximum response from $CD8^+$ T cells in the peritoneal cavity and a bias, perhaps, toward FasL expression.

I first examined the $CD8^+$ T cell response to lower levels of allogeneic tumor cells. Mice were therefore injected ip with titrated doses of P815 cells ranging from $0.02x10^6$ to $2.5x10^6$ cells on day zero. On day eight, the $CD8^+$ T cell response was assessed in terms of infiltrating cell numbers, percentage among total PEL population and also the percentage of $CD8^+$ T_{eff} among $CD8^+$ T cells found in the peritoneal

cavity. As expected, with a low P815 injection dose ($0.02x10^6$), a significantly lower presence of $CD8^+$ T cells were found in the peritoneum as compared to higher P815 injection doses ($2.5x10^6$). These differences were observed when comparing total infiltrating $CD8^+$ T cell numbers, roughly $1x10^6$ compared to $10x10^6$ $CD8^+$ T cells, as well as proportion of $CD8^+$ T cells found among total PELs, approximately 10% compared to 25% (Figure 3-9 A & B). Additionally, among the responding $CD8^+$ T cells in the peritoneum, I observed a significantly lower percentage of $CD8^+$ T_{eff} cells among total $CD8^+$ T cells in mice challenged with lower rather than higher doses of P815. Only about 50% of the total $CD8^+$ T cell population in the peritoneum was of T_{eff} $CD44^{hi}CD62L^{lo}$ phenotype in $0.02x10^6$ P815 injected mice. In contrast, at higher doses of P815 injection ($2.5x10^6$), over 90% of $CD8^+$ T cells in the peritoneum were $CD8^+$ T_{eff} cells (Figure 3-9 C and D). Collectively, these results demonstrate that by reducing the dose of P815 injected, a sub-maximum state of $CD8^+$ T cell response can be induced in the peritoneal cavity. Importantly, this experimental setup allowed me to examine how antigen availability from the quantity of tumor cell injection influences the expression patterns of FasL and GrB in responding $CD8^+$ T_{eff} cells.

Intracellular FasL expression requires a lower antigen dose than granzyme B

Using the titrated P815 injection doses described above, I next examined the expression pattern of intracellular FasL and GrB in $CD8^+$ T_{eff} cells in the peritoneum eight days post-injection. At low doses of P815 injection ($0.02x10^6$), while only half of the responding $CD8^+$ T cells are of effector phenotype (Figure 3-9 C), approximately only half of the $CD8^+$ T_{eff} cells expressed detectable levels of GrB. As expected, at high doses, the percentage of GrB positive $CD8^+$ T_{eff} cells increased. At an injection dose of $2.5x10^6$ P815 cells, over 90% of $CD8^+$ T_{eff} cells expressed GrB (Figure 3-10 A). In contrast, roughly 75% of $CD8^+$ T_{eff} cells expressed FasL eight days following low level of P815 injection. When the injection dose of P815 cells was increased to $0.1x10^6$ cells, nearly 90% of the $CD8^+$ T_{eff} cells in the peritoneum

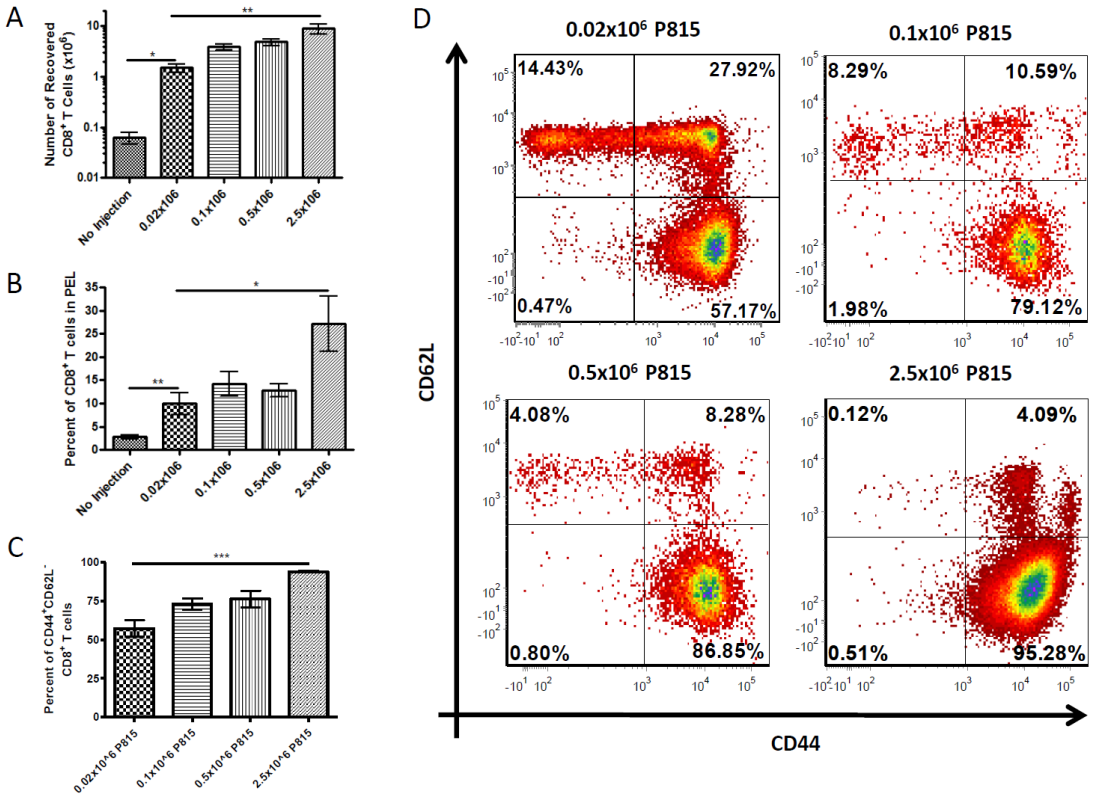

Figure 3-9: Sub-maximum PEL CD8$^+$ T cell response to lower P815 injection. C57BL/6 mice were ip injected with 0.02, 0.1, 0.5 or 2.5x10^6 P815 cells on day zero. On day eight, the total number (A) and percent of CD8$^+$ T cells (B) in PEL of day zero mice or day eight mice receiving the indicated tumor doses are shown. The proportion of PEL CD8$^+$ T_{eff} cells among total CD8$^+$ T cells (C) and a representative dot plot of CD44 and CD62L staining of CD8$^+$ T cells from mice injected with P815 eight days prior are shown (D). Data represent mean ± SEM of at least three experiments with a total of at least three mice per day in A, B and C. Statistical significance was determined using unpaired two-tailed t tests. *p<0.05** p<0.01 and ***p<0.001.

expressed detectable levels of FasL. Additionally, there was no significant difference in the percent of FasL positive $CD8^+$ T_{eff} in mice treated with 0.1, 0.5 or $2.5x10^6$ P815 cells on day eight (Figure 3-10 B). When co-expression of FasL and GrB were examined, at low doses of tumor challenge ($0.02x10^6$), half of the $CD8^+$ T_{eff} cells expressed both FasL and GrB with a substantial population of FasL only expressing $CD8^+$ T_{eff} cells. Additionally, as the injection dose increases, a diminished proportion of FasL only and increased FasL/GrB double expressing $CD8^+$ T_{eff} cells was observed (Figure 3-10 C). There was a significant increase in the percentage of FasL/GrB double expressing and decrease in FasL only expressing $CD8^+$ T_{eff} cells in mice exposed to 0.02 or $2.5x10^6$ P815 cells, respectively (Figure 3-10 D).

Collectively, my results suggest that in circumstances of limiting antigen availability, expression of FasL, is more pronounced in $CD8^+$ T_{eff} cells, compared to a strong antigen challenge. Previous studies have also suggested a lower antigen threshold of FasL expression and function than GrB (171, 210, 212). However, none of these studies had compared the expression levels of intracellular FasL and GrB from *in vivo* stimulated $CD8^+$ T cells. My data demonstrates that at low P815 doses, a higher percentage of $CD8^+$ T_{eff} cells express FasL than GrB. Additionally, my results also suggest that a lower antigen burden level may be more optimal for $CD8^+$ T_{eff} expression of FasL compared to GrB *in vivo*. It would seem that under very low levels of activation signal strength, activated $CD8^+$ T cells preferentially utilize FasL over degranulation mediated immunity, as previously postulated (210).

Summary

In this chapter, I examined the expression patterns of intracellular FasL and GrB in *ex vivo* and *in vivo* stimulated $CD8^+$ T cells. The results suggest that FasL expression dose not correlate with GrB expression in activated $CD8^+$ T cells. While activation does induce the expression of both effector molecules, strong activation signal strength seems to favor a rapid and robust expression of GrB. In contrast, $CD8^+$

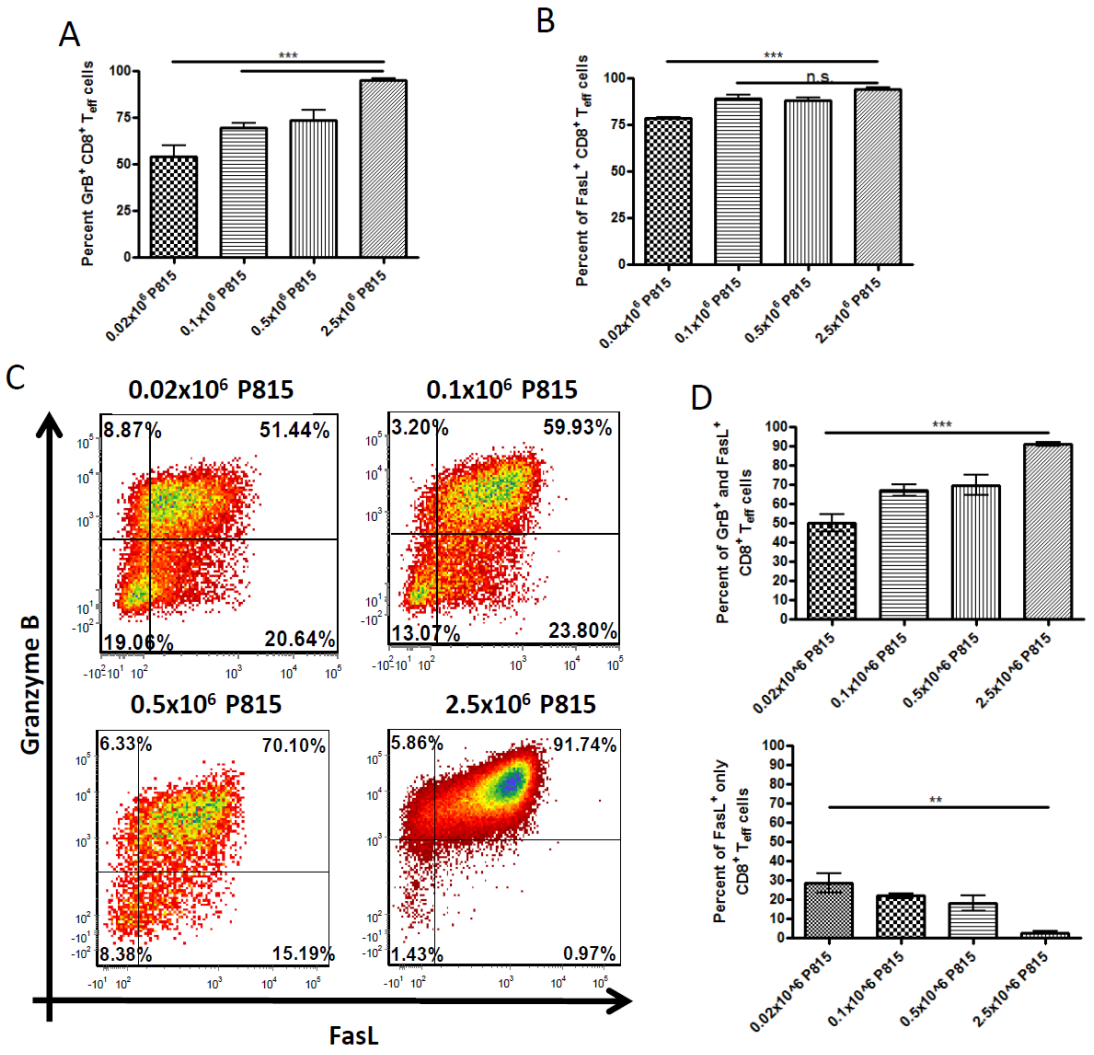

Figure 3-10: Intracellular FasL expression in T_{eff} $CD8^+$ T cells require a lower P815 stimulation dose than granzyme B.

C57BL/6 mice were ip injected with 0.02, 0.1, 0.5 or $2.5x10^6$ P815 cells on day zero. On day eight, intracellular GrB and FasL expression in PEL $CD8^+$ T_{eff} cells were examined by flow cytometry. The percent of GrB expressing (A) and intracellular FasL expressing (B) T_{eff} $CD8^+$ T cells are shown. A representative dot plot of intracellular GrB and FasL staining of PEL $CD8^+$ T_{eff} cells from day eight P815 injected mice are shown (C). In addition, the percent of PEL $CD8^+$ T_{eff} cells positive for both intracellular FasL and GrB or intracellular FasL only (D) are also shown. Data represent mean ± SEM of three experiments with a total of at least three mice per day in A, B and D. Statistical significance was determined using unpaired two-tailed t tests. ** $p<0.01$, ***$p<0.001$ and n.s. not significant.

T cells seem to favor FasL expression over GrB expression in situations of weak activation signal strength. Using knock-out mice models, several groups have suggested the importance of FasL during low level antigen stimulation situations against tumor and viral infections (165, 210, 218).

From the *ex vivo* experiments, I observed that both medium and high levels of both B7.1 and ICAM-1 co-stimulation induce a robust GrB response in stimulated $CD8^+$ T cells, however, FasL expression, while induced early following T cell activation, is not sustained over time. Low levels of both B7.1 and ICAM-1, while augmenting GrB expression more slowly than higher levels of co-stimulation, induced a sustained expression of FasL in stimulated $CD8^+$ T cells. Additionally, since no difference in FasL expression patterns were observed between B7.1 and ICAM-1, it is possible that either co-stimulation with B7.1 and ICAM-1 results in a similar kinetic induction of FasL or that neither B7.1 nor ICAM-1 specifically amplify FasL expression. It would therefore be interesting to examine additional co-stimulatory molecules for their potential effect on FasL expression in activated $CD8^+$ T cells. However, these *ex vivo* stimulating results suggest a positive correlation between collective activation signal strength and expression of GrB in stimulated $CD8^+$ T cells, while maintenance of FasL expression is inversely correlated with initial activation signal strength.

My *in vivo* examination of $CD8^+$ T_{eff} cells also suggested a similar correlation between activation signal strength and FasL and GrB expression. Shortly after challenge with high numbers of allogeneic tumor cells, nearly all infiltrating $CD8^+$ T_{eff} cells were high expressers of GrB. In contrast, about half of the infiltrating $CD8^+$ T_{eff} cells expressed detectable levels of FasL. Over a three week period, as tumor immunity progresses, presumably decreasing tumor antigen availability, GrB production and the proportion of GrB expressing $CD8^+$ T_{eff} cells decline significantly. In contrast, FasL production and expression among $CD8^+$ T_{eff} cells remained relatively constant throughout. These findings are reminiscent of a previous study examining mRNA levels of degranulation dependent perforin and FasL in tumor

injected mice (211). Here, Meiraz *et al.* ultimately concluded that during late stages of a tumor immune response by $CD8^+$ T cells, a switch from degranulation/FasL mediated immunity to largely FasL dependent was a result of reduced tumor antigen availability (211). Interestingly, when I examined the effects of very low doses of tumor cell challenge, a higher percentage of FasL than GrB expressing $CD8^+$ T_{eff} cells were observed eight days post injection. Compared to GrB induction, optimum induction of FasL in $CD8^+$ T_{eff} cells occurred at a much lower tumor injection dose. These results suggest that, similar to my *ex vivo* results, *in vivo,* FasL expression is not correlated with GrB expression in activated PEL $CD8^+$ T_{eff} cells. Additionally, the relative expression patterns of FasL and GrB may in part be determined by antigen availability and consequently, perceived activation signal strength by $CD8^+$ T cells.

Collectively, the *ex vivo* and *in vivo* results suggest that FasL and GrB expression in stimulated and activated $CD8^+$ T cells are regulated differentially. The differential expression patterns of FasL and GrB may reflect the distinct roles and importance of FasL and GrB in response to low and high antigen challenge situations, respectively. *In vivo*, the importance of low antigen dependent FasL mediated immunity may likely occur in one of two scenarios: first, early during a natural infection or tumor development; second, during late stages of tumor and acute viral clearance or control of a chronic infection. While a number of studies have demonstrated the importance of FasL in one or both of these scenarios to a tumor or viral challenge (165, 211, 212, 218), none of these studies examined the possibility of both scenarios using the same stimulation system. From the complexity of the immune system, it may be likely that not every viral or tumor challenge would require FasL engagement, however, my experiments have demonstrated a predominant protein expression of FasL over GrB expression by activated $CD8^+$ T cells during lower antigen stimulation conditions.

Chapter 4: High Expression of Ly-6C Identify Resting Memory $CD8^+$ T Cells and Long-Lived Splenic NK Cells

Table 4-1 and Figures 4-1 and 4-2 were previously generated by Dr. Chew Shun Chang.
Figure 4-3 was previously generated by Dr. Andy I. Kokaji.

Introduction

Ly-6C is a member of the Ly-6 superfamily. Encoded on murine chromosome 15, Ly-6 molecules are C-terminal GPI anchored cell surface proteins. While a number of Ly-6 family proteins are expressed in mice, rat and humans, no Ly-6C syntenic region is present in rats and humans. In mice, Ly-6C is expressed on a number of cell populations, including T cells, neutrophils, macrophages and NK cells (191, 192). While the specific function of Ly-6C has not been determined, stimulation of Ly-6C has previously been shown to induce T cell activation and enhanced Ly-6C expression has been observed following stimulation with type I and II IFN (191, 219-221). Ly-6C has also been reported to contribute to $CD8^+$ T cell adhesion to high endothelial venules and trafficking into lymph nodes (197, 198). However, the specific ligand for Ly-6C is also currently undetermined. In many cases, Ly-6C expression has been associated with higher differentiation states in developing lymphocyte and leukocyte populations. Prominent expression of Ly-6C has been observed on myeloid cells as they differentiate into neutrophils and monocytes, Ly-6C also identifies plasma cells from other subsets of B cells and Ly-6C has been utilized as a memory $CD8^+$ T cell marker (191, 193, 196, 201). Additionally, recently identified memory NK cells following MCMV infections have been suggested to be present in the Ly-6C expression subset of NK cells (73). These observations raise the possibility that Ly-6C expression may be utilized to identify late stages of differentiation on a number of different cell types. Additionally, not all anti-Ly-6C

antibodies demonstrate the same reactivity towards Ly-6C (193, 219). As such, it is important to examine Ly-6C using multiple anti-Ly-6C monoclonal antibodies.

In this chapter, we characterize and describe a novel monoclonal anti-Ly-6C antibody, iMAP (immunological memory associated protein). While iMAP was initially generated in our laboratory against adherent lymphokine activated killer (A-LAK) cells from C57BL/6 mice to search for novel NK cell markers, iMAP showed specificity towards a subset of Ly-6C expressing lymphocytes. iMAP demonstrated some overlapping recognition patterns of Ly-6C compared to AL-21, a commercially available anti-Ly-6C monoclonal antibody. In uninfected mice, AL-21 identified Ly-6C expressed on $CD4^+$ and $CD8^+$ T cells, whereas iMAP only recognized Ly-6C expressed on $CD8^+$ T cells. Following the clearance of an acute LCMV infection, iMAP reactivity on $CD8^+$ T cells identified IFNγ responding antigen specific memory $CD8^+$ T cells. Additionally, iMAP recognition of Ly-6C partially interferes with AL-21 recognition of Ly-6C on *ex vivo* splenocytes. In contrast, AL-21 staining does not interfere with iMAP staining of Ly-6C. We also demonstrated a higher percentage of Ly-6C expressing NK cells among long-lived splenic NK cells, but not long-lived hepatic NK cells, thus Ly-6C may be a potential marker to identify long-lived splenic NK cells.

Results

iMAP recognizes a distinct Ly-6C subsets from clone AL-21

Using previously published methods and C57BL/6 A-LAK cells from spleens, our laboratory generated an IgM producing hybridoma, iMAP, in BALB/c mice (204). The iMAP antibody recognized A-LAK cells generated from different mouse strains, including C57BL/6, 129/J, AKR/J, C57BL/10 and DBA/2. However, iMAP failed to react with A-LAK cells from BALB/c, C3H/He, CBA/J and NOD/LtJ mice (Table 4-1). iMAP reactivity to A-LAK cells corresponded closely with Ly-6.2 haplotype expressing mice (191). Therefore, to determine the specific Ly-6 family allele

Mouse strain	iMap reactivity on A-LAKs[a,b]	Ly-6 haplotype
C57BL/6	++++	Ly-6.2
C57BL/10	++++	Ly-6.2
DBA/2	++++	Ly-6.2
129/J	++++	Ly-6.2
AKR/J	++++	Ly-6.2
BALB/c	-	Ly-6.1
C3H/He	-	Ly-6.1
CBA/J	-	Ly-6.1
NOD/LtJ	-	Ly-6.1

Table 4-1: iMAP stain A-LAK and bone marrow granulocytes derived from different Ly-6 haplotype mouse strains.

[a] The anti-HLA-B27, B27M2, was used as an isotype control. In all instances, the mean fluorescence intensity of the isotype control samples was between 3 to 6 relative log fluorescence units.

[b] When positive staining of A-LAKs were observed, two distinct populations, Ly-6C^{iMAP+} and Ly-6C^{iMAP-} were detected.

"–" sign indicates no iMap staining was detected.

recognized by iMAP, EL4 and HEK293T cells were transfected with Ly-6.2 allele members and iMAP antibody reactivity examined by flow cytometry. When examined, iMAP only recognized EL4 and HEK293T cells transfected with Ly-6C but not Ly-6A/E, G or I, indicating iMAP reactivity against Ly-6C (Figure 4-1 A). Additionally, iMAP reactivity to Ly-6C did not mirror that of AL-21 exactly, a commercial anti-Ly-6C clone known to stain expression of Ly-6C in Ly-6.1 and Ly-6.2 mice (197, 201). AL-21 was able to stain Ly-6.2 haplotype expressing RF33.70, RMA and MDAY-D2 cells whereas iMAP staining was not observed (Figure 4-1 B). Additionally, as iMAP and AL-21 fluorescence staining pattern of Ly-6C transfected EL4J and HEK293T cells were very similar, it is therefore unlikely that differential staining of iMAP and AL-21 staining on RF33.70 and RMA cells was due to weak antibody affinities of iMAP for Ly-6C. Collectively, our results suggest that iMAP not only recognizes Ly-6C, it is likely recognizing a different Ly-6C epitope from that of AL-21.

Monoclonal iMAP antibody specifically recognizes Ly-6C expressed on CD8$^+$ T cells but not CD4$^+$ T cells

Since Ly-6.2 haplotype T cell lines demonstrated differential iMAP and AL-21 recognition patterns of Ly-6C, we next sought to determine if these differences would be observed in *ex vivo* cells from C57BL/6 mice. Thymocytes and bone marrow granulocytes were isolated and expression of Ly-6C determined by iMAP and AL-21 staining. Not surprisingly, Gr1$^+$ granulocytes expressed Ly-6C and were iMAP and AL-21 reactive, however, thymocytes were largely Ly-6C negative (Figure 4-2 A) (191, 193, 221). When splenic and lymph node T cells were examined, Ly-6C expression was observed on a population of CD4$^+$ and CD8$^+$ T cells. Of note, Ly-6C expressing CD8$^+$ T cells were identifiable using AL-21 or iMAP antibody staining. In contrast, Ly-6C expression on CD4$^+$ T cells was only observed when stained with AL-21 but not iMAP (Figure 4-2 B). AL-21 may represent a pan-Ly-6C recognizing antibody capable of reacting to Ly-6C expression on both resting CD4$^+$ and CD8$^+$ T

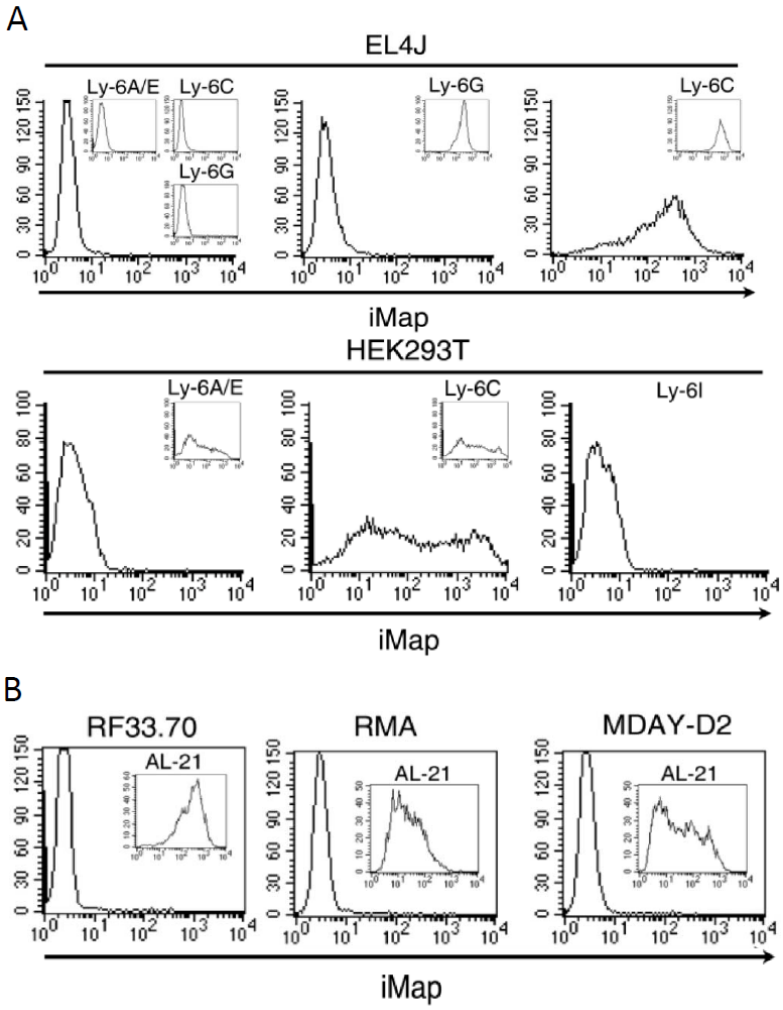

Figure 4-1: iMAP recognizes Ly-6C.
EL4J or HEK293T cells transfected with Ly-6A/E, C, G or I and untransfected EL4J cells (top left histogram) were stained with iMAP. Insert histograms represent staining of transfected Ly-6 proteins with respective antibodies. Expression of Ly-6A/E, C and G were examined using monoclonal antibodies clones D7, AL-21 and Rb6-8C5, respectively. No Ly-6I antibodies are commercially available (A). Distinctive Ly-6C detection by AL-21 and iMAP. Expression of Ly-6C on RF33.70 T cell hybridoma, RMA lymphoma and MDAY-D2 lymphosarcoma cells were not detected using iMAP. Insert histograms show Ly-6C expression on the indicated cell lines detected by AL-21 (B).

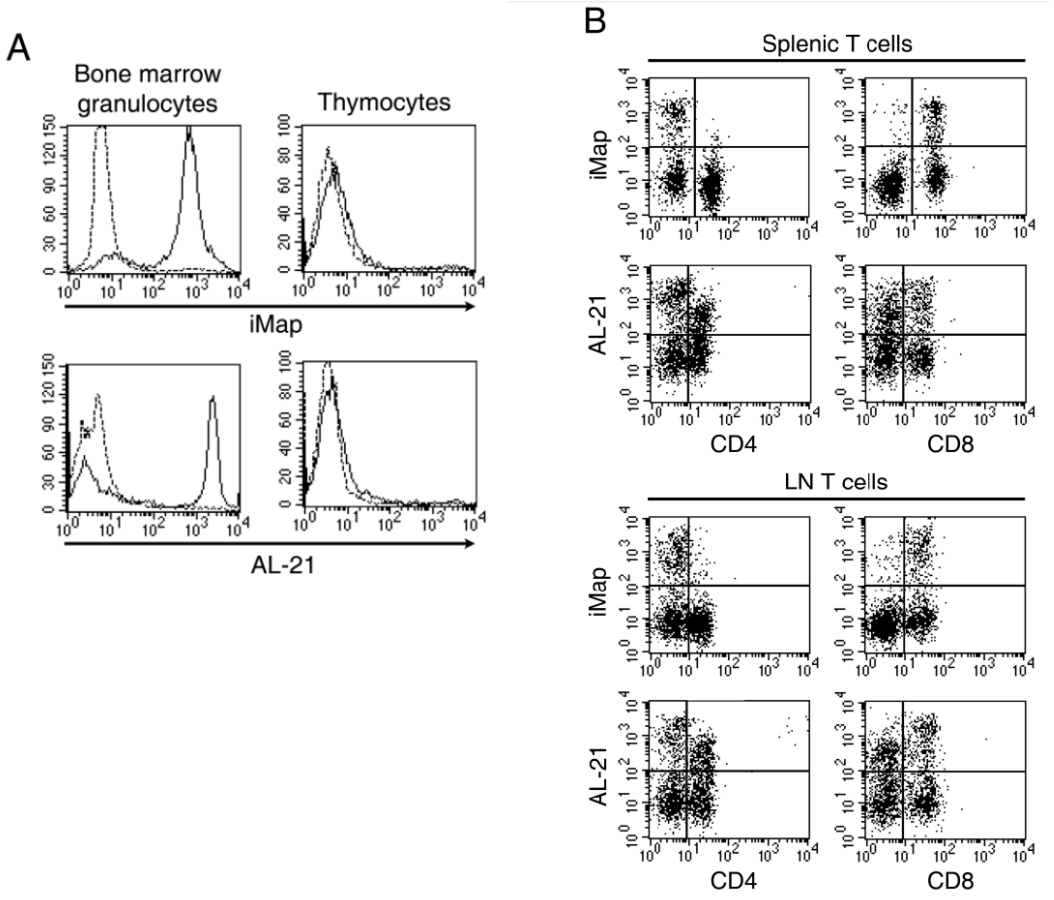

Figure 4-2: Detection of Ly-6C expression in resting *ex vivo* hematopoietic cells using AL-21 and iMAP.
Ly-6C expression on Gr-1$^+$ bone marrow granulocytes and thymocytes were detected using iMAP (top panel) or AL-21 (bottom panel). Dashed and solid lines represent isotype and anti-Ly-6C antibody (iMAP or AL-21) staining, respectively (A). Splenic and lymph node T cells were identified using anti-CD4 or anti-CD8 antibodies. Expression of Ly-6C on CD4$^+$ and CD8$^+$ T cells were examined using AL-21 and iMAP (B).

cells in C57BL/6 mice. Collectively, our results suggest that monoclonal iMAP antibody is capable of recognizing Ly-6C in *ex vivo* cell from C57BL/6 mice. Additionally, unlike monoclonal AL-21 antibody, which is reactive to Ly-6C expressed on both $CD4^+$ and $CD8^+$ T cells, among T cell subsets, iMAP only recognized Ly-6C expressed on resting $CD8^+$ T cells from the spleen and lymph nodes.

Dynamic expression of iMAP reactive Ly-6C on $CD4^+$ and $CD8^+$ T cells following LCMV infection

Previous studies have demonstrated Ly-6C is up regulated on T cells upon TCR stimulation and IFNα/β and IFNγ stimulation (196, 220). Additionally, Ly-6C expression has been shown to closely correlate with CD44 expression on TCR stimulated $CD8^+$ T cells and has been suggested to be a memory $CD8^+$ T cell marker (195, 196, 222). However, as iMAP antibody uniquely recognizes Ly-6C on resting $CD8^+$ but not $CD4^+$ T cells (Figure 4-2 B), we next sought to examine the kinetic expression of iMAP reactivity to Ly-6C during a primary response to an acute infection. To investigate this, C57BL/6 mice were infected ip with LCMV and iMAP reactive T cells in the spleen and lymph nodes were analyzed over the course of the infection. As previously demonstrated, on day zero, iMAP only stained $CD8^+$ but not $CD4^+$ T cells from the spleen and lymph nodes. From day three to nine after LCMV infection, we observed a dramatic increase in the proportion of iMAP reactive $CD8^+$ T cells from the spleen as well as from the lymph nodes. In fact, during this period, nearly all of the $CD8^+$ T cells found in the spleen and lymph nodes were iMAP reactive. By day 32 after infection, the level of iMAP staining on $CD8^+$ T cells returned to pre-infection expression levels in the spleen and lymph nodes (Figure 4-3 A). Surprisingly, while iMAP was non-reactive to resting $CD4^+$ T cells, iMAP strongly stained splenic and lymph node $CD4^+$ T cells on day three and day six after LCMV infection. However, $CD4^+$ T cells quickly lost reactivity to iMAP antibody by day nine post-infection (Figure 4-3 A).

Our observations demonstrated dynamic iMAP reactivity to Ly-6C expression pattern on $CD8^+$ and $CD4^+$ T cells following LCMV infection. During the peak of $CD8^+$ T cell response, nearly all $CD8^+$ T cells expressed iMAP reactive Ly-6C molecules. Furthermore, while iMAP did not recognize Ly-6C expressed on resting $CD4^+$ T cells, LCMV infection strongly induced expression of iMAP reactive Ly-6C in $CD4^+$ T cells. However, into the memory phase of T cell responses, only $CD8^+$ T cells retained expression of iMAP reactive Ly-6C.

Antigen-specific $CD8^+$ T cells found within highly iMAP reactive $CD8^+$ T cell subset

As Ly-6C expression can account for as high as 40% of $CD8^+$ T cells in the spleen of an unchallenged mice (193, 220), it is unlikely that all Ly-6C expressing $CD8^+$ T cells are LCMV specific memory $CD8^+$ T cells (Figure 4-3 A). However, as iMAP staining of splenic T cells after viral clearance was once again exclusive to $CD8^+$ T cells, iMAP reactivity may be used to distinguish between antigen-specific memory $CD8^+$ T cells from other $CD8^+$ T cells subsets and $CD4^+$ T cell. To examine the relationship between memory $CD8^+$ T cell specificity and iMAP reactivity, splenic $CD8^+$ T cells from LCMV infected mice >70 days were sorted into Ly-$6C^{iMAP(hi)}$, Ly-$6C^{iMAP(int)}$, Ly-$6C^{iMAP(lo)}$ and Ly-$6C^{iMAP(Neg)}$ reactive cells. The ability of each isolated $CD8^+$ T cell subset to respond to secondary antigen challenge was then assessed. Sorted $CD8^+$ T cells were stimulated with EL4 cells pulsed with a LCMV or influenza peptide for five hours and IFNγ production by stimulated $CD8^+$ T cells was assessed by ELISPOT. Our results demonstrated that when stimulated with LCMV peptide pulsed cells, a high level of Ly-$6C^{iMAP(hi)}$ and Ly-$6C^{iMAP(int)}$ $CD8^+$ T cells were able to secrete IFNγ (Figure 4-3 B). In contrast, a relatively low number of stimulated Ly-$6C^{iMAP(lo)}$ and Ly-$6C^{iMAP(Neg)}$ $CD8^+$ T cells produced IFNγ (Figure 4-3 B). In contrast, a significantly higher number of Ly-$6C^{iMAP(hi)}$ sorted $CD8^+$ T cells produced IFNγ than Ly-$6C^{iMAP(int)}$ $CD8^+$ T cells (Figure 4-3 B). As expected, sorted $CD8^+$ T cells did not produce any noticeable level of IFNγ secretion when stimulated

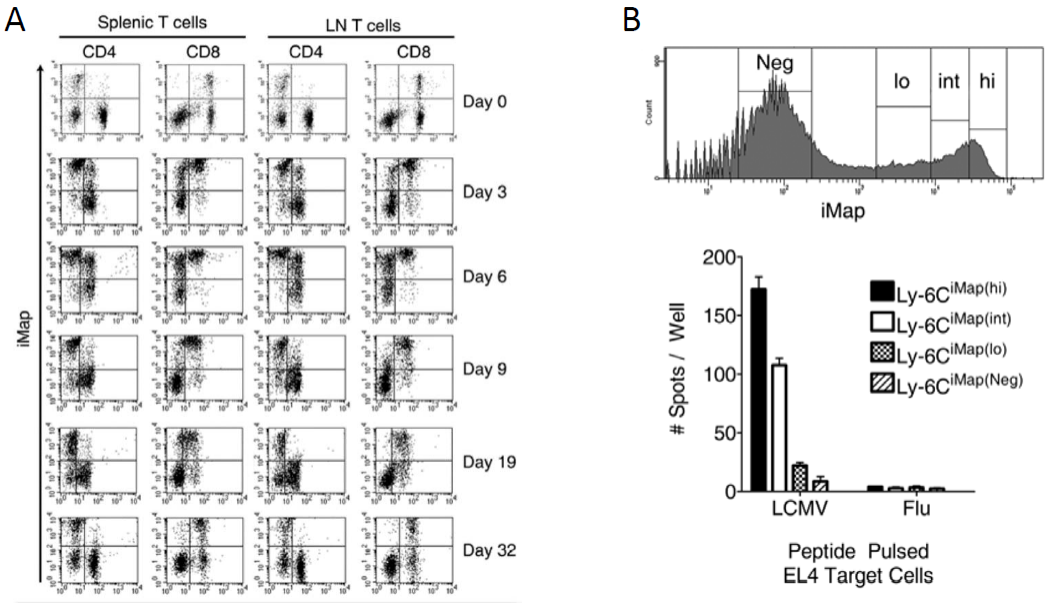

Figure 4-3: iMAP recognizes *in vivo* activated CD4$^+$ and CD8$^+$ T cells and resting antigen specific memory CD8$^+$ T cells.
CD4$^+$ and CD8$^+$ T cells from C57Bl/6 mice were isolated on days 0, 3, 6, 9, 19 and 32 following LCMV infection. Expression of Ly-6C on splenic and lymph node CD4$^+$ and CD8$^+$ T cells were determined by iMAP staining. Fluorescence intensity of CD4 or CD8 staining is indicated on the x-axis and iMAP staining is indicated on the y-axis (A). CD8$^+$ T cells from previously LCMV infected mice (>70 days) were sorted into Ly-6C$^{iMAP(Neg)}$, Ly-6C$^{iMAP(lo)}$, Ly-6C$^{iMAP(int)}$ and Ly-6C$^{iMAP(hi)}$ populations, as indicated on the histogram. The sorted subsets of CD8$^+$ T cells were incubated with LCMV or influenza peptide pulsed EL4 target cells for five hours and secretion of IFNγ was detected by ELISPOT as described in the Materials and Methods chapter (B).

with EL4 cells pulsed with influenza peptides (Figure 4-3 B). Our results suggest that following LCMV infection, antigen-specific memory $CD8^+$ T cells are found primarily in the Ly-$6C^{iMAP(hi)}$ and Ly-$6C^{iMAP(int)}$ population and contain a higher frequency of IFNγ producing cells than Ly-$6C^{(Neg)}$ naïve $CD8^+$ T cells. Our findings demonstrate that antigen-specific memory $CD8^+$ T cells can be identified by high iMAP antibody staining.

iMAP recognizes Ly-6C expression on splenic NK cells

In addition to Ly-6C expression on splenic $CD4^+$ and $CD8^+$ T cells, Ly-6C expression has also be described on splenic NK cells but not splenic B cells (201, 223). Additionally, with the preferential recognition of iMAP for Ly-6C expression on $CD8^+$ T cells compared to $CD4^+$ T cells, we next sought to further characterize iMAP reactivity to Ly-6C on other splenic lymphocyte populations. Splenocytes from uninfected mice were stained with anti-CD3ε and anti-NK1.1 antibodies, to identify NK cells, plus iMAP or AL-21 monoclonal antibody and examined by flow cytometry. Based on AL-21 reactivity, a notable population of NK cells expressed Ly-6C (Figure 4-4). Not surprisingly, as the iMAP hybridoma was generated against A-LAK cells, a previously published method to generate monoclonal hybridomas against NK cells (204), iMAP stained Ly-6C expressed on NK cells. Our results indicated that in addition to $CD8^+$ T cells, splenic NK cells also express AL-21 and iMAP reactive Ly-6C. However, from these results, it was difficult to determine whether AL-21 and iMAP reactive Ly-6C was expressed on the same cells or different cells. Additionally, since iMAP failed to recognize Ly-6C on resting $CD4^+$ T cells (Figure 4-2 B), it is likely that iMAP and AL-21 recognize different Ly-6C epitopes. It was therefore possible that distinct subsets of Ly-6C expressing $CD8^+$ T and NK cells may be further defined through a closer examination of iMAP and AL-21 reactivity.

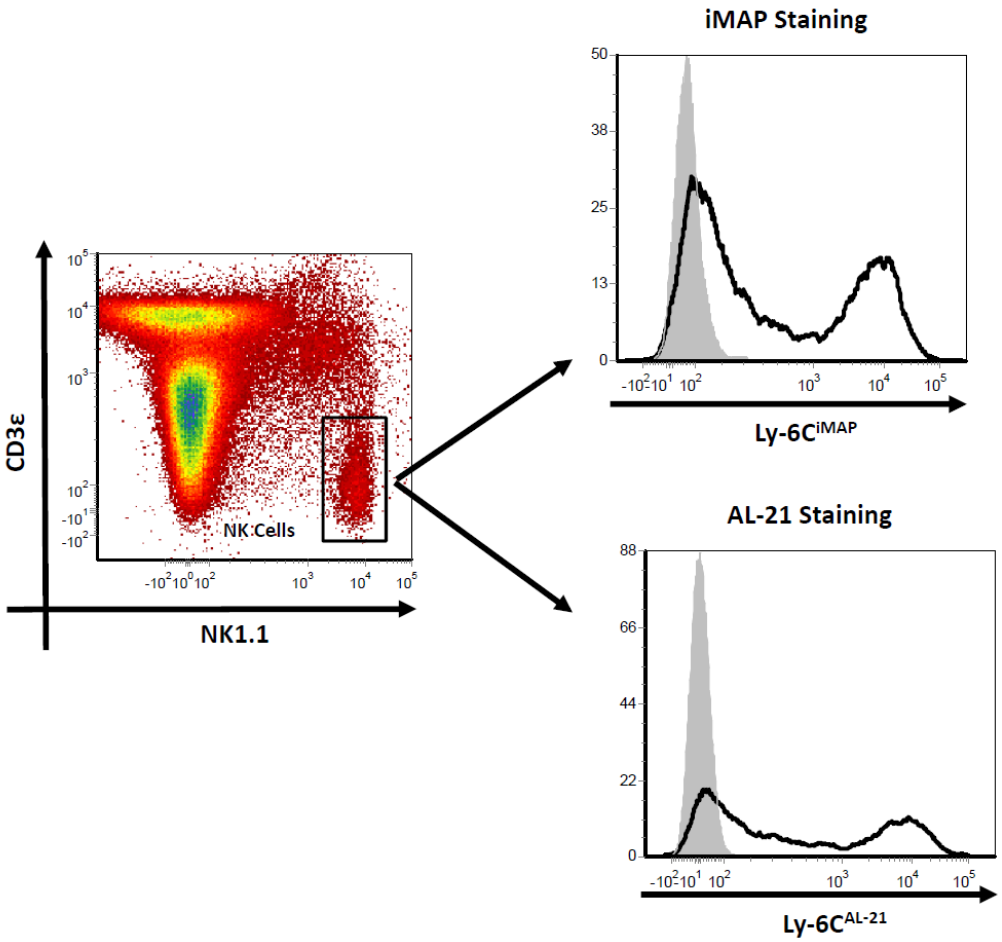

Figure 4-4: iMAP recognizes Ly-6C expressed by NK cells.
Splenic NK cells were identified as NK1.1$^+$ CD3ε$^-$ splenocytes (left). Ly-6C expression on NK cells were determined by iMAP staining (top right) or AL-21 staining (bottom right) by flow cytometry. Shaded histogram represents isotype staining. Flow cytometry plots are representative of one of two experiments.

iMAP antibody partially interferes with monoclonal AL-21 antibody recognition of Ly-6C on splenic CD8$^+$ T and NK cells

A number of anti-Ly-6C monoclonal antibodies have been described in the past and a number of anti-Ly-6C antibody pairs have been reported to compete for binding of Ly-6C on splenic T lymphocyte populations (193, 197, 219, 221). For example, immunoprecipitation and Western blotting of Ly-6C from BALB/c splenocytes demonstrated blocking of AL-21 recognition of Ly-6C by 5E9, another anti-Ly-6C monoclonal antibody. However, when immunoprecipitation was performed with a separate anti-Ly-6C monoclonal antibody, G10, Ly-6C detection by AL-21 was reduced but not completely inhibited (197). Therefore, we sought to further define the binding characteristics of iMAP monoclonal antibody to Ly-6C in relation to AL-21.

Splenic CD8$^+$ T and NK cells were identified as CD3ε$^+$ CD8$^+$ and CD3ε$^-$ NK1.1$^+$, respectively, and stained with three different concentrations of iMAP or AL-21. Typically, for cell surface staining, antibody concentrations between 0.5μg to 0.05μg per 100μl of staining volume yield sufficient separation of positive and negative populations of cells. As such, CD8$^+$ T cells (Figure 4-5 A) and NK cells (Figure 4-5 B) from whole splenic lymphocytes were single stained for Ly-6C expression using iMAP (0.03μg ~ 0.65μg per 100μl volume) or AL-21 (0.05μg~0.4μg per 100μl volume). From our results, Ly-6C expressing CD8$^+$ T and NK cells were easily identified by iMAP and AL-21 even at low concentrations (Figure 4-5 A and B). At high iMAP and AL-21 staining concentrations, Ly-6C positive CD8$^+$ T and NK cells are highly fluorescent, as expected (Figure 4-5 A and B). However, at low antibody concentrations, while fluorescence intensity is reduced, Ly-6C positive CD8$^+$ T and NK cells are still clearly distinguishable from Ly-6C negative cells (Figure 4-5 A and B).

Next, to determine potential dependent staining characteristics of iMAP and AL-21, staining of Ly-6C on splenocytes using AL-21 or iMAP were performed in

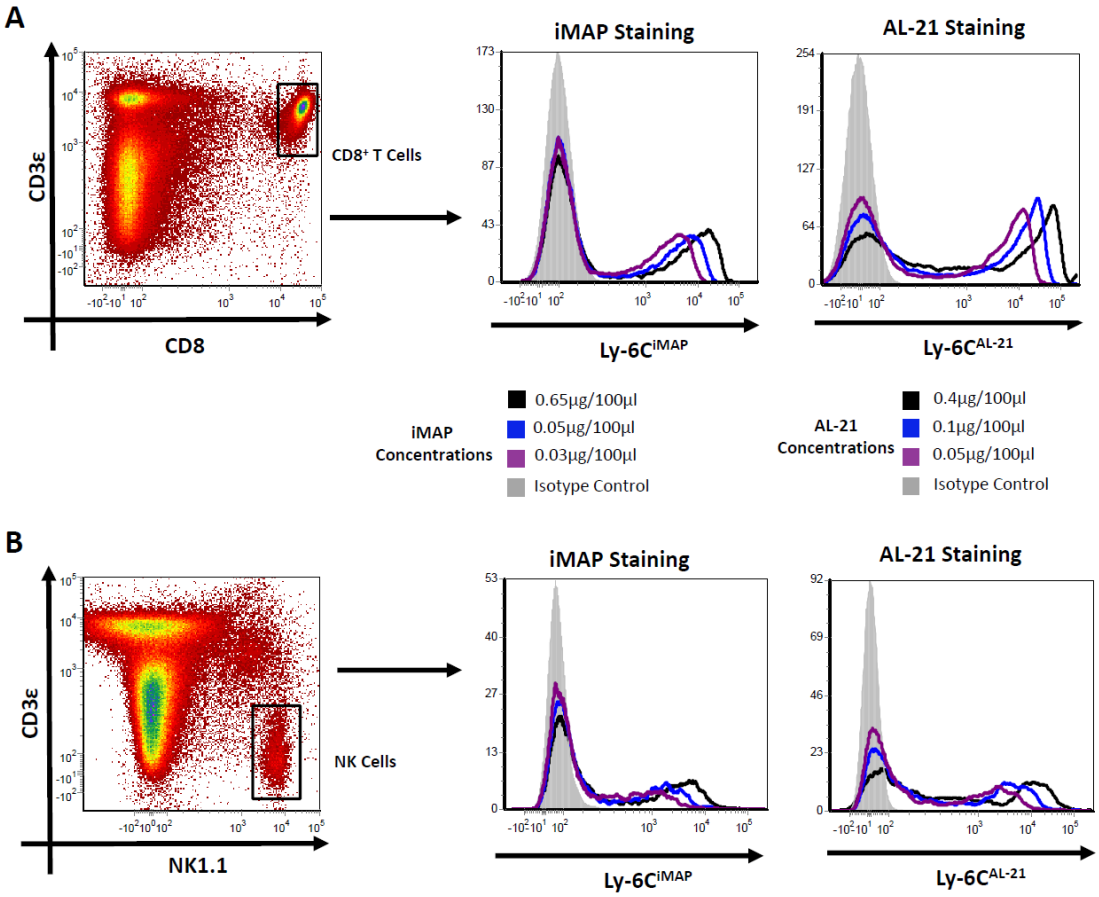

Figure 4-5: iMAP and AL-21 titration staining on $CD8^+$ T and NK cells. Splenic $CD8^+$ T cells were identified as $CD3\varepsilon^+CD8^+$ (A left panel) and NK cells identified by $CD3\varepsilon^-NK1.1^+$ staining (B left panel). Additionally, 0.65µg/100µl (black), 0.05µg/100µl (blue) and 0.03µg/100µl (purple) of iMAP (middle panel) or 0.4µg/100µl (black), 0.1µg/100µl (blue) and 0.05µg/100µl (purple) of AL-21 (right panel) was used to determine the expression of Ly-6C on $CD8^+$ T and NK cells. The shaded histograms represent isotype control staining of Ly-6C expression on $CD8^+$ T and NK cells. Flow cytometry plots are representative of one of two experiments.

consecutive stages of antibody labeling. The binding ability of each antibody was then determined through fluorescence intensity examined by flow cytometry.

Splenocytes from unchallenged mice were first incubated with 4% mouse serum plus monoclonal 2.4G2 antibody, to block Fc receptors and limit non-specific binding by fluorescently labeled antibodies, and followed by staining with anti-CD3ε, CD8 and NK1.1 plus iMAP (0.03µg~0.65µg) and subsequently 0.05µg of AL-21 (Scheme 1) or AL-21 (0.05µg~0.4µg) followed by 0.03µg of iMAP antibody (Scheme 2) (Figure 4-6 A). Additional samples of splenocytes were also stained with anti-CD3ε, CD8α and NK1.1 with either iMAP or AL-21 antibodies only followed by the respective isotype controls of AL-21 or iMAP as positive and negative controls. All antibody staining steps were performed at 4^{o}C in the dark for 20 minutes.

When CD8^{+} T cells and NK cells were stained with AL-21 in the absence of iMAP, high levels of AL-21 fluorescence was observed among Ly-6C expressing cells (Figure 4-6 B and C top panel). When CD8^{+} T cells and NK cells were first incubated with iMAP antibody, at low quantities, fluorescence due to AL-21 remained relatively high (Figure 4-6 B and C top panels). However, at higher iMAP pre-incubation concentrations, staining of AL-21 on both CD8^{+} T cells and NK cells was noticeably decreased (Figure 4-6 B and C top panels). The fluorescence intensity of AL-21 staining was maintained when splenocytes were first stained with 0.03µg of iMAP antibody, however, when pre-incubated with 0.65µg of iMAP, the fluorescence intensity from AL-21 binding was nearly a log lower than on CD8^{+} T cells and NK cells stained without any iMAP antibody (Scheme 1) (Figure 4-6 B and C top panels). As expected, when CD8^{+} T cells and NK cells were stained with iMAP with no addition of AL-21, Ly-6C positive cells were highly stained by iMAP (Figure 4-6 B and C bottom panels). Ly-6C positive and negative CD8^{+} T cells and NK cells were easily identified. However, in contrast to Scheme 1, when AL-21 was used for Ly-6C staining prior to iMAP staining, at all tested AL-21 concentrations, the fluorescence intensity of iMAP stained CD8^{+} T cells and NK cells remained relatively high (Figure 4-6 B and C bottom panels). We did not observe a large decrease in iMAP staining

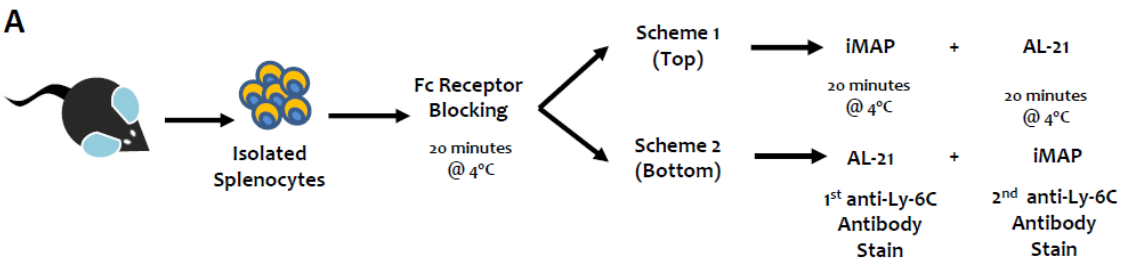
A
Isolated Splenocytes
Fc Receptor Blocking
20 minutes @ 4°C
Scheme 1 (Top)
Scheme 2 (Bottom)
iMAP
+
AL-21
20 minutes @ 4°C
20 minutes @ 4°C
AL-21
+
iMAP
1st anti-Ly-6C Antibody Stain
2nd anti-Ly-6C Antibody Stain

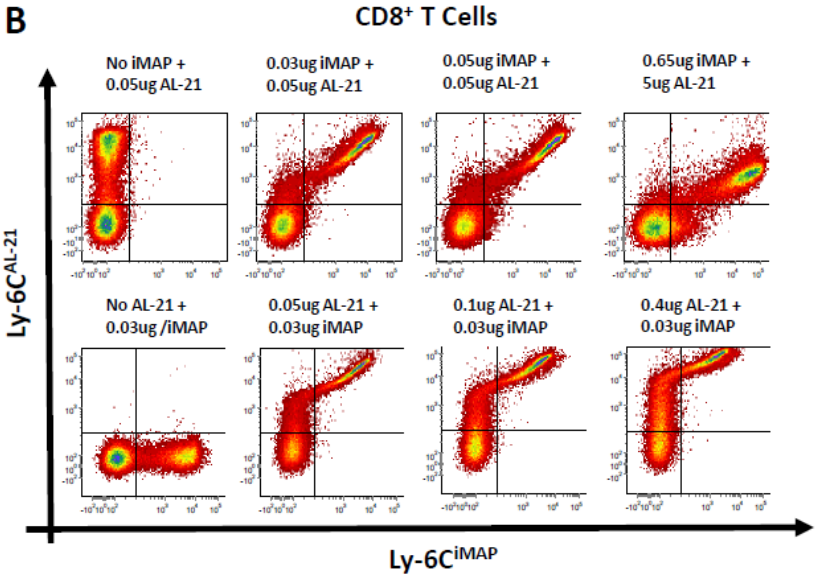
B
CD8+ T Cells
No iMAP + 0.05ug AL-21
0.03ug iMAP + 0.05ug AL-21
0.05ug iMAP + 0.05ug AL-21
0.65ug iMAP + 5ug AL-21
No AL-21 + 0.03ug /iMAP
0.05ug AL-21 + 0.03ug iMAP
0.1ug AL-21 + 0.03ug iMAP
0.4ug AL-21 + 0.03ug iMAP
Ly-6CAL-21
Ly-6CiMAP

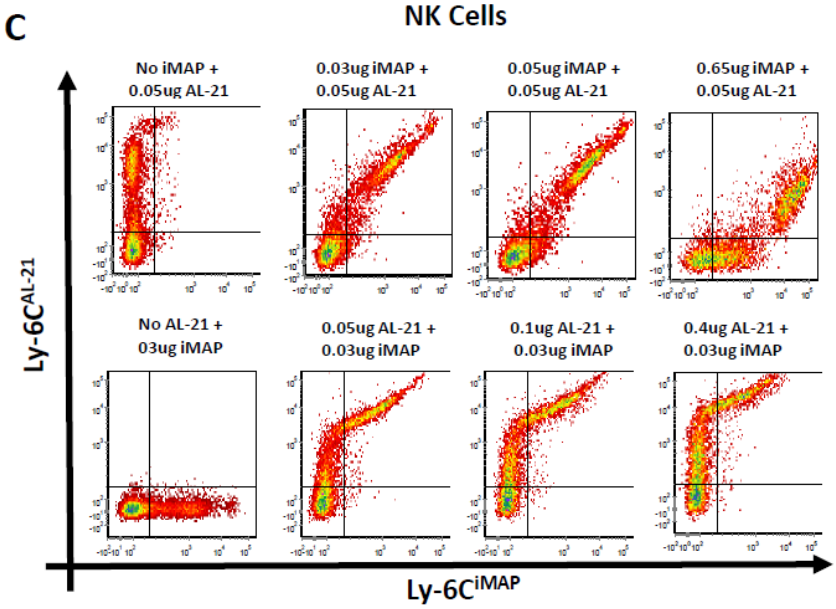
C
NK Cells
No iMAP + 0.05ug AL-21
0.03ug iMAP + 0.05ug AL-21
0.05ug iMAP + 0.05ug AL-21
0.65ug iMAP + 0.05ug AL-21
No AL-21 + 03ug iMAP
0.05ug AL-21 + 0.03ug iMAP
0.1ug AL-21 + 0.03ug iMAP
0.4ug AL-21 + 0.03ug iMAP
Ly-6CAL-21
Ly-6CiMAP

Figure 4-6: iMAP antibody partially interferes with AL-21 recognition of Ly-6C. Isolated splenocytes from mice were incubated with 4% mouse serum plus Fc blocking antibody, 2.4G2, for 20 minutes followed by stained with anti-CD3ε, CD8 and NK1.1 antibodies and first anti-Ly-6C antibody of either 0.03μg ~ 0.88μg of iMAP (Scheme 1) or 0.05μg ~ 0.4μg of AL-21(Scheme 2). Following the first 20 minute staining, the second anti-Ly-6C antibody was added; either 0.05μg of AL-21 (Scheme 1) or 0.03μg of iMAP (Scheme 2) for 20 minutes (A). Staining of iMAP and AL-21 on $CD8^+$ T cells (B) and NK cells (C) using Scheme 1 (top panels) and Scheme 2 (bottom panels) are shown. Top left dot plots show Ly-6C staining using only AL-21 and bottom left dot plots show Ly-6C staining using only iMAP on $CD8^+$ T cells (B) and NK cells (C). Flow cytometry plots are representative of one of two experiments.

with pre-incubation of AL-21 (Scheme 2) (Figure 4-6 B and C bottom panel). Collectively, our results suggest an intriguing dynamic between AL-21 and iMAP staining of Ly-6C; AL-21 recognition of Ly-6C may be inhibited partially by iMAP binding whereas iMAP recognition of Ly-6C is independent of AL-21. Importantly, using both anti-Ly-6C antibodies, we have identified two distinct subsets of Ly-6C expressing $CD8^+$ T and NK cells; an AL-21 only single stained and an AL-21/iMAP double stained Ly-6C positive population.

Increased percentage of Ly-6C expression among long-lived splenic NK cells

Recent studies of NK cell functions have revealed previously unappreciated adaptive immune features of NK cells (145, 146, 149). Using the MCMV infection model, Sun *et al.* demonstrated that while Ly-6C expressing NK cells can be found in naïve unchallenged mice, long-lived $Ly49H^+$ NK cells six weeks after MCMV infection are highly enriched in the Ly-6C expressing population of NK cells (73). Additionally, stimulation with pro-inflammatory cytokines IL-12, IL-18 and IL-15 have also been shown to generate long-lived murine and human NK cells (142, 144). Murine memory-like NK cells, so termed as the NK cells are not activated by a specific foreign antigen or ligand, were found to persist for at least three weeks and possess enhanced IFNγ production capabilities following re-stimulation (142). However, Ly-6C expression on memory-like cytokine stimulated NK cells had not been previously examined. We therefore sought to determine the expression pattern of Ly-6C in cytokine generated long-lived memory-like NK cells using monoclonal AL-21 and iMAP antibodies. Additionally, since iMAP staining of Ly-6C on NK cells was not inhibited by AL-21, to characterize Ly-6C expression, we therefore first stained NK cells with AL-21 followed by iMAP (Scheme 2) (Figure 4-6 A). From our previous data, staining of NK cells with Scheme 2 identified three subsets of NK cells based on Ly-6C expression; cells absent in Ly-6C expression ($Ly\text{-}6C^{Neg}$), cells expressing Ly-6C stained by AL-21 only ($Ly\text{-}6C^{AL\text{-}21}$) and cells stained by both AL-21 and iMAP ($Ly\text{-}6C^{AL\text{-}21/iMAP}$) (Figure 4-6 B bottom panel). Mouse splenic NK cells

were sorted based on NK1.1^{+} CD3ε^{-} staining and stimulated for 14~16 hours with either IL-12, IL-18 and low levels of IL-15 or low level of IL-15 only as a control, as previously published (142). Following stimulation, cultured NK cells were adoptively transferred into CD45.1 age-matched congenic mice via tail vein injection. The usage of congenic mice allowed us to easily differentiate between transferred and host NK cells based on the expression of CD45.2. After a six week rest period, Ly-6C expression profile of long-lived transferred NK cells were examined. Ly-6C on recipient mouse NK cells, based on the absence of CD45.2 marker, was also examined for comparison (Figure 4-7 A). To ensure sort purity, percentage of NK cells pre- and post-sort were also determined by flow cytometry. Before sorting, less than 3% of splenocytes were NK cells based on NK1.1^{+} CD3ε^{-} staining. Post-sort, NK cell purity was >95% (Figure 4-7 B). Additionally, prior to adoptive transfer, IL-12, IL-18 and IL-15 cultured NK cells were stimulated to produce IFNγ whereas NK cells cultured with low levels of IL-15 only, served as a control, did not produce detectable amounts of IFNγ (Figure 4-7 C).

Six weeks after adoptive transfer, Ly-6C expression on splenic NK cells from congenic mice receiving IL-12, IL-18 and IL-15 stimulated NK cells, or IL-15 only cultured NK cells are shown in Figure 4-7 D top and bottom panel, respectively. Long-lived NK cells pre-cultured with either IL-12, IL-18 and IL-15 or IL-15 only, represented less than 2% of the total recipient mouse splenic NK cells population, based on CD45.2 expression. Interestingly, while around 40% of the recipient CD45.2 deficient NK cells stained positive for Ly-6C, greater than 60% of the long-lived transferred CD45.2 expressing NK cells expressed Ly-6C, regardless of previous stimulation. Furthermore, we observed an increase in the proportion of Ly-6C$^{AL\text{-}21/iMAP}$ NK cells within the transferred CD45.2 NK cell population (~30%) compared to host NK cells (~15%) (Figure 4-7 D). These findings suggest that Ly-6C expression may be associated with NK cell longevity. Additionally, much of the increase in Ly-6C positive long-lived NK cells are reactive to both AL-21 and iMAP monoclonal antibodies.

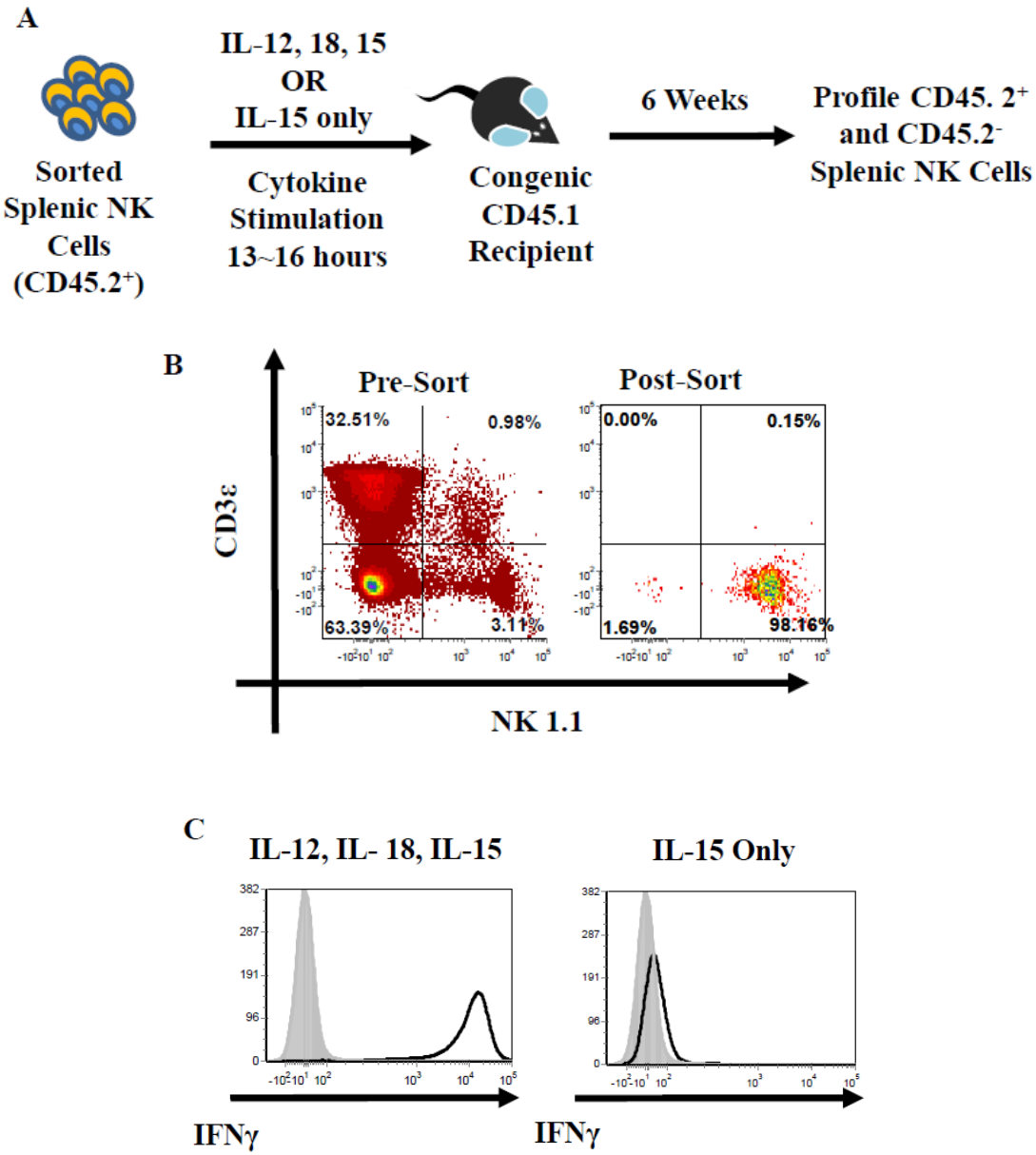
A
Sorted Splenic NK Cells (CD45.2+)
IL-12, 18, 15 OR IL-15 only
Cytokine Stimulation 13~16 hours
Congenic CD45.1 Recipient
6 Weeks
Profile CD45. 2+ and CD45.2- Splenic NK Cells
B
Pre-Sort
Post-Sort
32.51%
0.98%
63.39%
3.11%
0.00%
0.15%
1.69%
98.16%
CD3ε
NK 1.1
C
IL-12, IL- 18, IL-15
IL-15 Only
IFNγ
IFNγ

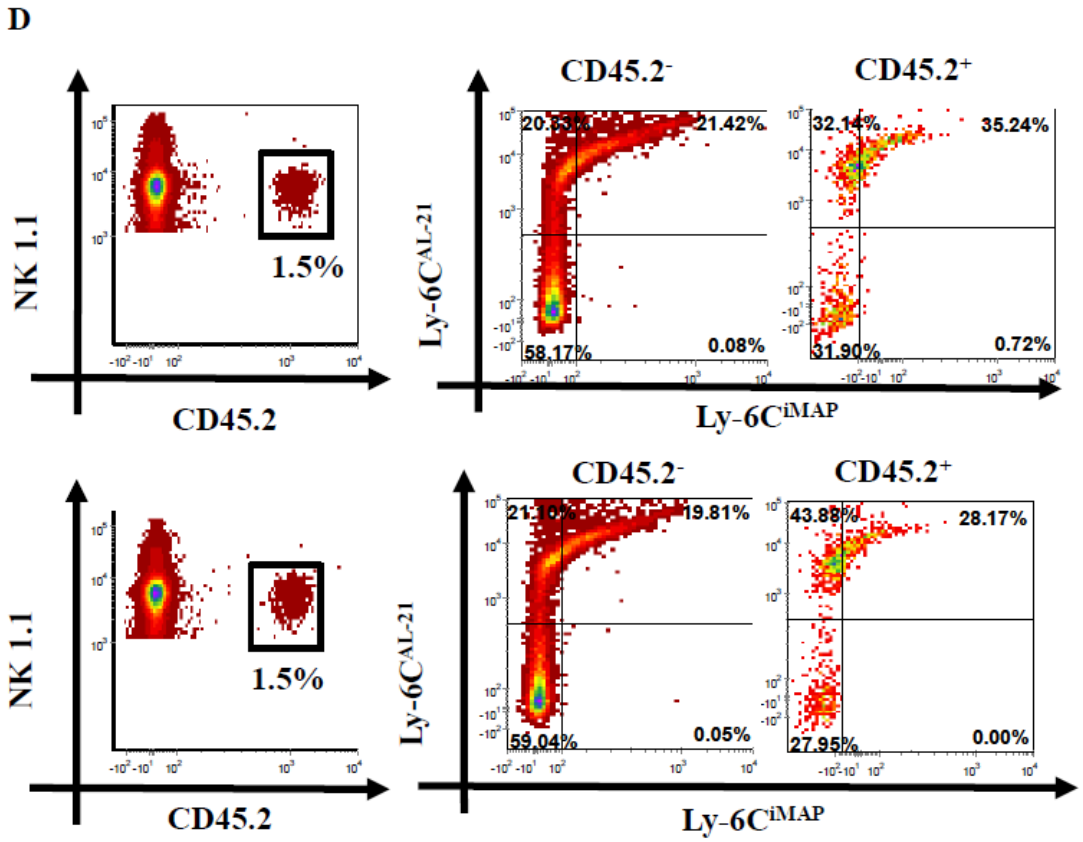

Figure 4-7: Increased percentage of Ly-6C expression among long-lived splenic NK cells.

Sorted NK cells ($NK1.1^+$ $CD3\varepsilon^-$) from 7~8 week old C57BL/6 mice were cultured overnight with IL-12, IL-18 and IL-15, or IL-15 only, and transferred into age matched $CD45.1^+$ congenic mice. Following a six week rest period, Ly-6C expression using AL-21 and iMAP of splenic NK cells in the recipient mice were analyzed by flow cytometry. Pre-incubated long-lived NK cells were distinguished from recipient NK cells by expression of the congenic CD45.2 marker (A). Percentage of NK cells were examined pre- and post-sort based on anti-NK1.1 and CD3ε staining (B). Production of IFNγ was examined in IL-12, IL-18 and IL-15 stimulated and IL-15 only treated sorted NK cells after overnight culture by flow cytometry. Solid histogram line represents intracellular staining of IFNγ and shaded histogram represents intracellular staining using an isotype control antibody (C). Six weeks post transfer, using AL-21 and iMAP staining (Scheme 2), Ly-6C expression on NK cells in the spleen of recipient mice were analyzed using flow cytometry. NK cells were identified as $NK1.1^+$ $CD3\varepsilon^-$ and transferred and host NK cells distinguished by $CD45.2^+$ and $CD45.2^-$ expression, respectively. Top panel are NK cells from recipient mice that received IL-12, IL-18 and IL-15 cultured NK cells, whereas the bottom

panel are NK cells from recipient mice that received NK cells cultured with IL-15 only overnight (D).

Long-lived hepatic NK cells are negative for Ly-6C expression

Thus far, we have showed a higher representation of Ly-6C positive NK cells among long-lived splenic NK cells compared to splenic NK cells isolated from a conventionally housed untreated mouse. Furthermore, recent studies of memory NK cells have suggested hepatic rather than splenic NK cells mediate antigen specific adaptive immune features in response to haptens and some viral sensitizations (5, 150, 151). Recent studies have also identified unique NK cell markers associated with the generation of hapten and viral specific memory NK cells from the liver, such as CXCR6 and CD49a expression, which are not highly expressed on splenic NK cells, and a lack of expression of DX5, which is expressed on nearly all splenic NK cells (151, 155). Liver restriction of hapten specific memory NK cells may reflect a unique immunological feature of hepatic NK cells and/or possibly a result of a distinct NK cell developmental pathway unique to liver resident NK cells (224, 225). However, a specific marker for liver derived long-lived memory NK cells has not yet been identified. Therefore, we next sought to examine Ly-6C expression on hepatic NK cells and, specifically, long-lived hapten sensitized hepatic NK cells.

To evaluate changes in Ly-6C expression in hepatic NK cells, we first compared the Ly-6C expression pattern between hepatic and splenic NK cells in untreated mice using Ly-6C staining Scheme 2 (Figure 4-6 A). To examine hepatic NK cells, the liver was first perfused with PBS to remove lymphocytes in the circulating blood supply in the liver and then using a previously published mechanical disruption protocol, described in the Materials and Methods chapter, isolated hepatic lymphocytes (203). Both hepatic and splenic NK cells from unchallenged mice displayed a similar distribution of Ly-6C expression. While the majority of NK cells from both organs do not express Ly-6C, populations of splenic and hepatic Ly-$6C^{AL-21}$ and Ly-$6C^{AL-21/iMAP}$ NK cells were observed (Figure 4-8 A). To induce hapten specific memory NK cells, mice were sensitized with 0.5% DNFB in acetone on the surface of their shaved abdomens on day zero and day one, as previously reported (150, 151). On day four, hepatic NK cells were purified via cell sorting of $NK1.1^{+}$

$CD3\varepsilon^-$ cells and adoptively transferred into age-matched CD45.1 congenic recipient mice. Six weeks post transfer, Ly-6C expression on transferred hapten pre-sensitized CD45.2 positive and host CD45.2 negative hepatic NK cells were examined by flow cytometry (Figure 4-7 B). To ensure sorting efficacy, hepatic NK cell purity pre- and post-sort was analyzed via flow cytometry. Pre-sort, roughly 7% of total hepatic lymphocytes were NK cells, whereas, post-sort, hepatic NK cell purity was greater than 95% (Figure 4-8 C). The sorting purity of hepatic NK cells was very similar to the sorting purity seen with splenic NK cells (Figure 4-7 B). Six weeks post transfer, Ly-6C expression on hepatic NK cells in the recipient mice were examined. A small, population of adoptive transferred hepatic NK cells was easily distinguished from recipient host hepatic NK cells based on CD45.2 expression (Figure 4-8 D left). While the majority of host CD45.2 negative hepatic NK cells did not express Ly-6C, a noticeable population of hepatic NK cells expressed Ly-6C molecules reactive to AL-21 antibody or both AL-21 and iMAP antibodies (Figure 4-8 D right). This phenotype closely resembled the Ly-6C staining profile seen on hepatic NK cells from unchallenged mice (Figure 4-8 A). Interestingly, adoptively transferred long-lived hapten pre-sensitized NK cells were nearly all negative in Ly-6C expression (Figure 4-8 D right). These findings are in stark contrast to our findings in long-lived splenic NK cells (Figure 4-7). Collectively, our findings suggest that Ly-6C may not be a suitable marker for long-lived and, by extension, memory hepatic NK cell.

Summary

In this chapter we characterized the expression profile of the Ly-6C epitope identified by the monoclonal antibody iMAP. Interestingly, iMAP and AL-21, a widely utilized anti-Ly-6C antibody, displayed distinct staining patterns of Ly-6C. AL-21 recognized Ly-6C on a broad spectrum of Ly-6C transfected cell lines and C57BL/6 hybridoma clones, as well as resting $CD4^+$ and $CD8^+$ T cells. In contrast, while iMAP stained Ly-6C transfected cell lines, iMAP did not recognize Ly-6C expression on C57BL/6 derived hybridoma clones (Figure 4-1 & 4-2). iMAP

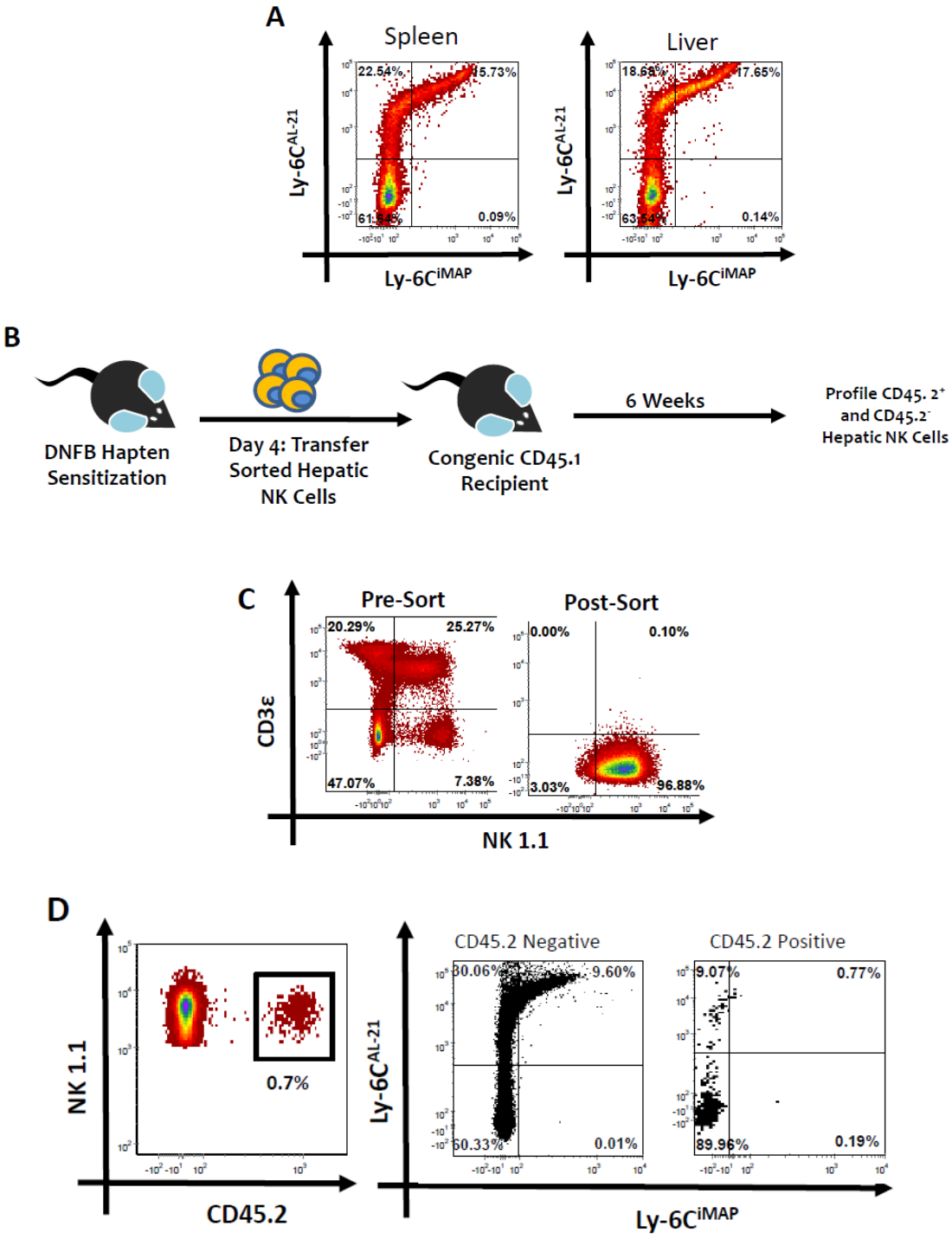

Figure 4-8: Long-lived hepatic NK cells are negative for Ly-6C expression.

Ly-6C expression on splenic and hepatic isolated NK cells ($NK1.1^{+}CD3\varepsilon^{-}$) from unchallenged mice using AL-21 and iMAP staining (Scheme 2) (A). C57BL/6 mice were sensitized with DNFB hapten on the abdomen on days zero and one. On day four, hepatic NK cells were sorted based on $NK1.1^{+}CD3\varepsilon^{-}$ expression and transferred to age matched CD45.1 congenic mice. Six weeks post transfer, Ly-6C expression of $CD45.2^{+}$ and $CD45.2^{-}$ hepatic NK cells in recipient mice were examined by flow cytometry (B). Purity of NK cells pre- and post-sort were examined by flow cytometry based on $NK1.1^{+}CD3\varepsilon^{-}$expression (C). Six weeks post transfer, using AL-21 and iMAP staining (Scheme 2), Ly-6C expressed by hepatic NK cells from recipient mice were analyzed using flow cytometry. NK cells were identified as $NK1.1^{+}$ $CD3\varepsilon^{-}$ and transferred and host NK cells distinguished by $CD45.2^{+}$ and $CD45.2^{-}$ expression, respectively (D). Experiment demonstration of n=1.

recognition of Ly-6C is similar to the 143-4-2 monoclonal antibody. Leo *et al.* demonstrated that 143-4-2 is an anti-Ly-6C with reactivity towards Ly-6C expression on $CD8^+$ T cells but not $CD4^+$ T cells in C57BL/10 mice, a Ly-6.2 haplotype strain (219). Additionally, iMAP recognized Ly-6C expressed on $CD8^+$ T cells and NK cells while only staining $CD4^+$ T cells following an acute LCMV infection (Figure 4-3). During competitive binding assays, pre-incubation of splenocytes with iMAP antibody partially interfered with AL-21 recognition of Ly-6C. In contrast, pre-staining of splenocytes with AL-21 did not affect iMAP reactivity to Ly-6C (Figure 4-6). Collectively, our results suggest that iMAP may recognize a distinct subset of Ly-6C and a separate epitope from AL-21. Our results suggest that binding of the iMAP epitope may result in a less accessible conformation for AL-21 binding. However, future epitope mapping studies will be needed to further clarify these observations.

Recently, NK cells capable of adaptive immune features have been described following a wide variety of stimulations (73, 142, 151). Ly-6C expression has also been demonstrated to be up-regulated on long-lived memory $Ly\text{-}49H^+$ NK cells following MCMV infection (73). Therefore, we examined Ly-6C expression on cytokine stimulated and hapten sensitized long-lived NK cells from spleen and liver, respectively. After six weeks post stimulation and transfer, over 60% of long-lived splenic NK cells expressed Ly-6C, compared to roughly 40% from an unchallenged mouse. In contrast, only about 10% of long-lived hepatic NK cells expressed Ly-6C (Figure 4-7 & 4-8). The disparity in Ly-6C expression between long-lived splenic and hepatic NK cells may reflect intrinsic differences between the two NK cell populations as demonstrated by differential expression of surface markers and cytokine requirements for viral response (113, 151, 155). Collectively, our results suggest expression of Ly-6C may identify a subset of long-lived NK cells specific to the spleen.

To build upon these findings, it would be interesting to further define other cell surface markers in addition to Ly-6C to better define the phenotype of long-lived

splenic NK cells, in particular, NK cell maturation markers such as CD27, CD11b and KLRG1 (87-89). Additionally, it would also be interesting to determine if Ly-6C^{Neg}, Ly-6C^{AL-21} and Ly-6C$^{AL-21/iMAP}$ NK cells represented subsequent stages of splenic NK cell maturation or, possibly, distinct linages of splenic NK cells development.

Chapter 5: Ly-6C$^{AL-21/iMAP}$ NK Cells Represent a Highly Differentiated State of Long-lived NK Cells

Introduction

Natural killer (NK) cells are cytotoxic lymphocytes of the innate immune system and were first described for their "natural" cytotoxic ability against tumor cells without prior sensitization (70, 71, 78, 226). Early on, NK cells were identified as a distinct subset of lymphocytes from the T and B cells of the adaptive immune system (71). Unlike adaptive T and B cells, NK cells do not require somatic gene rearrangement of their receptor genes during development (7, 227). Instead, using a limited number of germ-line encoded activating and inhibitory receptors, NK cells detect the presence or absence of inhibitory receptor ligands, such as MHC molecules, or activating receptor ligands such as stress-induced ligands or virally encoded products on transformed or infected cells (96). The balance of activating and inhibitory receptor signals received by ligands on a target cell determines whether or not an NK cell will become activated or tolerant to a target cell (228). Not surprisingly, deficiencies in NK cell activity result in increased susceptibility to tumor formations and many infections both in mice and humans (229, 230).

During mouse cytomegalovirus (MCMV) infections, early NK cell recognition of viral products is vital to the survival of an infected host (229). In MCMV resistant C57BL/6 and Ma/My mice strains, Ly-49H and Ly-49P expressed by NK cells recognize MCMV viral products m157 and m04 co-expressed with H-2D^k, respectively (229, 231-233). Upon activation, NK cells are also important early producers of a number of cytokines and chemokines, such as IFNγ (78, 229). Defects in NK cell cytotoxicity and IFNγ production render mice susceptible to MCMV infection (229). In addition to activation by direct receptor-ligand interactions, NK cells are also activated by pro-inflammatory cytokines such as IL-12, IL-18 and IL-15 (96, 115, 229). Both IL-12 and IL-18 have been demonstrated to be integral in the optimal induction of IFNγ during culture and viral infections (113, 234, 235).

Additionally, IL-15 trans-presented by activated dendritic cells have been shown to prime NK cells for enhanced IFNγ responses (123). While IL-12, IL-18 and IL-15 may function independently to stimulate NK cell responses under different conditions, IL-12, IL-18 and IL-15 have also been shown to work synergistically to enhance NK cell effector function (116, 123, 234). Using MCMV infection and cytokine stimulation models, recent studies have suggested additional characteristics of NK cell functions beyond the defined innate immune functions of NK cells (146).

While immunological memory has historically been attributed to T and B cells, recent studies have demonstrated previously unappreciated adaptive immune features of NK cells, including longevity and memory of antigen specificity (146, 147). Mature NK cells were previously thought to be short lived, however, recent studies have demonstrated that NK cells are able to persist several months after *in vivo* stimulation and are able to mount a secondary response (73, 151, 152, 228, 236). Using MCMV, Sun *et al.* generated Ly-49H$^+$ memory NK cells with enhanced protective capability compared to naïve NK cells months after initial MCMV infection (73). Additionally, memory NK cells have been shown to have remarkable antigen specificity to previous chemical haptens and virus like particle stimulations (5, 146, 147, 151). While the mechanisms of antigen specific recognition is still unknown, Paust *et al.* demonstrated that memory NK cells generated against influenza virus-like particles were not stimulated when treated with HIV virus like particles in mice, and vice versa (151). However, specific antigen stimulation of NK cells is not a requirement for memory NK cell generation. Cytokine stimulations of NK cells have also been shown to induce long-lived memory-like NK cells in mice and humans with enhanced IFNγ production capacity upon re-stimulation (142, 144). Additionally, IL-12 has recently been suggested to be indispensable for memory NK cell generation (129).While a number of studies have demonstrated adaptive immune characteristics of NK cells, a definitive memory NK cell marker or markers have not been described.

In this chapter, I aimed to further characterize long-lived Ly-6C expressing cytokine stimulated NK cells. In the previous chapter, and results obtained by others, splenic derived long-lived NK cells express high levels of Ly-6C (73, 237) (Chapter 4). Additionally, I have previously shown that Ly-6C positive NK cells can be sub-divided into two subsets; NK cells expressing Ly-6C reactive to monoclonal AL-21 antibody only (Ly-6C^{AL-21}) or to both monoclonal AL-21 and iMAP antibodies (Ly-6C$^{AL-21/iMAP}$). In this chapter I first characterized the maturation state of Ly-6C^{Neg}, Ly-6C^{AL-21}, Ly-6C$^{AL-21/iMAP}$ NK cell subsets using expression patterns of CD11b, CD27 and KRLG1, established markers for evaluating NK cell developmental maturity (86, 89). While only 50% of Ly-6C^{Neg} NK cells expressed high levels of CD11b and low levels of CD27 (CD11b^{+}CD27^{-}), the vast majority of Ly-6C^{AL-21} and Ly-6C$^{AL-21/iMAP}$ NK cells were CD11b^{+}CD27^{-}. Additionally, a higher percentage of Ly-6C positive NK cells express KLRG1 than Ly-6C^{Neg} NK. These findings collectively suggest Ly-6C^{AL-21} and Ly-6C$^{AL-21/iMAP}$ NK cells are fully mature NK cells and may be further differentiated than Ly-6C negative NK cells. Functionally, I was unable to detect significant differences in IFNγ production from Ly-6C^{Neg}, Ly-6C^{AL-21} and Ly-6C$^{AL-21/iMAP}$ NK cell subsets following cytokine stimulation. However, Ly-6C^{Neg} NK cells did display a slightly higher proliferative capability than Ly-6C positive NK cells seven days after cytokine activation. Furthermore, adoptive transfer of isolated Ly-6C^{Neg}, Ly-6C^{AL-21} and Ly-6C$^{AL-21/iMAP}$ NK cells into congenic hosts not only suggested a developmental progression of Ly-6C^{Neg} NK cells to Ly-6C positive NK cells, but also a differentiation progression from Ly-6C^{Neg}→Ly-6C^{AL-21}→Ly-6C$^{AL-21/iMAP}$ by NK cells. Collectively, I have described a novel stage of NK cells differentiation using Ly-6C reactivity to monoclonal AL-21 and iMAP antibodies expressed by NK cells.

Results

Ly-6C positive NK cells are phenotypically mature NK cells

In the previous chapter, I demonstrated distinct binding characteristics of iMAP and AL-21 to Ly-6C expressed on NK cells and by utilizing both anti-Ly-6C antibodies, I demonstrated three subsets of splenic NK cells based on Ly-6C expression; Ly-6C^{Neg}, Ly-6C$^{AL\text{-}21}$ and Ly-6C$^{AL\text{-}21/iMAP}$ (Chapter 4). Recent studies have suggested that NK cells, or a subset of NK cells, are able to acquire adaptive immune features such as longevity, antigen specificity and enhanced secondary responses in mice (73, 142, 150). In one study, Sun *et al.* demonstrated that MCMV induced Ly-49H$^+$ memory NK cells express high levels of KLRG1 and low levels of CD27, hallmarks of NK cell maturity (73, 87-89). Additionally, memory NK cells also expressed high levels of Ly-6C, a known marker for memory CD8$^+$ T cells (73, 196). However, a notable population of NK cells from uninfected mice also express Ly-6C (73). As such, these NK cells may represent memory NK cells from previous undocumented infections or perhaps generated through homeostatic proliferation, similar to memory phenotype CD8$^+$ T cells generated through homeostatic proliferation (238, 239). Therefore I next sought to further characterize the maturation state of Ly-6C expressing NK cells.

Splenic NK cells from >7 week old mice were identified as NK1.1$^+$CD3ε$^-$ and were further stained with anti-Ly-6C antibodies AL-21 and iMAP as well as anti-CD27, CD11b and KLRG1 antibodies. Based only on Ly-6C expression, the NK cell population was subdivided into Ly-6C^{Neg}, Ly-6C$^{AL\text{-}21}$ and Ly-6C$^{AL\text{-}21/iMAP}$ subsets. Similar to what was previously shown in Chapter 4, the majority of the NK cells were negative for Ly-6C expression, however, around 20% of the NK cells were stained by AL-21 and 10% were double stained by AL-21 and iMAP (Figure 5-1 A). In terms of NK cell maturity, NK cells develop through four distinct stages; CD11b$^-$CD27$^-$→ CD11b$^-$CD27$^+$→ CD11b$^+$CD27$^+$→ CD11b$^+$CD27$^-$ (79, 88). While CD11b$^+$ NK cells are considered mature NK cells, it is clear that CD11b$^+$CD27$^-$ NK cells are further differentiated than CD11b$^+$CD27$^+$ NK cells and are thought to be a population of terminally differentiated NK cells (86). Among the splenic NK cell population, there was a similar frequency of CD11b$^-$CD27$^+$, CD11b$^-$CD27$^+$ and CD11b$^+$CD27$^+$ NK

cells, with a separate population of $CD11b^{+}CD27^{-}$ NK cells making up a majority of the NK cells (Figure 5-1 A). As the bulk of NK cells were fully differentiated, I next sought to examine the specific relationship between Ly-6C, CD11b and CD27 expression on splenic NK cells. When sub-divided, based on Ly-6C expression and staining, around 50% of $Ly\text{-}6C^{Neg}$ NK cells displayed a mature $CD11b^{+}CD27^{-}$ phenotype. Additionally, I observed a similar distribution of $CD11b^{-}CD27^{-}$, $CD11b^{-}CD27^{+}$ and $CD11b^{+}CD27^{+}$ $Ly\text{-}6C^{Neg}$ NK cells when compared to the analysis of CD11b and CD27 expression from the whole splenic NK cell population (Figure 5-1 B). When $Ly\text{-}6C^{AL\text{-}21}$ and $Ly\text{-}6C^{AL\text{-}21/iMAP}$ NK cell subsets were analyzed, the majority of NK cells were $CD11b^{+}CD27^{-}$, 80% and 75%, respectively, with a small cluster of $CD11b^{-}CD27^{+}$ NK cells present in both Ly-6C expressing NK cell subsets (Figure 5-1 B).

In addition to CD11b and CD27 expression, KLRG1 has also been described as a marker of NK cells differentiation (89). Previous studies have suggested that NK cells acquire KLRG1 expression only during later stages of maturation, specifically, only on $CD11b^{+}CD27^{-}$ NK cells (87, 89). Among $Ly\text{-}6C^{Neg}$ NK cells, while nearly half of the cells are $CD11b^{+}CD27^{-}$, only a small subset of these NK cells express KLRG1 (Figure 5-1 C). In contrast, between 30% and 40% of $Ly\text{-}6C^{AL\text{-}21}$ and $Ly\text{-}6C^{AL\text{-}21/iMAP}$ NK cells were KLRG1 positive, respectively (Figure 5-1 C). Additionally, in accordance with previous studies, KLRG1 expression was not observed on $CD11b^{-}CD27^{-}$, $CD11b^{-}CD27^{+}$ and $CD11b^{+}CD27^{+}$ NK cells (Figure 5-1 D). Collectively, my results suggest that Ly-6C positive NK cells are mature based on CD11b expression and representing a subset of $CD11^{+}CD27^{-}$ NK cells. Additionally, as a much higher percentage of $Ly\text{-}6C^{AL\text{-}21}$ and $Ly\text{-}6C^{AL\text{-}21/iMAP}$ NK cells are also KLRG1 positive, Ly-6C expressing NK cells may be further differentiated NK cells than $Ly\text{-}6C^{Neg}$ NK cells.

Ly-6C expressing NK cells produce IFNγ at comparable levels to $Ly\text{-}6C^{Neg}$ NK cells

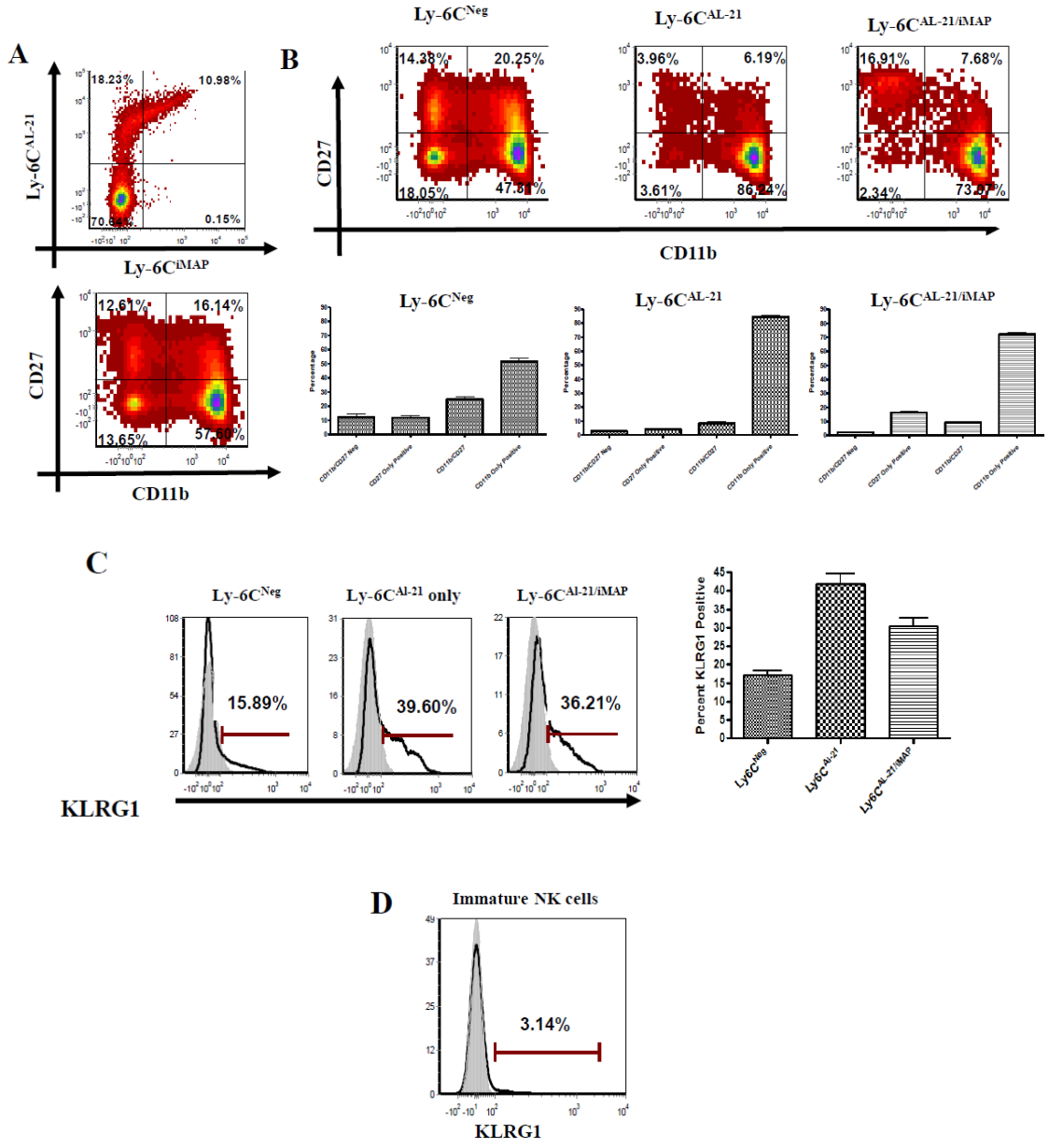

Figure 5-1: Ly-6C expressing NK cells express high levels of maturation markers CD11b and KLRG1.

Splenic NK cells from 7 week old mice were stained with AL-21, iMAP, anti-CD27, CD11b and KLRG1 antibodies. Dot plots represent expression of AL-21 or AL-21/iMAP double reactive Ly-6C molecules on whole splenic NK cells and staining of CD11b and CD27 on whole splenic NK cells (A). Ly-6C^{Neg}, Ly-6C^{AL-21} and Ly-6C$^{AL-21/iMAP}$ NK cell subsets were further analyzed for their expression of CD11b, CD27 and KLRG1. Dot plots represent typical distribution of CD11b and CD27 staining on

Ly-6C^{Neg}, Ly-6C^{AL-21} and Ly-6C$^{AL-21/iMAP}$ NK cell (B). Histogram represents expression patterns of KLRG1 on Ly-6C^{Neg}, Ly-6C^{AL-21} and Ly-6C$^{AL-21/iMAP}$ NK cell (C). KLRG1 was not detected on immature NK cells defined as CD11b negative and CD11b^{+}CD27^{+} NK cells (D). Shaded histograms represent isotype control staining. Bar graphs represent mean of at least three experiments ± SEM in B and C.

A primary response of NK cells during host defense against foreign pathogens is the production of cytokines (229). Upon activation from cytokines or engagement of NK cell activating receptors, mature NK cells are able to produce large quantities of IFNγ (87, 229). Additionally, Sato *et al.* had previously suggested enhanced IFNγ secretion capabilities among Ly-6C positive NK cells compared to Ly-6C^{Neg} NK cells (223). Because Ly-6C$^{AL\text{-}21}$ and Ly-6C$^{AL\text{-}21/iMAP}$ NK cells display a mature phenotype, I next sought to further define the functional properties of Ly-6C^{Neg}, Ly-6C$^{AL\text{-}21}$ and Ly-6C$^{AL\text{-}21/iMAP}$ NK cells; in particular, IFNγ production following pro-inflammatory cytokine stimulations.

To mitigate potential Ly-6C expression changes during stimulation, splenic NK cells from unchallenged mice were sorted into Ly-6C^{Neg}, Ly-6C$^{AL\text{-}21}$ and Ly-6C$^{AL\text{-}21/iMAP}$ subsets and stimulated separately with IL-12 (10ng/ml) and IL-15 (10ng/ml) or IL-15 (10ng/ml) only, as a control, as previously performed (142, 144). Brefeldin A (BFA), which inhibits protein trafficking from the ER to the Golgi, was then added to the culture after the first hour and intracellular IFNγ production in the NK cells examined via flow cytometry after four hours of stimulation (Figure 5-2 A). The sort purity of NK cells from spleens, based on CD3ε^{-} NK1.1^{+} phenotype, was typically >90% (Figure 5-2 B). Additionally, the purity of sorted Ly-6C^{Neg}, Ly-6C$^{AL\text{-}21}$ and Ly-6C$^{AL\text{-}21/iMAP}$ NK cell subsets was typically between 70% to 90% (Figure 5-2 C). Following culture, IL-15 only stimulated NK cells did not produce notable levels of IFNγ. Not surprisingly, no more than 10% of the Ly-6C^{Neg}, Ly-6C$^{AL\text{-}21}$ and Ly-6C$^{AL\text{-}21/iMAP}$ unstimulated NK cells expressed IFNγ above background levels from my flow cytometry data (Figure 5-2 D). In contrast, between 35% and 40% of the Ly-6C^{Neg}, Ly-6C$^{AL\text{-}21}$ and Ly-6C$^{AL\text{-}21/iMAP}$ NK cells stimulated with IL-12 and IL-15 stained positive for IFNγ production (Figure 5-2 D). From the histogram, a distinct population of IFNγ producing NK cells was clearly observed based on the fluorescence intensity (Figure 5-2 D). However, the fluorescence intensity of IFNγ expressing NK cells was comparable between Ly-6C^{Neg}, Ly-6C$^{AL\text{-}21}$ and Ly-6C$^{AL\text{-}21/iMAP}$ NK cell subsets (Figure 5-2 D). Collectively, my results suggest that Ly-6C^{Neg},

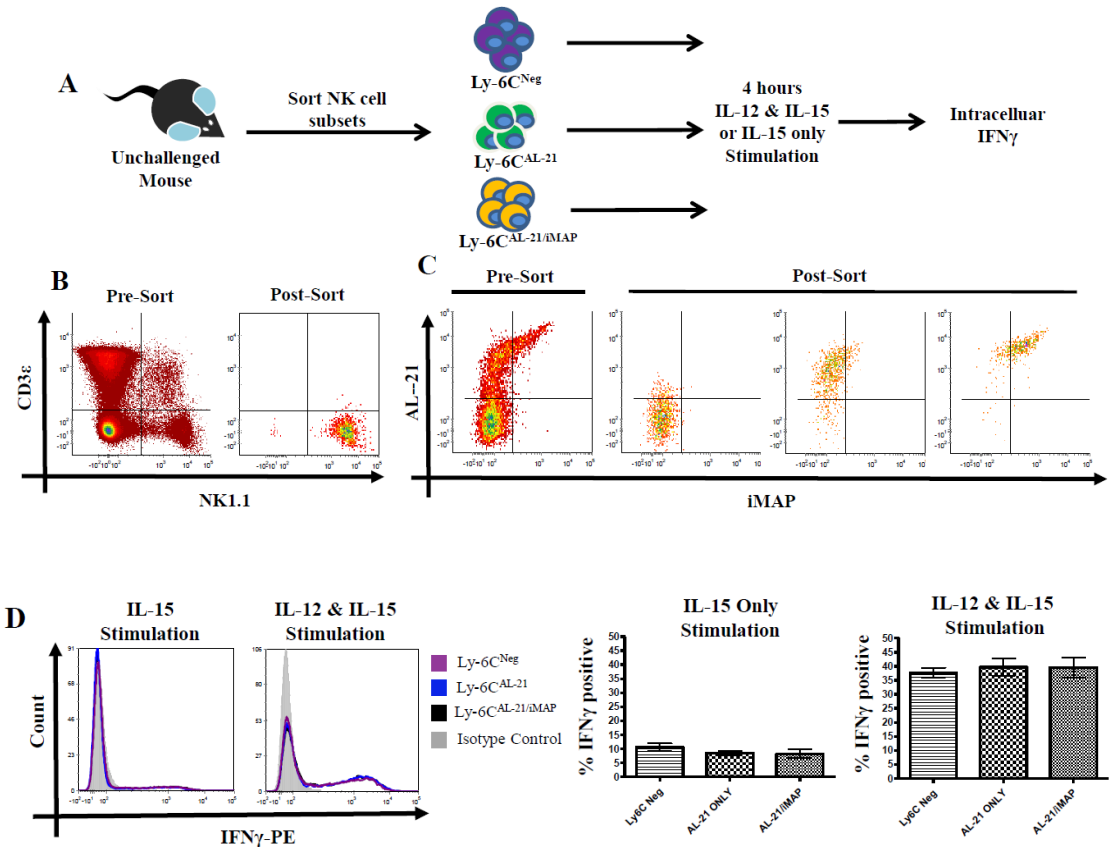

Figure 5-2: Ly-6C^{Neg,} Ly-6C^{AL-21} and Ly-6C$^{AL-21/iMAP}$ NK Cells produce IFNγ equivalently following cytokine stimulation.
Ly-6C^{Neg}, Ly-6C^{AL-21} and Ly-6C$^{AL-21/iMAP}$ NK cells were isolated from unchallenged mice via cell sorting and stimulated with IL-12 and IL-15, or IL-15 only, for fours. Intracellular production of IFNγ was then determined by flow cytometry (A). Distribution of NK1.1 and CD3ε positive splenocytes pre- and post-sort are shown. NK cells purity was generally greater than 95% purity post sort (B). Pre- and post-sort distribution of Ly-6C^{Neg}, Ly-6C^{AL-21} and Ly-6C$^{AL-21/iMAP}$ NK cells are shown. Post sort, Ly-6C^{Neg}, Ly-6C^{AL-21} and Ly-6C$^{AL-21/iMAP}$ NK cell purity was typically between 70% to 90% (C). Histograms are representative of intracellular IFNγ production in Ly-6C^{Neg} (purple), Ly-6C^{AL-21} (blue) and Ly-6C$^{AL-21/iMAP}$ (black) sorted NK cells after four hour stimulation with IL-15 only (left) or IL-12 and IL-15 (right). Shaded histogram represents isotype staining control. Bar graphs represents mean of at least three experiments ± SEM in D.

Ly-6C^{AL-21} and Ly-6C$^{AL-21/iMAP}$ NK cell subsets are able to rapidly produce IFNγ following IL-12 and IL-15 stimulation. Furthermore, while a larger proportion of Ly-6C positive NK cells were fully mature (CD11b^{+}CD27^{-}), there were no significant differences in IFNγ production between all three subsets of NK cells.

Ly-6C expressing NK cells are less proliferative than Ly-6C^{Neg} NK cells

From previous studies, CD11b positive NK cells have been suggested to have a diminished homeostatic proliferative capability compared to CD11b negative NK cells while matured CD11b^{+}CD27^{-} NK cells have a further reduced proliferative ability than CD11b^{+}CD27^{+} NK cells (87, 88). In addition, in line with KLRG1 as a marker for further differentiated NK cells, KLRG1^{+} NK cells have also been suggested to have a lower proliferative capacity than KLRG1 negative NK cells (89). As Ly-6C expressing NK cells have a notably higher proportion of CD11b^{+}CD27^{-}KLRG1^{+} NK cells than Ly-6C^{Neg} NK cells, I next wanted to examine the proliferative potential of Ly-6C^{Neg}, Ly-6C^{AL-21} and Ly-6C$^{AL-21/iMAP}$ NK cells.

NK cells were sorted into Ly-6C^{Neg}, Ly-6C^{AL-21} and Ly-6C$^{AL-21/iMAP}$ subsets and stimulated overnight with IL-12 (10ng/ml), IL-18 (50ng/ml) and IL-15 (10ng/ml), as previously described (142). The next day the cells were labeled with CellTrace Violet Proliferation Kit, a fluorescent membrane permeable dye, and transferred via tail vain injection at equal numbers into separate age-matched sub-lethally irradiated mice. CellTrace Violet Proliferation Kit allowed for the tracking of the cytokine stimulated NK cells as well as cell proliferation by flow cytometry. An advantage of using proliferation dyes, such as CellTrace Violet, is the ability to identify the specific number of rounds of cell division for proliferating daughter cells. *In vivo* proliferation of NK cells are readily observed as early as seven days following stimulation (142, 143).

First I examined possible changes in Ly-6C expression following overnight cytokine stimulation. Ly-6C^{Neg}, Ly-6C^{AL-21} and Ly-6C$^{AL-21/iMAP}$ splenic NK cells were isolated via cell sorting (Figure 5-3 A). The cells were then stimulated with IL-

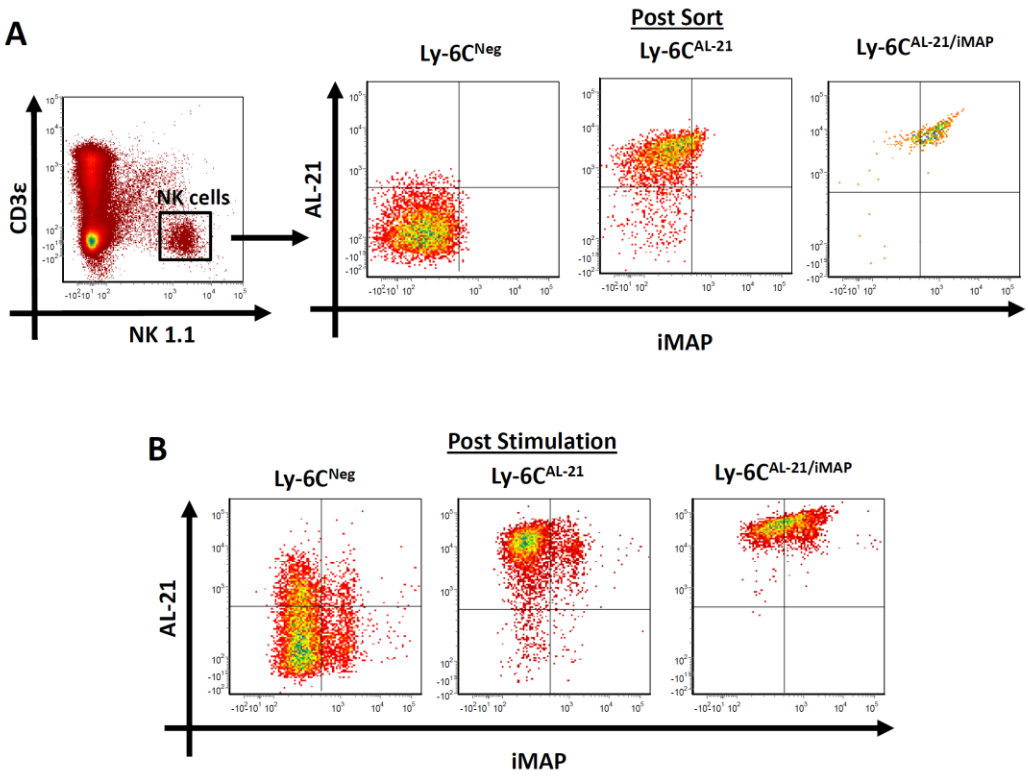

Figure 5-3: Ly-6C expression is largely unchanged during overnight cytokine stimulations.
Ly-6C^{Neg}, Ly-6C$^{AL\text{-}21}$ and Ly-6C$^{AL\text{-}21/iMAP}$ NK cells were isolated from NK1.1^{+}CD3ε^{-} splenocytes by cell sorting (A). Post-sort, Ly-6C^{Neg}, Ly-6C$^{AL\text{-}21}$ and Ly-6C$^{AL\text{-}21/iMAP}$ NK cells were stimulated overnight with IL-12, IL-18 and IL-15. The next day, stimulated Ly-6C^{Neg}, Ly-6C$^{AL\text{-}21}$ and Ly-6C$^{AL\text{-}21/iMAP}$ NK cells were re-stained with AL-21 and iMAP antibodies and Ly-6C expression determined by flow cytometry (B). Dot plot is representative of three experiments.

12, IL-18 and IL-15 overnight and the next day, re-stained with AL-21 and iMAP and expression of Ly-6C examined by flow cytometry. No dramatic changes in Ly-6C expression were observed following stimulation (Figure 5-3 B). The expression levels and pattern of Ly-6C^{Neg}, Ly-6C$^{AL\text{-}21}$, Ly-6C$^{Al\text{-}21/iMAP}$ NK cells remained relatively similar after stimulation compared to after isolation (Figure 5-3 B).

Seven days post-transfer, of sorted and stimulated NK cell subsets, I examined the proliferation of Ly-6C^{Neg}, Ly-6C$^{AL\text{-}21}$ and Ly-6C$^{AL\text{-}21/iMAP}$ NK cells in the spleen based on CellTrace Violet dye dilution by flow cytometry (Figure 5-4 A). From my results, cytokine stimulated Ly-6C^{Neg}, Ly-6C$^{AL\text{-}21}$ and Ly-6C$^{AL\text{-}21/iMAP}$ NK cells all proliferated extensively *in vivo* (Figure 5-4 B). Based on the number of violet dye dilutions, a number of Ly-6C^{Neg}, Ly-6C$^{AL\text{-}21}$ and Ly-6C$^{AL\text{-}21/iMAP}$ NK cells progressed through four to five rounds of division in seven days (Figure 5-4 B). While the majority, over 80%, of Ly-6C^{Neg}, Ly-6C$^{AL\text{-}21}$ and Ly-6C$^{AL\text{-}21/iMAP}$ NK cells proliferated, there was no observable difference in the percentage of proliferated cells between the different NK cell subsets (Figure 5-4 C). However, upon closer examination, there was a significantly higher proportion of Ly-6C^{Neg} NK cells (>50%) that proliferated four or more times than Ly-6C$^{AL\text{-}21}$ and Ly-6C$^{AL\text{-}21/iMAP}$ NK cells (<40%) (Figure 5-4 C). Collectively, my results suggest that while Ly-6C$^{AL\text{-}21}$ and Ly-6C$^{AL\text{-}21/iMAP}$ NK cells are highly proliferative following cytokine stimulation, Ly-6C^{Neg} NK cells are more capable of sustaining extensive rounds of proliferation than Ly-6C expressing NK cells. These results further support the notion that Ly-6C expressing NK cells may represent a further differentiated population of NK cells as proliferation potential typically diminishes with differentiation cell state (89).

Sub-lethal irradiation enhances survival of adoptive transferred NK cells without altering Ly-6C expression on host and transferred NK cells six weeks post transfer

From my preliminary results in Chapter 4, I showed that long-lived NK cells are present within the Ly-6C^{+} population of NK cells. My previous findings resemble memory NK cell phenotypes generated following MCMV infections (73). Among

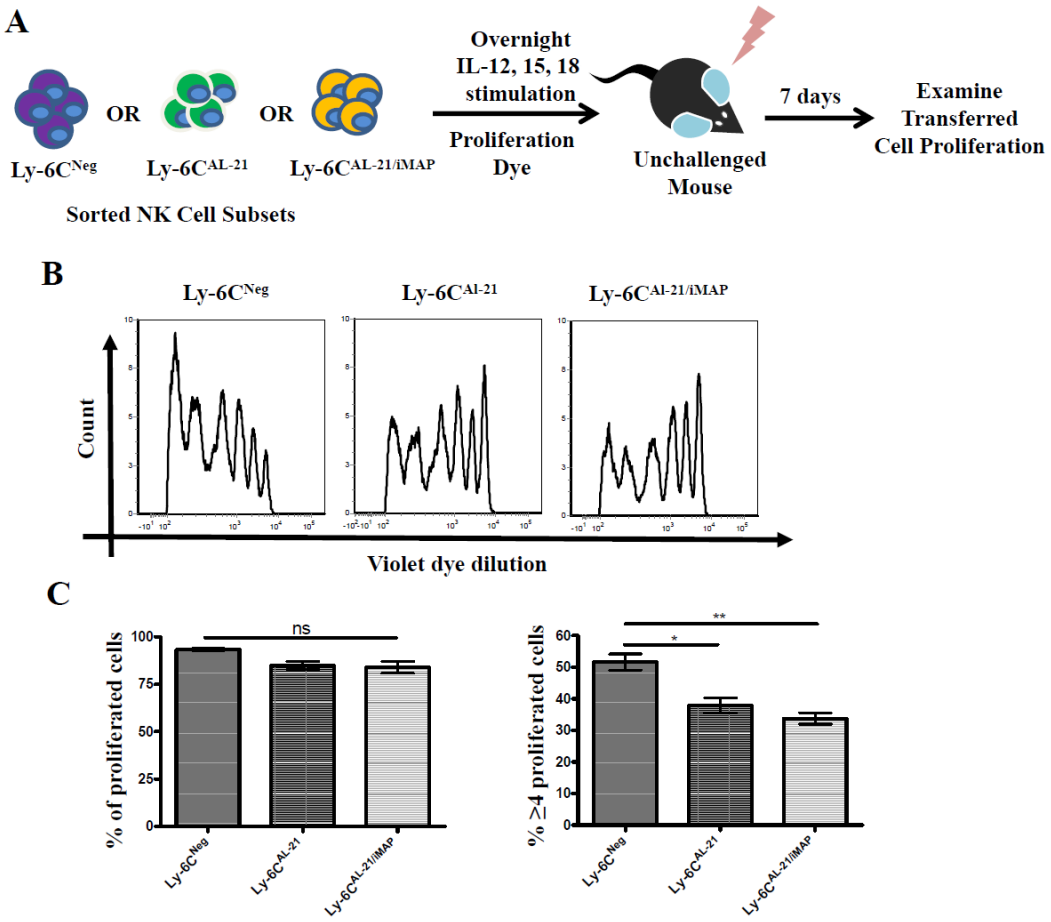

Figure 5-4: Ly-6C^{Neg} NK cells have higher proliferative capabilities than Ly-6C^{AL-21} and Ly-6C$^{AL-21/iMAP}$ NK cells.
Sorted Ly-6C^{Neg}, Ly-6C^{AL-21} and Ly-6C$^{AL-21/iMAP}$ NK cells were activated separately overnight with IL-12, IL18 and IL-15. The next day the NK cells were labeled with CellTrace Violet Dye from Life Technologies and adoptively transferred via tail vein injection into separate sub-lethally irradiated recipient mice. Seven days post-transfer, proliferation of transferred NK cells was determined by examining violet dye dilutions via flow cytometry (A). Histogram show typical violet dye dilution peaks of stimulated Ly-6C^{Neg}, Ly-6C^{AL-21} and Ly-6C$^{AL-21/iMAP}$ NK cells seven days post transfer (B). Bar graphs display percentage of proliferated NK cells (left) or percentage of NK cells that have undergone ≥4 rounds of proliferation (right) (C). Bar graphs represent mean of at least three experiments ± SEM in C. * $p<0.05$, **$p<0.01$ and n.s. not significant.

long-lived Ly-6C expressing NK cells, I observed a large increase in the percentage of Ly-6C$^{AL\text{-}21/iMAP}$ NK cells (Chapter 4). However, in those preliminary experiments, recipient congenic mice were fully immune competent at the time of adoptive transfer of cytokine stimulated NK cells. Consequently, the recovery of transferred NK cells six weeks post transfer were extremely low and posed significant difficulties to the further analysis of these long-lived NK cells. As a result, to increase recovery of long-lived NK cells, recipient mice were sub-lethally irradiated prior to adoptive transfer of stimulated NK cells. Sub-lethal irradiation of recipient mice temporarily reduces host lymphocyte populations and enhances establishment of transferred NK cells (116).

Sorted splenic NK cells were stimulated with IL-12, IL-18 and IL-15 overnight and adoptively transferred into age-matched sub-lethally irradiated CD45.1^{+} congenic mice the next day. Six weeks after transfer, Ly-6C expression on transferred and host NK cells from the spleen were examined using AL-21 and iMAP (Figure 5-5 A). Host and adoptively transferred NK1.1^{+}CD3ε^{-} NK cells from the spleen were identified based on CD45.2^{-}CD45.1^{+} and CD45.2^{+}CD45.1^{-}, respectively. Six weeks post transfer, sub-lethal irradiation of recipient mice significantly increased the recovery of adoptively transferred NK cells. Without irradiation, transferred NK cells represented less than 2% of the total NK cell population (Chapter 4). In contrast, following sub-lethally irradiation of recipient congenic mice, transferred NK cells represented greater than 5% of the NK cell population (Figure 5-5 B). Six weeks post transfer, half of the unstimulated splenic host NK cells did not express Ly-6C while around 40% and 10% of host NK cells were stained by AL-21 or AL-21 and iMAP, respectively (Figure 5-5 C). These findings were similar to previous results of NK cells from naïve unchallenged >7 week old mice (Chapter 4). In contrast, less than 20% of cytokine stimulated long-lived transferred CD45.2^{+} NK cells were Ly-6C negative while the majority of transferred NK cells expressed Ly-6C (Figure 5-5 C). Among these NK cells, over 50% of the cytokine stimulated long-lived NK cells were stained by AL-21 only while Ly-6C$^{AL\text{-}21/iMAP}$ NK cells represented nearly 30% of the

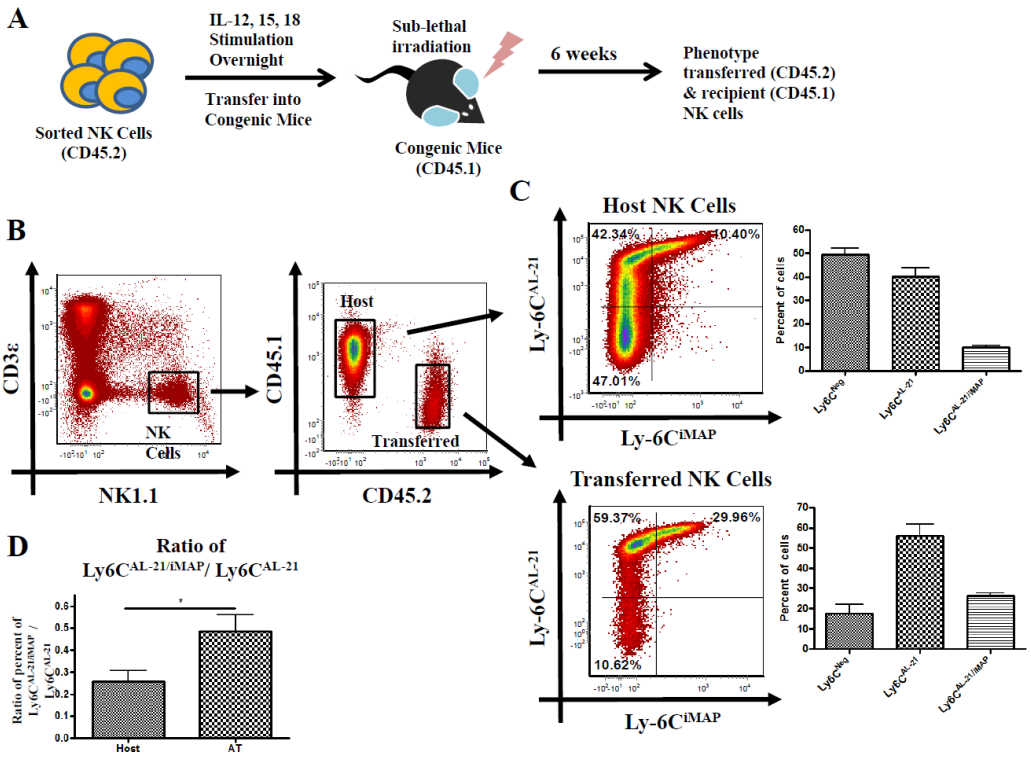

Figure 5-5: Long-lived NK cells are high expressers of Ly-6C.
Sorted NK1.1^{+}CD3ε^{-} NK cells from wild-type CD45.2^{+} C57BL/6 mice were stimulated overnight with IL-12, IL-18 and IL-15 and adoptively transferred into sub-lethally irradiated age-matched congenic CD45.1^{+} mice. Six weeks post transfer, staining of AL-21 and iMAP on host (CD45.1^{+}) and transferred (CD45.2^{+}) NK cells were examined by flow cytometry (A). Host (CD45.1^{+}) and transferred (CD45.2^{+}) NK cells were sub-gated from NK1.1^{+}CD3ε^{-} splenocytes (B). Representative distribution of host (CD45.1^{+}) and transferred (CD45.2^{+}) Ly-6C^{Neg}, Ly-6C^{AL-21} and Ly-6C$^{AL-21/iMAP}$ NK cells six weeks post transfer of stimulated NK cells are shown (C). Relative ratio of the percentage of Ly-6C^{AL-21} and Ly-6C$^{AL-21/iMAP}$ of host and adoptive transferred NK cells (D). Bar graphs in C and D represent mean of at least three experiments ± SEM. * $p<0.05$.

long-lived transferred NK cells (Figure 5-5 C). Among all Ly-6C positive NK cells, long-lived transferred NK cells had a significantly higher ratio of Ly-6C$^{AL\text{-}21/iMAP}$ to Ly-6C$^{AL\text{-}21}$ NK cells compared to host NK cells in the spleen (Figure 5-5 D). Collectively, my results suggest that cytokine stimulated long-lived splenic NK cells express high levels of Ly-6C with a higher proportion of long-lived NK cells from spleen expressing Ly-6C stained by both AL-21 and iMAP compared to unstimulated host NK cells from age-matched recipient mice. While these results may be influenced by the activation of transferred NK cells with cytokines, previous preliminary data using NK cells cultured with low dose of IL-15, which is required for NK cell survival and does not induce NK cell activation, suggests that increase in Ly-6C expressing NK cells over time may be an intrinsic property of long-lived splenic NK cells (Chapter 4). Additionally, sub-lethal irradiation of recipient mice enhanced the recovery of the adoptively transferred NK cells six weeks post transfer without prevent the expression of Ly-6C on host and cytokine pre-activated transferred NK cells.

Long-lived NK cells display a mature phenotype

Phenotypically, expression of KLRG1 and CD11b have been utilized to identify mature NK cells (87-89). Interestingly, splenic memory NK cells generated from MCMV infections have also been shown to express low levels of CD27 and high levels of KLRG1 >70 days after infection (73). Therefore, I next wanted to determine the distribution and expression level of CD27, CD11b and KLRG1 on cytokine stimulated long-lived NK cells.

As before, NK cells were purified via sorting of NK1.1^{+}CD3ε^{-} splenocytes and stimulated overnight with IL-12, IL-18 and IL-15 and adoptively transferred into sub-lethally irradiated CD45.1^{+} congenic mice. Six weeks post transfer, expression of CD27, CD11b and KLRG1 were examined on NK cells isolated from the spleen. To distinguish host and transferred NK cells, NK1.1^{+}CD3ε^{-} NK cells were further divided into CD45.2^{+}CD45.1^{-} transferred NK cells and CD45.2^{-}CD45.1^{+} host NK

cells. Not surprisingly, in accordance with my previous observations in unchallenged mice, host NK cells displayed a similar distribution of CD11b and CD27 expression (Figure 5-6 A). Around half of the host NK cells were matured NK cells expressing a $CD11b^{+}CD27^{-}$ phenotype while no more than 20% of the host NK cells were found in each of the other $CD11b^{-}CD27^{-}$, $CD11b^{-}CD27^{+}$ or $CD11b^{+}CD27^{+}$ NK cell subsets (Figure 5-6 A). In contrast, greater than 90% of long-lived adoptively transferred NK cells were $CD11b^{+}CD27^{-}$ while only a low percentage of long-lived NK cells were found in the $CD11b^{-}CD27^{-}$, $CD11b^{-}CD27^{+}$ or $CD11b^{+}CD27^{+}$ NK cell subsets (Figure 5-6 A). In terms of KLRG1 expression, a significantly higher percentage of long-lived NK cells expressed KLRG1 compared to host NK cells (Figure 5-6 B). In fact, less than half of the host NK cells expressed high levels of KLRG1 compared to over 90% of long-lived transferred NK cells (Figure 5-6 B). Collectively, my results suggest that long-lived splenic NK cells may be found in the population of $CD11b^{+}CD27^{-}$ and KLRG1 expressing NK cells; a phenotype associated with fully mature and fully differentiated NK cells.

Long-lived NK cell respond to cytokine re-stimulation

Thus far, I have characterized long-lived splenic NK cells as a population of Ly-6C expressing NK cells with an increased ratio of $Ly\text{-}6C^{AL\text{-}21/iMAP}$ NK cells to $Ly\text{-}6C^{Al\text{-}21}$ NK cells compared to unstimulated NK cells. Not surprisingly, long-lived splenic NK cells expressed high levels of KLRG1 and CD11b and lacked CD27 expression (Figure 5-6); a phenotype of mature NK cells (87-89). Additionally, Cooper *et al.* previously demonstrated enhanced IFNγ production from long-lived cytokine stimulated NK cells compared to untreated NK cells (142). However, their study was performed using Rag1-deficient mice which contains enhanced NK cell numbers and lack any mature B and T cells (7, 227). Interestingly, Andrews *et al.* recently suggested a potential role for Rag1 in NK cell development independent of known Rag1-dependent cells such as T and B cells (240). Therefore, I next wanted to examine the functionality of long-lived NK cells generated in Rag1sufficient

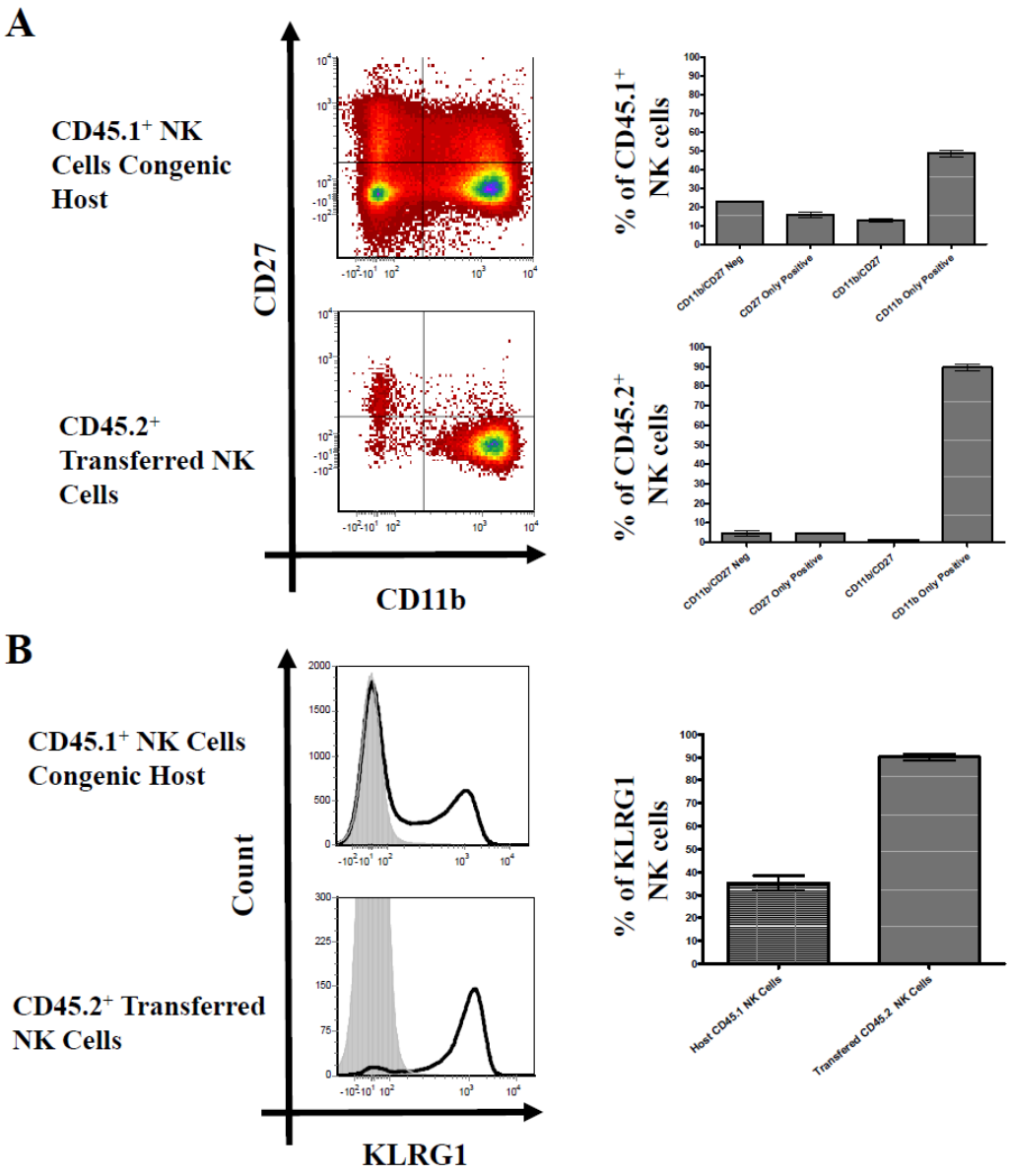

Figure 5-6: Long-lived NK cells express high levels of CD11b and KLRG1. NK cells were sorted from C57BL/6 mice, activated with IL-12, IL-18 and IL-15 and transferred into sub-lethally irradiated age-matched CD45.1$^+$ congenic mice as depicted in Figure 5-4 A. Distribution of CD11b, CD27 and KRLG1 was examined by flow cytometry on host (CD45.1$^+$) and pre-activated adoptively transferred (CD45.2$^+$) NK cells six weeks post adoptive transfer. Dot plot shows representative expression patterns of CD11b and CD27 on CD45.1$^+$and CD45.2$^+$ NK cells from

spleen (A). Histogram displays typical expression of KLRG1 on $CD45.1^+$ and $CD45.2^+$ NK cells from spleen (B). Shaded histograms represent isotype staining control. Bar graphs represent mean of at least three experiments ± SEM in A and B.

wild-type mice.

Splenic NK1.1^{+}CD3ε^{-} NK cells were sorted and stimulated with IL-12, IL-18 and IL-15 overnight and transferred via tail vein injection into sub-lethally irradiated CD45.1^{+} congenic mice (Figure 5-7 A). Six weeks post transfer, NK cells from the spleen of the recipient mice were purified again by cell sorting of NK1.1^{+}CD3ε^{-} cells and stimulated with IL-12 and IL-15 or IL-15 only, as control, for four hours. After the first hour, BFA was added and NK cell intracellular production of IFNγ was determined by flow cytometry (Figure 5-7 A). Host and transferred NK1.1^{+}CD3ε^{-} NK cells were distinguished based on CD45.1^{+}CD45.2^{-} and CD45.1^{-}CD45.2^{+} expression, respectively (Figure 5-7 B). Following culture, as expected, IL-15 stimulation did not induce IFNγ production from CD45.1^{+} host or CD45.2^{+} pre-activated transferred NK cells (Figure 5-7 C). Following IL-12 and IL-15 stimulation, host and pre-activated long-lived transferred NK cells had a similar percentage of IFNγ producing cells and level of IFNγ production (Figure 5-7 C). Collectively, these results suggest that cytokine pre-activated long-lived NK cells generated from Rag1 sufficient mice do not have enhanced IFNγ production capabilities compared to the unchallenged NK cells. Interestingly, my results differ significantly from previous cytokine pre-activated long-lived NK cells experiments conducted using Rag1 deficient mice (142). However, as cytokine pre-activated long-lived NK cells are greatly enriched among the Ly-6C positive population of NK cells, I therefore next sought to examine the IFNγ production capabilities of long-lived NK cells within each Ly-6C^{Neg}, Ly-6C^{AL-21} and Ly-6C$^{AL-21/iMAP}$ subset.

As before, isolated splenic NK cells were stimulated with IL-12, IL-15 and IL-18 overnight and adoptively transferred into sub-lethally irradiated congenic mice, as described before. Six weeks post transfer, Ly-6C^{AL-21}, Ly-6C$^{Al-21/iMAP}$ and Ly-6C^{Neg} NK cells from recipient mice spleens were isolated via cell sorting and stimulated separately with IL-12 and IL-15 for four hours with the addition of BFA after the first hour of stimulation (Figure 5-8 A). Host and previously transferred NK cells were again identified based on CD45.1 and CD45.2 staining (Figure 5-8 B).

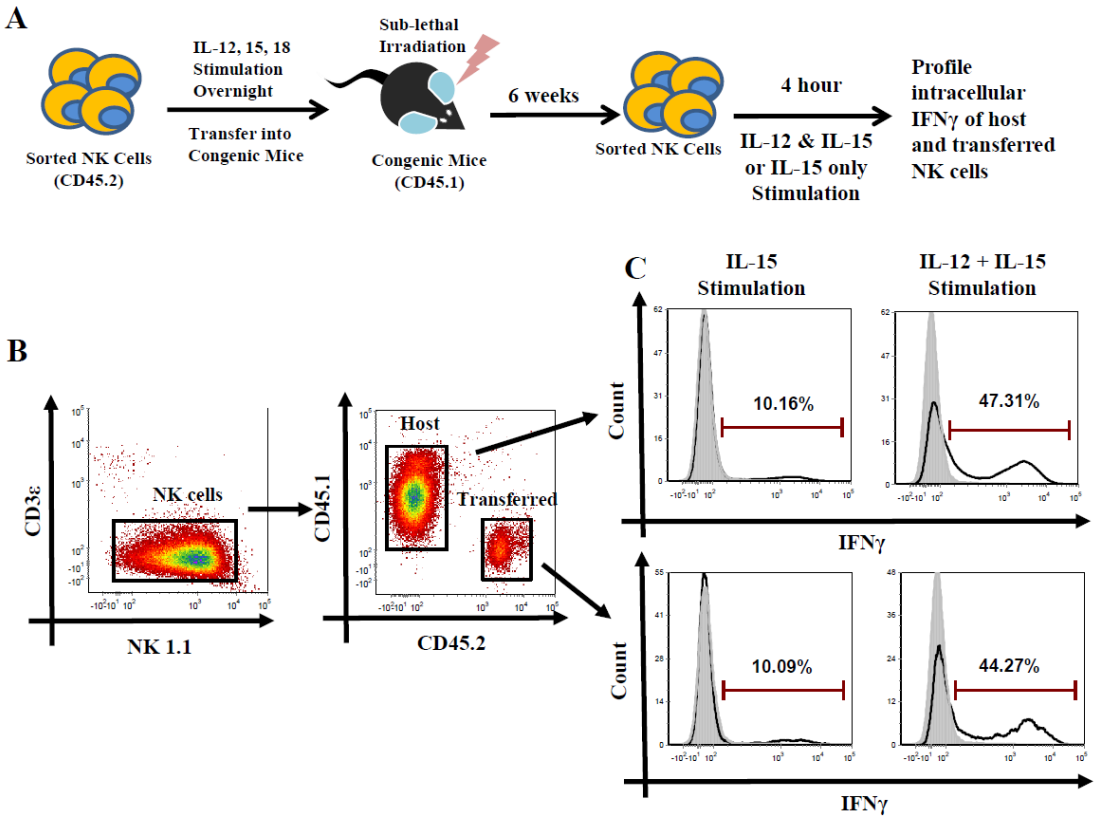

Figure 5-7: Long-lived NK cells as a whole do not have enhanced IFNγ production capacity.
NK cells from CD45.2$^+$ C57BL/6 mice were isolated via cell sorting and stimulated with IL-12, IL-18 and IL-15 overnight and transferred into sub-lethally irradiated age-matched CD45.1$^+$ congenic mice the next day. Six weeks post transfer, NK cells from the recipient mice spleens were sorted and stimulated for four hours with IL-12 and IL-15 or IL-15 only and intracellular IFNγ production was determined by flow cytometry in host CD45.1$^+$ and adoptively transferred CD45.2$^+$ NK cells (A). Following a four hour stimulation, host (CD45.1$^+$) and transferred (CD45.2$^+$) NK cells were sub-gated from NK1.1$^+$CD3ε$^-$ NK cells (B). Histogram is a representative of intracellular IFNγ by host (top) and adoptively transferred (bottom) NK cells post stimulation with IL-15 only (left) or IL-12 and IL-15 (right) (C). Histogram represents one of two experiments.

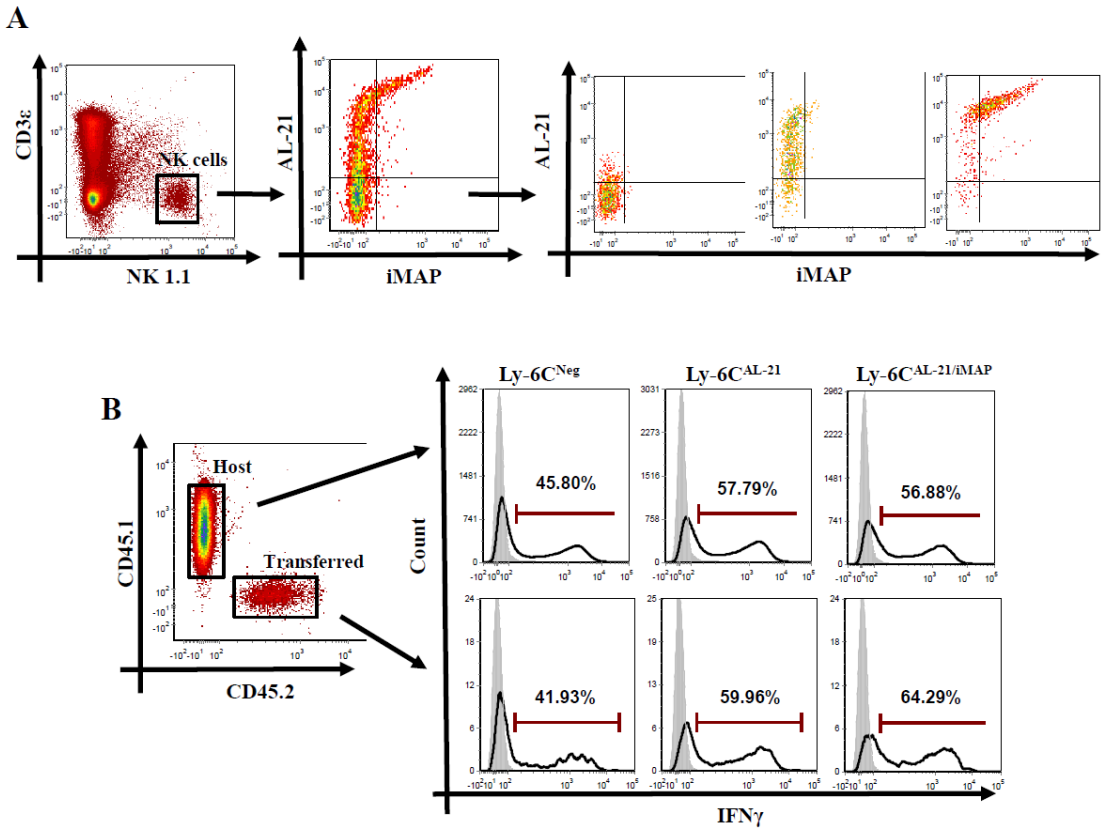

Figure 5-8: Long-Lived Ly-6C^{AL-21} and Ly-6C$^{AL-21/iMAP}$ NK cells have slightly enhanced IFNγ capacity.
Cytokine activated long-lived NK cells were generated as previously described in Figure 5-4 A. Six weeks post transfer, Ly-6C^{Neg}, Ly-6C^{AL-21} and Ly-6C$^{AL-21/iMAP}$ NK cells were purified from NK1.1^{+} CD3ε^{-} splenocyte population via cell sorting (A). Post sort, Ly-6C^{Neg}, Ly-6C^{AL-21} and Ly-6C$^{AL-21/iMAP}$ NK cells were stimulated with IL-12 and IL-15 for four hour, as previously described. Post culture, host and long-lived previously transferred NK cells were identified by CD45.1 and CD45.2 surface staining. Intracellular production of IFNγ of Ly-6C^{Neg} (left), Ly-6C^{AL-21} (middle) and Ly-6C$^{AL-21/iMAP}$ (right) host (top) and adoptively transferred long-lived (bottom) NK cells were determined by flow cytometry (B). Shaded histograms represent isotype control staining. Data presented is representative of one of two experiments.

Following stimulation, a substantial population of host NK cells produced IFNγ with over 50% of host Ly-6C^{AL-21} and Ly-6C$^{AL-21/iMAP}$ NK cells and 40% of Ly-6C^{Neg} NK cells staining positive for IFNγ production (Figure 5-8 B). For CD45.2^{+} long-lived NK cells, roughly 40% of Ly-6C^{Neg} long-lived NK cells produced IFNγ while approximately 60% or more of Ly-6C^{AL-21} and Ly-6C$^{AL-21/iMAP}$ long-lived NK cells produced high levels of IFNγ following stimulation, respectively (Figure 5-8 B). Collectively, my results suggest that among cytokine stimulated long-lived NK cells, Ly-6C^{AL-21} and Ly-6C$^{AL-21/iMAP}$ NK cells have a slightly enhanced IFNγ production capability compared to long-lived Ly-6C^{Neg} NK cells.

Ly-6C$^{AL-21/iMAP}$ NK cells mature from Ly-6C^{AL-21} and Ly-6C^{Neg} NK cells

From my results and others, long-lived NK cells are enriched within the Ly-6C positive population of NK cells (73, 237) (Figure 5-5 C). Additionally, I have demonstrated two distinct populations of Ly-6C expressing NK cells, Ly-6C^{AL-21} and Ly-6C$^{AL-21/iMAP}$ NK cells. While these results suggest Ly-6C expression may be used as a potential cell surface marker for long-lived or "memory" NK cells, whether acquisition of Ly-6C expression represents a developmental progress for long-lived NK cells or expression of Ly-6C represents a distinct subset of NK cells capable of longevity has not been fully examined. Therefore, I next sought to examine the relationship between Ly-6C^{Neg}, Ly-6C^{AL-21} and Ly-6C$^{AL-21/iMAP}$ NK cells.

To determine the relationship of Ly-6C expression to long-lived NK cell development, purified Ly-6C^{Neg}, Ly-6C^{Al-21} and Ly-6C$^{AL-21/iMAP}$ NK cells were stimulated separately with IL-12, IL-15 and IL-18 overnight and adoptively transferred into separate sub-lethally irradiated CD45.1^{+} congenic mice. Six weeks post transfer, expression of Ly-6C, CD11b, CD27 and KLRG1 on long-lived CD45.2^{+} adoptively transferred NK cells from spleen were examined by flow cytometry (Figure 5-9 A). Six weeks post transfer, a clear trend of Ly-6C expression on long-lived NK cells was observed (Figure 5-9 B). When I examined CD45.2^{+}

transferred NK cells from the recipient mouse of Ly-6C^{Neg} NK cells, a small population of NK cells remained negative for Ly-6C expression (Figure 5-9 B). However, the majority of Ly-6C negative origin NK cells now expressed detectable levels of Ly-6C, with a substantial population of Ly-6C$^{AL\text{-}21}$ and Ly-6C$^{AL\text{-}21/iMAP}$ NK cells observed (Figure 5-9 B). When I examined Ly-6C$^{AL\text{-}21}$ origin transferred CD45.2^{+} NK cells, a large proportion remained Ly-6C$^{AL\text{-}21}$ with a substantial percentage of the NK cells now expressing Ly-6C recognized by both AL-21 and iMAP (Figure 5-9 B). From the density plots, two distinct populations of Ly-6C positive NK cells were clearly visible; Ly-6C$^{AL\text{-}21}$ and Ly-6C$^{AL\text{-}21/iMAP}$ (Figure 5-9 B). Finally, when CD45.2^{+} Ly-6C$^{AL\text{-}21/iMAP}$ origin NK cells were examined six weeks post transfer, the vast majority of the NK cells retained their reactivity towards AL-21 and iMAP (Figure 5-9 B). Although less than 20% of the NK cells were solely expressing the AL-21 recognized epitope, Ly-6C$^{AL\text{-}21/iMAP}$ NK cells represented over 70% of the long-lived NK cells recovered (Figure 5-9 B).

Next I sought to further define the relationship between KLRG1, CD11b and CD27 maturation markers to Ly-6C expression during long-lived NK cell development. Given my prior results, not surprisingly, greater than 90% of the long-lived NK cells generated from the transfer of Ly-6C^{Neg}, Ly-6C$^{AL\text{-}21}$ and Ly-6C$^{Al\text{-}21/iMAP}$ origin NK cells expressed KLRG1 (Figure 5-9 C). In terms of CD11b and CD27, the majority of long-lived Ly-6C^{Neg} origin CD45.2^{+} NK cells expressed a mature CD11b^{+}CD27^{-} phenotype (Figure 5-9 D left). Long-lived CD45.2^{+} NK cells that acquired expression of Ly-6C were exclusively CD11b^{+}CD27^{-} (Figure 5-9 D left). A noticeable population of long-lived Ly-6C^{Neg} origin CD45.2^{+} NK cells that remained Ly-6C^{Neg} after six weeks were found to be negative for CD11b expression after six weeks (Figure 5-9 D left). In contrast long-lived NK cells generated from the transfer of CD45.2^{+} Ly-6C$^{AL\text{-}21}$ and Ly-6C$^{Al\text{-}21/iMAP}$ NK cells, were exclusively CD11b^{+}CD27^{-} (Figure 5-9 D center and right).

My results demonstrate that Ly-6C expressing NK cells do not represent a distinct subset of NK cells. Rather, long-lived NK cells acquired and/or maintained

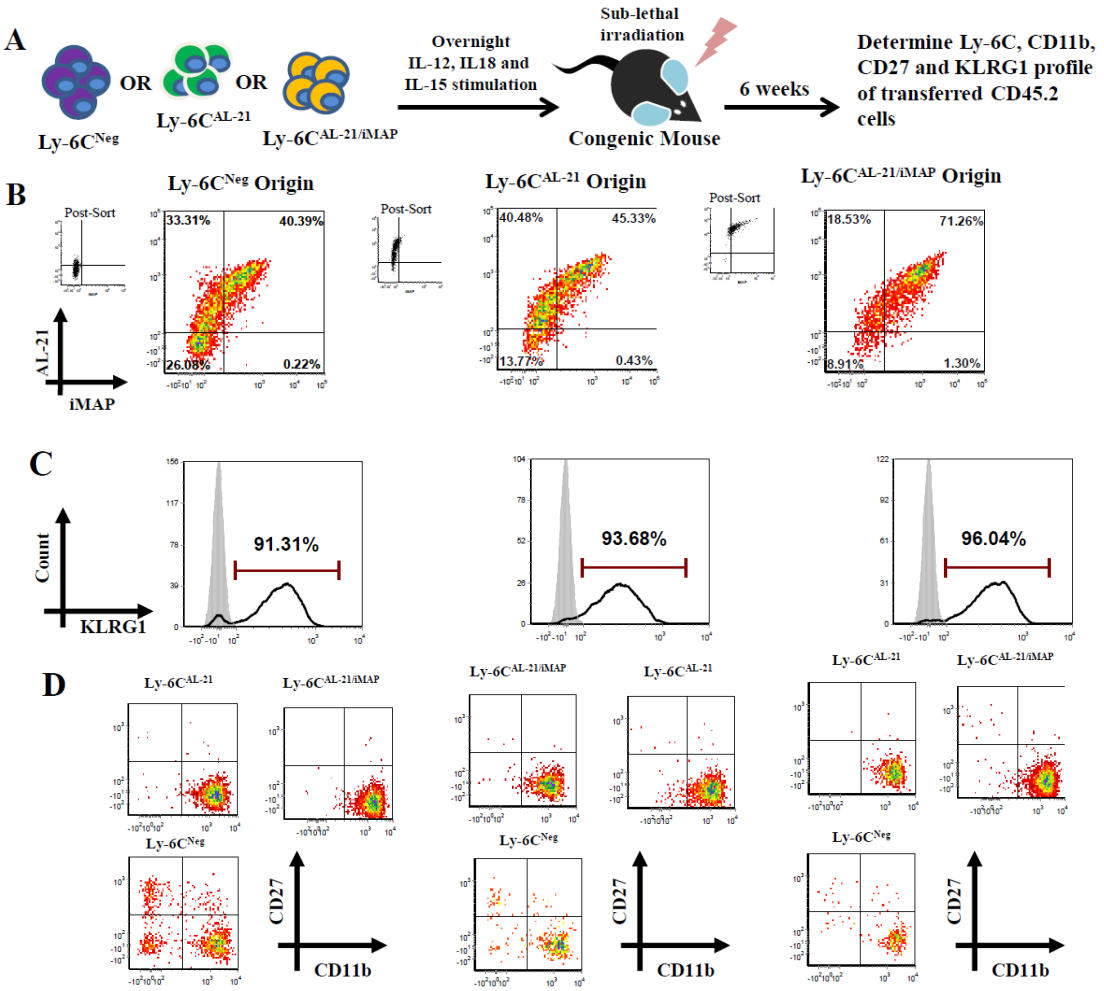

Figure 5-9: Ly-6C$^{AL-21/iMAP}$ NK cells are further differentiated NK cells. Sorted Ly-6C^{Neg}, Ly-6C^{AL-21} and Ly-6C$^{AL-21/iMAP}$ NK cells were stimulated overnight with IL-12, IL-18 and IL-15 and transferred into separate age-matched sub-lethally irradiated mice the next day. Six weeks post transfer Ly-6C expression based on AL-21 and iMAP staining and CD11b, CD27 and KLRG1 on splenic long-lived CD45.2^{+} NK cells were profiled by flow cytometry (A). Insert dot plots depict purity of sorted Ly-6C^{Neg}, Ly-6C^{AL-21} and Ly-6C$^{AL-21/iMAP}$ NK cell prior to overnight cytokine stimulation (B). Six weeks post transfer, staining of CD45.2^{+} NK cells by AL-21 and iMAP is shown for recipient mice initially receiving stimulated Ly-6C^{Neg} (left), Ly-6C^{AL-21} (middle) and Ly-6C$^{AL-21/iMAP}$ (right) NK cells. KLRG1 on CD45.2^{+} long-lived NK cells are also shown from recipient mice injected with Ly-6C^{Neg} (left), Ly-6C^{AL-21} (middle) and Ly-6C$^{AL-21/iMAP}$ (right) NK cells. Shaded histograms represent isotype staining controls (C). CD45.2^{+} long-lived NK cells resulting from recipient mice injection with Ly-6C^{Neg} (left), Ly-6C^{AL-21} (middle) and Ly-6C$^{AL-21/iMAP}$ (right) NK

cells, were divided into Ly-6C^{Neg}, Ly-6C^{AL-21} and Ly-6C$^{AL-21/iMAP}$ NK cell subsets and expression of CD11b and CD27 were examined for each subset (D). Data presented is a representative of one of two experiments with one mouse per treatment.

Ly-6C expression over time following cytokine stimulation. Additionally, within Ly-6C expressing long-lived NK cells, there is a progression of Ly-6C$^{AL\text{-}21}$ NK cells to Ly-6C$^{AL\text{-}21/iMAP}$ NK cells. While not definitive, the majority of transferred Ly-6C$^{AL\text{-}21/iMAP}$ origin NK cells remained reactive to both AL-21 and iMAP six weeks post transfer and may suggest a Ly-6C expression equilibrium favorable to expression of Ly-6C reactive to AL-21 and iMAP over time. Additionally, my results suggest that expression of KLRG1 and CD11b and lack of CD27 may also be used in conjunction with Ly-6C epitope expression to identify long-lived NK cells. Collectively, these results suggest that Ly-6C expression is a further stage of NK cell differentiation beyond the acquisition of CD11b and KLRG1 expression. In fact, within Ly-6C expressing NK cells, the most differentiated stage of NK cells observed in my experiments are NK cells simultaneously expressing AL-21 and iMAP epitope Ly-6C molecules.

Summary

In this chapter, I first aimed to determine the differentiation and functional relationship of Ly-6C^{Neg}, Ly-6C$^{AL\text{-}21}$ and Ly-6C$^{AL\text{-}21/iMAP}$ NK cells. Using CD11b, CD27 and KLRG1, I characterized the maturation states of Ly-6C^{Neg}, Ly-6C$^{AL\text{-}21}$ and Ly-6C$^{AL\text{-}21/iMAP}$ NK cells from the spleen. Only Ly-6C^{Neg} NK cells had a significant proportion of immature CD11b negative NK cells. In contrast, Ly-6C$^{AL\text{-}21}$ and Ly-6C$^{AL\text{-}21/iMAP}$ NK cells were almost exclusively CD11b^{+}CD27^{-}. Additionally, Ly-6C positive NK cells also had a significantly higher percentage of KLRG1 expressing cells than Ly-6C^{Neg} NK cells. These results collectively suggested that Ly-6C expressing NK cells are mature and, as they are exclusively CD11b^{+}CD27^{-}, may be a highly differentiated subset of NK cells. Additionally, immature CD11b negative and CD11b^{+}CD27^{+} NK cells were largely represented in the population of Ly-6C^{Neg} NK cells, suggesting that Ly-6C expression may be acquired during NK cell development mainly on mature CD11b^{+}CD27^{-} NK cells. In this sense, Ly-6C is similar to KLRG1 where both are expressed almost exclusively on mature CD11b^{+}CD27^{-} NK cells (87,

89). Additionally, while Ly-6C^{Neg}, Ly-6C$^{AL\text{-}21}$ and Ly-6C$^{AL\text{-}21/iMAP}$ NK cells were all highly proliferative, Ly-6C^{Neg} NK cells were clearly better able to sustain a higher percentage of NK cells past four or more rounds of cell division than Ly-6C$^{AL\text{-}21}$ and Ly-6C$^{AL\text{-}21/iMAP}$ NK cells. This finding also suggests that Ly-6C expressing NK cells may be a further differentiated subset of NK cells than Ly-6C negative NK cells. However, in terms of cytokine production, the frequency of IFNγ producing cells in all three subsets of NK cells were equivalent following stimulation with pro-inflammatory cytokines. However, my findings differ from previous findings of Sato *et al.* where Ly-6C positive NK cells were found to secrete larger quantities of IFNγ than Ly-6C negative NK cells (223). A possible explanation of the discrepancy may be in the stimulation methodology used. Sato *et al.* stimulated sorted Ly-6C positive and negative NK cells for 48 hours and examined secreted IFNγ in the supernatant via ELISA, whereas I, and others, examined intracellular accumulation of IFNγ after a short four hour stimulation (142). Consequently, it would be interesting to examine IFNγ secretion from Ly-6C^{Neg}, Ly-6C$^{AL\text{-}21}$ and Ly-6C$^{AL\text{-}21/iMAP}$ NK cells following prolonged pro-inflammatory cytokine stimulation.

Additionally, I also examined phenotypic characteristics and functional properties of long-lived Ly-6C expressing NK cells. As demonstrated in the previous chapter, long-lived NK cells expressed high levels of Ly-6C (Chapter 4). Not surprisingly, these results were confirmed in sub-lethally irradiated recipient hosts, where sub-lethal irradiation enhanced the recovery of long-lived NK cells six weeks post transfer. My results are also consistent with previous findings in MCMV generated memory splenic NK cells (73). However, in the previous report, Ly-6C NK cells were not further sub-divided. Among long-lived NK cells, I observed a significantly higher ratio of Ly-6C$^{AL\text{-}21/iMAP}$ to Ly-6C$^{AL\text{-}21}$ NK cells compared to host NK cells. This finding suggested that while NK cell longevity may be associated with Ly-6C expression, over time, there is an increase in co-expression of AL-21 and iMAP reactive Ly-6C on long-lived NK cells. As expected, long-lived NK cells expressed high levels of KLRG1 and were almost completely CD11b^{+}CD27^{-}; a

phenotype representative of a highly differentiated NK cell (87-89). However, functionally, I did not observe greatly enhanced IFNγ production capabilities to a cytokine stimulation from long-lived NK cells compared to unstimulated naïve NK cells, as previously reported (142). A possible explanation for the discrepancy may stem from the use of Rag deficient mice by Cooper *et al*. Rag deficient mice are often used for NK cell experiments as NK cells do not require somatic gene rearrangement for expression of activating receptors, such as T cell receptors and B cell receptors (7). Additionally, without any T or B cells, Rag deficient mice have a higher percentage of NK cells in the spleen and slightly enhanced splenic NK cell numbers allowing for easier and more efficient isolation of NK cells (227). However, recently, by comparing NK cell accumulation during ontogeny, Andrews *et al.* suggested that Rag-1 may have a previously unappreciated contribution to optimum splenic NK cell development (240). Additionally, Karo *et al.* also suggested that Rag gene expression during development enable a higher level of cellular fitness in NK cells (241).

Finally, I examined the differentiation relationship between Ly-6C^{Neg}, Ly-6C$^{AL\text{-}21}$ and Ly-6C$^{AL\text{-}21/iMAP}$ NK cells. Interestingly, after a six week period *in vivo*, I observed a distinct developmental progression of cytokine stimulated long-lived NK cells from Ly-6C^{Neg}→ Ly-6C$^{AL\text{-}21}$→ Ly-6C$^{AL\text{-}21/iMAP}$. My results support the possibility that expression of Ly-6C on NK cells occurs during later stages of NK cell differentiation and may be used as a long-lived or memory splenic NK cell marker. This conclusion is further supported by previous findings that memory Ly-49H^{+} NK cells generated from MCMV infections are high expressers of Ly-6C (73). However, in the previous report, whether the Ly-6C expressing Ly-49H^{+} memory NK cells can originated from less differentiated NK cells, such as Ly-6C negative NK cells, or existing Ly-6C positive NK cells was not addressed (73).

From my results, it is clear that in an unstimulated state, once acquired, NK cells do not readily lose expression of Ly-6C. Cytokine stimulated NK cells were able to progress from Ly-6C^{Neg} to Ly-6C$^{AL\text{-}21/iMAP}$ within six weeks. However, even after six weeks, approximately 25% of cytokine stimulated Ly-6C^{Neg} origin NK cells

remained negative for expression of Ly-6C (Figure 5-9). As Ly-6C^{Neg} NK cells have an enhanced proliferative capability (Figure 5-4), it is possible that the small percentage of long-lived Ly-6C^{Neg} NK cells represent a self-renewing population of previously stimulated long-lived NK cells able to sustain a population of highly differentiated Ly-6C$^{AL\text{-}21}$ and Ly-6C$^{AL\text{-}21/iMAP}$ NK cells over a period of time. Sun *et al.* have reported findings that memory NK cells following MCMV infection persist up to six months post infection (236). However, the steadily declining number of memory NK cells did make their observation more difficult (236). Additionally, it is also possible that once Ly-6C is expressed on long-lived NK cells, expression of AL-21 and iMAP reactive Ly-6C may still be reversible. Recently, Omi *et al.* suggested that while Ly-6C negative NK cells start to acquire Ly-6C expression *in vivo* in as little as two weeks, Ly-6C positive NK cells lose Ly-6C expression following IL-15 stimulation (242). In the future, it would therefore be interesting to examine the expression of Ly-6C on long-lived NK cells beyond six weeks to further determine the long-term contributions of Ly-6C^{Neg}, Ly-6C$^{AL\text{-}21}$ and Ly-6C$^{AL\text{-}21/iMAP}$ NK cells to a sustained long-lived memory NK cell population.

Finally, it would be interesting to examine the expression of AL-21 and iMAP Ly-6C epitopes on viral specific splenic memory NK cells, such as Ly-49H^{+} MCMV specific memory NK cells, where Ly-6C expression was first described on memory NK cells. Additionally, while no difference in production of IFNγ between cytokine stimulated long-lived NK cells and unstimulated NK cells was observed, titration of the quantity of cytokines used to re-stimulate long-lived NK cells may reveal enhanced sensitivity of long-lived NK cells to a secondary stimulation.

Chapter 6: General Discussion

Summary of Results:

FasL expression in CD8$^+$ T cells

Cell mediated cytotoxicity is largely directed by CD8$^+$ T cells and NK cells of the adaptive and innate immune systems, respectively. Cytotoxic lymphocytes lyse target cells through two mechanisms, a perforin/granzyme degranulation dependent mechanism and a degranulation independent FasL-Fas receptor/ligand mechanism. While both systems are utilized by CD8$^+$ T cells and NK cells, it still remains unclear as to the purpose and importance of retaining both systems. In particular, the FasL-Fas receptor/ligand killing mechanism which is kinetically a slower inducer of target cell apoptosis and in many systems, is seemingly redundant to degranulation mediated immunity. This question is of great importance in understanding CD8$^+$ T cell effector functions, which are tasked with providing sterilizing immunity against intracellular pathogens.

Recently, new studies have reported that FasL is important in CD8$^+$ T cells for limiting viral infections and in situations of low antigen availability, vital for tumor surveillance and control of persistent infections (165, 169, 170, 212). While a number of co-stimulatory molecules and pro-inflammatory cytokines have been demonstrated to augment degranulation mediated immunity in CD8$^+$ T cells, mediators of FasL expression have been much less characterized (19, 35). In the first part of my thesis, I investigated the role of B7.1 and ICAM-1 on intracellular FasL expression in sub-optimally activated CD8$^+$ T cells *ex vivo*. The co-stimulator ligand, B7.1 and ICAM-1 enhance GrB expression in stimulated naïve CD8$^+$ T cells in a density dependent manner. Interestingly, while B7.1 and ICAM-1 initially augmented intracellular FasL expression in a density dependent manner, highly co-stimulated naïve CD8$^+$ T cells lost FasL expression over time in culture. *In vivo*, initial ip injections of high numbers of allogeneic P815 tumor cells induced a strong CD8$^+$ T cell response in the

peritoneal cavity, with nearly all responding $CD8^+$ T cells expressing GrB and roughly half expressing intracellular FasL, eight days after injection. However, as immunity progressed over the span of 21 days, the responding $CD8^+$ T cells noticeably lost expression of GrB while the percentage of FasL expressing $CD8^+$ T cells was not significantly altered. In contrast, when mice were challenged with reduced numbers of P815, this induced a sub-optimum response from infiltrating $CD8^+$ T cells. Interestingly, while a lower percentage of responding T cells expressed GrB, a high percentage of T cells expressed intracellular FasL. Additionally, a substantial portion of the T cells stimulated under these conditions expressed intracellular FasL without expressing GrB. Taken together, these findings support the conclusion that FasL may be preferentially expressed over GrB by $CD8^+$ T cell undergoing low level stimulation.

Ly-6C expression on long-lived NK cells

In the latter half of my thesis, I explored markers of long-lived NK cells, the prototypical cellular cytotoxic innate immune cells in mammalian organisms. At the beginning of my studies, NK cells were still largely recognized as traditional innate immune cells: short lived cytotoxic lymphocytes with limited foreign antigen recognition capabilities and believed not to have enhanced immune responses upon a second challenge. However, around the same time, the first few studies describing adaptive immune features of hepatic NK cells against chemical haptens, a number of different virus-like particles and splenic NK cells against MCMV had just been published (73, 151). In one study, memory $Ly49H^+$ MCMV specific NK cells were characterized as high Ly-6C expressing NK cells (73). Our laboratory had previously generated a monoclonal anti-Ly-6C antibody, iMAP, and identified high iMAP recognized epitope expression on antigen specific memory $CD8^+$ T cells generated from a previous LCMV infection. Additionally, while $CD4^+$ T cells also express Ly-6C, under resting conditions, iMAP only recognized Ly-6C expressed on $CD8^+$ T cells. Additionally, non-ligand/antigen specific pro-inflammatory cytokine induced

'memory-like' splenic NK cells with enhanced cytokine production capabilities were reported from the Yokoyama laboratory (142). While these findings described a new arm of NK cell function, phenotypic characterization of these cells had not been fully examined, particularly, cytokine induced 'memory-like' NK cells.

I hypothesized that since highly iMAP reactive $CD8^+$ T cells identify antigen specific memory $CD8^+$ T cells, the cell mediated cytotoxic arm of the adaptive immune, iMAP may also be used to identify long-lived or 'memory-like' NK cells. From my initial examinations, I showed that iMAP not only recognized $CD8^+$ T cells, but also splenic NK cells. Additionally, in conjunction with clone AL-21, a commercially available anti-Ly-6C monoclonal antibody, splenic $CD8^+$ T cells and NK cells can be divided into three subsets: Ly-6C negative, Ly-$6C^{AL\text{-}21}$ and Ly-$6C^{AL\text{-}21/iMAP}$ expressing cells. As iMAP partially interferes with AL-21 staining of Ly-6C, these three subsets were most easily identified when AL-21 staining preceded iMAP staining for Ly-6C expression. I also demonstrated that long-lived splenic 'memory-like' NK cells had enhanced expression of Ly-6C identified by AL-21 or iMAP. These results were in accordance with previous MCMV generated memory NK cell studies demonstrating high Ly-6C expression (73). Of particular interest, I observed an increased percentage of Ly-$6C^{AL\text{-}21/iMAP}$ cells among long-lived NK cells six weeks post adoptive transfer. Using AL-21 and iMAP, I demonstrated two subsets of Ly-6C expressing long-lived NK cells that had not been previously described; Ly-$6C^{AL\text{-}21}$ and Ly-$6C^{AL\text{-}21/iMAP}$ NK cells. In contrast, long-lived hapten sensitized hepatic NK cells did not have an accumulation of Ly-6C expressing NK cells six weeks post transfer.

From these studies, I sought to further characterize Ly-6C expressing NK cells. Using multi-parameter flow cytometry, I showed that Ly-6C expressing NK cells, Ly-$6C^{AL\text{-}21}$ and Ly-$6C^{AL\text{-}21/iMAP}$, were mature NK cells expressing a $CD11b^+CD27^-$ phenotype. In addition, Ly-6C expressing splenic NK cells from six to eight week old mice possessed a higher percentage of KLRG1 positive NK cells than Ly-$6C^{Neg}$ NK cells. However, when isolated, Ly-$6C^{Neg}$, Ly-$6C^{AL\text{-}21}$ and Ly-$6C^{AL\text{-}21/iMAP}$ did not

differ in their ability to produce IFNγ following pro-inflammatory cytokine stimulation. Interestingly, Ly-6C^{Neg} NK cells did demonstrate a higher proliferative rate compared to Ly-6C positive NK cells following pro-inflammatory cytokine stimulation *in vivo*. In adoptive transfer experiments, long-lived NK cells expressed high levels of KLRG1 and CD11b, as well as high levels of Ly-6C. When re-stimulated with pro-inflammatory cytokines, adoptively transferred long-lived NK cells and endogenous NK cells produced similar levels of IFNγ. However, among the long-lived transferred NK cells, a higher percentage of Ly-6C positive NK cells expressed produced IFNγ than Ly-6C^{Neg} NK cells. Finally, I examined the developmental relationship between NK cell differentiation and Ly-6C expression. Over a six week period, I showed a clear trend of NK cells progressing from Ly-6C^{Neg} to Ly-6C$^{AL\text{-}21}$ to Ly-6C$^{AL\text{-}21/iMAP}$. Importantly, the transition from Ly-6C$^{AL\text{-}21}$ to Ly-6C$^{AL\text{-}21/iMAP}$ seemed to be subsequent to acquisition of KLRG1 and CD11b expression, thus AL-21 and iMAP reactivity towards long-lived NK cells represents a previously undefined stage of NK cell differentiation.

Major Contributions:

FasL expression levels in activated CD8$^+$ T cells

FasL expression in CD8$^+$ T cells are vital to combat against viral infections and tumor progression. Recent studies have demonstrated reduced protection by CD8$^+$ T cells against LCMV, influenza and tumor metastases in the absence of FasL mediated immunity (164, 166, 170). While a number of studies have examined FasL mRNA expression, intracellular FasL expression at the protein level in CD8$^+$ T cells has not been closely examined. In a recent study, Meiraz *et al*. demonstrated that following ip injection of allogeneic tumors in BALB/c mice, responding CD8$^+$ T cells initially expressed both perforin and FasL mRNA (211). However, as the immune response progressed, CD8$^+$ T cells lost expression of perforin mRNA while FasL mRNA was still detected (211). These results suggested that during an immune

response, $CD8^+$ T cells switch from an early perforin/FasL joint killing mechanisms to a predominantly FasL killing mechanism later on and is dependent upon antigen availability (211). However, in this study, FasL protein expression was never directly assessed. Using a similar allogeneic model, I showed *in vivo* for the first time that responding $CD8^+$ T cells in the peritoneum maintain extended expression of intracellular FasL protein, whereas GrB expression slowly diminishes over time. My results may suggest a higher dependence of FasL than degranulation mediated response by $CD8^+$ T cells during late stages of an allogeneic challenge; similar to what had been previously suggested from mRNA expression patterns (211).

Additionally, a number of studies have suggested that FasL mediated immunity against viral and tumor infections is particularly important during low antigen stimulation situations (212, 218). In a few studies, cytolysis by FasL requires a notably lower level of activation compared to degranulation mediated killing (171, 210). In accordance, Meiraz *et al.* further suggested that the down-regulation of perforin in $CD8^+$ T cells during late stages of allogeneic tumor challenge was due to decreased tumor antigen availability (211). While Meiraz *et al*. focused on limited antigen availability resulting from an immunological response, previous finds have also suggested that FasL expressed on $CD8^+$ T cells are vital in preventing the initial stages of tumor cell development *in vivo* (212). To further examine the relationship between antigen dose and FasL/GrB expression, I showed *in vivo* that a sub-optimal $CD8^+$ T cell stimulation to an allogeneic tumor cell injection favors expression of FasL over GrB in responding T cells in the peritoneum. Sub-optimum stimulation from a low tumor dose was able to induce FasL expression but not GrB expression in a significant percentage of responding T cells. Collectively, from my *in vivo* data and previous findings discussed above, it would seem that during the course of a natural infection or tumor development, initial $CD8^+$ T cell immunity may rely strongly on FasL mediated killing of infected or transformed cells. As the disease progresses and antigen availability increases, $CD8^+$ T cells likely engage both FasL and degranulation mediated immune mechanisms. Finally, as the insult subsides, resulting

in lower levels of antigen, $CD8^+$ T cells decrease dependence on degranulation mediated immunity (Figure 6-1). Additionally, FasL induction of apoptosis has previously been determined to be kinetically slower than GrB mediated apoptosis by multiple studies (206, 207). These findings also suggest a correlation between antigen levels and killing mechanism; the slower FasL and faster degranulation driven immunity during low and high antigen availability conditions, respectively.

Additionally, I also showed differential co-stimulatory requirements for FasL and GrB expression in *ex vivo* stimulated $CD8^+$ T cells. While early induction of FasL and GrB are augmented by higher levels of co-stimulation, FasL expression over time decreases in T cells receiving high levels of B7.1 or ICAM-1 co-stimulation, whereas GrB expression does not. As co-stimulatory molecules augment TCR stimulation and therefore enhance T cell activation signals, these *ex vivo* experiments would suggest that lower collective activation signal strength allows for sustained FasL expression. While these findings may seem counter-intuitive, Seki *et al.* previously reported that a number of key pro-inflammatory cytokines, such as IL-12, IL-18, IFNα, TNFα and IFNγ, had minimal effect on FasL expression in tumor specific $CD8^+$ T cells in culture (168). While it is likely that other co-stimulatory molecule(s) and cytokine(s) may augment and sustain FasL expression, an alternative possibility is that optimum FasL expression can be reached at lower levels of T cell stimulation. As a number of studies have indicated, FasL seems important under low foreign antigen stimulation situations *in vivo*. Therefore, effective FasL expression may not require high levels of co-stimulation and/or pro-inflammatory cytokines. As such, FasL may be an early line of defense utilized by cytotoxic T cells during the early stages of $CD8^+$ T cell responses to an infection or tumor cell transformation without the need for generating a highly inflammatory environment.

Long-lived NK cells

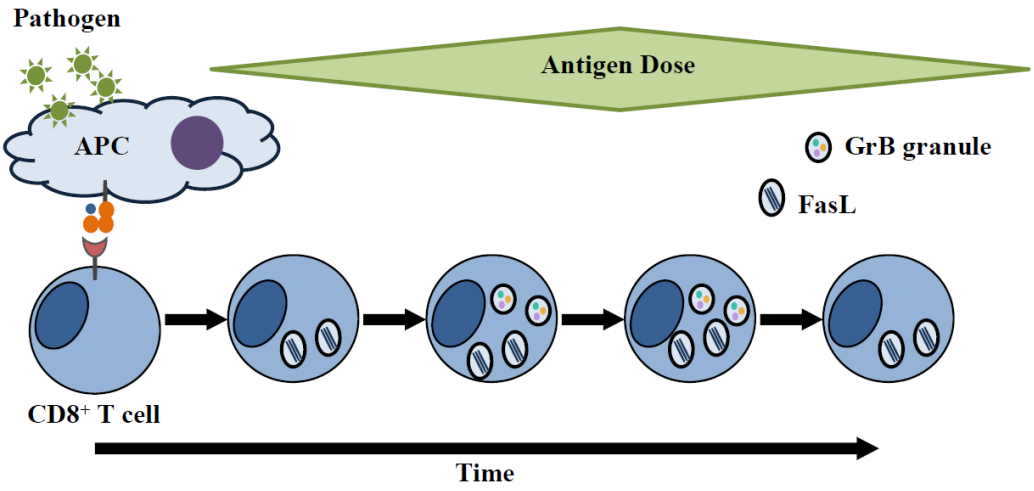

Figure 6-1: FasL and cytolytic granule expression in CD8$^+$ T cells.

Activated CD8$^+$ T cells may express cytolytic granule components such as GrB and/or FasL to lyse pathogen infected or transformed cells. The kinetics of GrB and FasL expression may depend on antigen availability. Early during an infection or early stages of tumor cell formation, antigen availability is low. CD8$^+$ T cells activated during this time express intracellular FasL but lack GrB expression. As time progresses and the infection and tumor cells grow, antigen dose increases and stimulated CD8$^+$ T cells at this time may express high levels of GrB and FasL. However, as time further progresses and the infection or tumor subsides, antigen levels are reduced resulting in late stage stimulated CD8$^+$ T cells to lose expression of GrB. The expression patterns of GrB and FasL may very well reflect the relative importance of degranulation and FasL mediated immunity provided by CD8$^+$ T cells during varying levels of antigen availability; a higher priority for FasL mediated cytotoxicity during low antigen doses and degranulation during high antigen doses.

NK cells are an integral part of anti-viral immunity in mammals. Deficiencies in NK cell recognition of MCMV infected cells have been demonstrated to result in viral susceptibility in otherwise resistant C57BL/6 mice (243). Using the MCMV infection model, Sun *et al.* demonstrated Ly49H$^+$ memory NK cells can be generated following an MCMV infection with a specificity towards m157 (73). Additionally, NK cells have been shown to be activated independently of Ly49H expression during early stages of MCMV infections through activation by pro-inflammatory cytokines (109, 110). Consequently, it is possible that pro-inflammatory cytokine stimulated NK cells may also possess adaptive immune features. Indeed, Cooper *et al.* demonstrated that splenic NK cells activated with pro-inflammatory cytokines IL-12, IL-18 and IL-15 possess enhanced IFNγ capabilities when re-stimulated following a rest period of several weeks (142). These results demonstrated functional properties of NK cells previously thought to be reserved for T and B cells. However, unlike Ly49H expressing memory NK cells, no long-lived NK cell markers were described by Cooper *et al.* (142). Therefore, in the latter half of my thesis, I examined potential markers for long-lived NK cells following IL-12, IL-18 and IL-15 stimulation. Using previously established NK cell maturation markers and markers found on Ly49H$^+$ memory NK cells, I examined expression of CD11b, CD27, KLRG1 and Ly-6C on long-lived cytokine stimulated NK cells (73, 88, 89). From my data in Chapters 4 and 5, I have determined a previously undescribed state of NK cell differentiation using AL-21 and iMAP antibody staining of Ly-6C expressed on cytokine stimulated long-lived NK cells.

Ly-6C expression on long-lived NK cells

Previous unpublished work from our laboratory, presented in this thesis, demonstrated a novel monoclonal anti-Ly-6C antibody, iMAP, developed in our laboratory that uniquely stains Ly-6C expressed on CD8$^+$ T cells but not CD4$^+$ T cells. In contrast, clone AL-21 was found to recognize Ly-6C expressed by both CD4$^+$ and CD8$^+$ T cells. These results suggest that CD4$^+$ and CD8$^+$ T cells may express

different forms of Ly-6C identified through AL-21 and iMAP staining. Interestingly, iMAP recognized antigen-specific $CD8^+$ T cells with high IFNγ production capabilities following LCMV infections in C57BL/6 mice. From my studies, I observed that iMAP also recognized NK cells isolated from spleen and liver. In both $CD8^+$ T and NK cells, I observed a partial interference by iMAP on AL-21 recognition of Ly-6C. However, AL-21 was not observed to interfere with iMAP staining. From these competitive staining experiments, it is possible that two forms of Ly-6C may be expressed by T cells and NK cells in C57BL/6 mice. The first form of Ly-6C may only express an epitope for AL-21 but not iMAP, as expressed by $CD4^+$ T cells. Second, $CD8^+$ T and NK cells may express Ly-6C molecules that express epitopes for both AL-21 and iMAP, however, binding of iMAP may hinder access of AL-21 recognition of Ly-6C. Finally, as iMAP interference of AL-21 staining is only partial, it is possible that $CD8^+$ T and NK cells may also express Ly-6C molecules that contain only the epitope for AL-21 binding.

From these results, it was then prudent to examine Ly-6C expression on NK cells with a two-step staining process; staining with AL-21 followed by staining with iMAP. With this procedure, I was able to identified two subsets of NK cells within the Ly-6C positive population; $Ly\text{-}6C^{AL\text{-}21}$ and $Ly\text{-}6C^{AL\text{-}21/iMAP}$. Additionally, since previous studies have shown Ly-6C to be a potential memory NK cell marker (73), I therefore further examined Ly-6C expression on NK cells using AL-21 and iMAP antibodies. From my preliminary adoptive transfer studies, I observed an increased percentage of Ly-6C positive NK cells among splenic long-lived NK cells. In contrast, long-lived adoptively transferred hepatic NK cells were almost exclusively Ly-6C negative even though a noticeable population of host hepatic NK cells expressed Ly-6C, to a similar degree as previously reported for hepatic NK cells (242). While it is unclear why I observed this difference, it is possible that differential Ly-6C expression may be an inherent distinction between hepatic and splenic origin NK cells.

Recent analysis of NK cell accumulation during development suggests potential differences between hepatic and splenic NK cells (240). In their study, maturation of hepatic NK cells appeared complete by five weeks of age compared to eight weeks of age needed for splenic NK cells (240). Additionally, a liver specific $CD49a^{+}$ $DX5^{-}$ NK cell subset, not found in spleen, was observed to mediate hapten specific memory (155). Using surgically joined congenic mice by parabiosis, Peng *et al.* demonstrated that the liver specific $CD49a^{+}$ $DX5^{-}$ NK cells do not enter peripheral circulation without a peripheral stimulus and do not migrate to the liver of the opposite conjoined mouse (155). However, hapten generated memory NK cells have been shown to migrate to the site of a secondary stimulation in a hapten dependent manner (150, 151). Since NK cells have been found and circulate among many peripheral organs, one possible origin of the Ly-6C positive NK cells in the liver may be from circulating splenic NK cells that have taken up residence in the liver. In contrast, hepatic origin NK cells and hepatic origin memory NK cells may not naturally express Ly-6C. While collectively these findings may explain discrepancies between Ly-6C staining on long-lived hepatic and splenic NK cells, examination of Ly-6C expression on $CD49a^{+}$ $DX5^{-}$ hepatic NK cell will need to be examined in future studies.

Maturation markers expressed by Ly-6C positive NK cells

Splenic and peripheral NK cell maturation have been commonly defined through staining of CD11b and CD27. From immature to mature, NK cells progress through at least four stages; $CD11b^{-}CD27^{-}$, $CD11b^{-}CD27^{+}$, $CD11b^{+}CD27^{+}$ and $CD11b^{+}CD27^{-}$ (88). Additionally, NK cell maturation has also been shown to associate with KLRG1 expression, only found on $CD11b^{+}CD27^{-}$ NK cells (89). From my results, I found that while Ly-6C positive NK cells can be divided into $Ly\text{-}6C^{AL\text{-}21}$ and $Ly\text{-}6C^{AL\text{-}21/iMAP}$ NK cells, most of the Ly-6C positive NK cells displayed a $CD11b^{+}CD27^{-}$ phenotype with a significant population of cells also expressing KLRG1. These findings suggest that Ly-6C positive NK cells are mature.

Additionally, as the vast majority of Ly-6C positive NK cells are $CD11b^{+}CD27^{-}$ compared to Ly-6C negative NK cells, it is likely that acquisition of Ly-6C expression may occur predominantly after down regulation of CD27 expression on developing NK cells.

Proliferative and IFNγ production by Ly-6C positive NK cells

Often, cells with an increased differentiation state have a lower proliferative potential, as with KRLG1 negative relative to positive NK cells (89). As such I examined the proliferative potential of NK cell subsets that differ in Ly-6C expression. My results showed that Ly-$6C^{Neg}$ NK cells are more proliferative than Ly-6C positive NK cells *in vivo*; suggesting that Ly-6C positive NK cells may be further differentiated than Ly-6C negative NK cells.

Additionally, I tested the IFNγ production capabilities of Ly-6C negative and positive NK cells following a four hour *ex vivo* cytokine stimulation. Of the Ly-6C sorted NK cell subsets, the percentage and quantity of IFNγ production, as measured by flow cytometry, were similar between Ly-6C negative and Ly-6C positive NK cells. Interestingly, my results differ from a recent publication on IFNγ production from NK cells with regard to Ly-6C expression. In a recent findings, Omi *et al.* reported higher IFNγ secretion from Ly-6C negative NK cells following 24 hour stimulation with IL-2 in combination with either IL-12 or IL-18 compared to Ly-6C positive NK cells (242). In this report, Omi *et al.* examined IFNγ over a much longer time frame than in my experiments, 24 hours compared to four hours, respectively. Additionally, Omi *et al.* stimulated NK cells with a much higher concentration of IL-12 or IL-18 at 100ng/ml. In contrast, my stimulations consisted of stimulations of 10ng/ml of IL-12, a concentration previously utilized by other groups for NK cell stimulations (142, 144). It is possible that at high cytokine stimulation concentrations and over a 24 hour period, Ly-6C negative NK cells may secrete larger quantities of IFNγ than Ly-6C positive NK cells. However, Ly-6C positive NK cells may have a lower threshold of sensitivity towards pro-inflammatory cytokine stimulations during

short term stimulations. Future studies with titrated levels of cytokine stimulations will be required to further clarify the differing findings.

IFNγ production of long-lived NK cells

While a number of studies have demonstrated foreign antigen dependent generation of memory NK cells, Cooper *et al.* were the first to describe an antigen independent and activating ligand independent mechanism for memory NK cell generation (142). Using Rag deficient mice, Cooper *et al.* demonstrated that long-lived 'memory-like' NK cells can be generated following cytokine stimulation of splenic NK cells with IL-12, IL-18 and low levels of IL-15, as a survival factor (142). The resulting 'memory-like' NK cells possess enhanced IFNγ production capabilities compared to previous unstimulated splenic NK cells (142). Additionally, a recent study based on NK cell accumulation during ontogeny suggested a possible role for Rag in NK cell development (240). In their study, based on CD27 and CD11b staining, the splenic NK cell population in WT mice were not fully developed until eight weeks after birth whereas the limited NK cell population present in the spleen of Rag deficient mice seemed to be developed by week two (240). Additionally, Karo *et al.* recently suggested that Rag gene expression at the CLP stage of NK cell development may enhance NK cell fitness and survival (241). In a comparison of NK cells from Rag deficient and Rag sufficient mice, Rag deficient mice displayed a higher killing potential of target tumor cells in vitro (241). However, in an *in vivo* competitive survival assay, Karo *et al.* also demonstrated that NK cell from Rag deficient mice possessed a reduced survival rate compared to NK cells isolated from Rag sufficient mice (241). Collectively, these studies suggest that the Rag gene may have previously unappreciated functions in NK cell development. Therefore, I sought to examine the responses of 'memory-like' NK cells generated from Rag-sufficient WT mice. I observed a similar NK cell IFNγ response from long-lived 'memory-like' NK cells previously stimulated with pro-inflammatory cytokines and NK cells that had not been previously stimulated; a contrast to results published by Cooper *et al.*

My results suggest that in Rag-sufficient mice, long-lived 'memory-like' NK cells may not have an enhanced IFNγ production capability. However, the responses of naïve and long-lived 'memory-like' NK cells to lower levels of cytokine stimulation were not examined. It is possible that long-lived 'memory-like' NK cell may have increased sensitivity towards pro-inflammatory cytokine stimulations than naïve NK cells. Interestingly, among the long-lived NK cells, a higher percentage of Ly-6C$^{AL-21/iMAP}$ NK cells produced IFNγ following IL-12 stimulation compared to Ly-6C^{Neg} long-lived NK cells.

Ly-6C$^{AL-21/iMAP}$ NK cells are highly differentiated NK cell subsets

From earlier experiments, Ly-6C expression on NK cells seemed to identify mature and highly differentiated NK cells. From past publications, Ly-6C has been associated with highly differentiated T and B cells, specifically memory CD8^{+} T cells and plasma B cells, respectively (196, 201). Indeed, through adoptive transfer experiments of sorted and stimulated Ly-6C^{Neg}, Ly-6C^{AL-21} and Ly-6C$^{AL-21/iMAP}$ NK cells, I observed a clear NK cell differentiation trend progressing from Ly-6C^{Neg} to Ly-6C^{AL-21} to Ly-6C$^{AL-21/iMAP}$. Six weeks post transfer of originally Ly-6C^{Neg} NK cells, a proportion of NK cells progressed to Ly-6C^{Al-21} or remained Ly-6C deficient. Similarly, of the transferred Ly-6C^{AL-21} NK cells, a significant percentage of the cells remained as Ly-6C^{AL-21} NK cells. These results suggest that while expression of Ly-6C is acquired on NK cells over time, continual development of NK cells from Ly-6C^{Neg} to Ly-6C^{AL-21} to Ly-6C$^{AL-21/iMAP}$ may continue beyond six weeks. Recently, Omi *et al.* also suggested that Ly-6C positive NK cells in mice develop from Ly-6C negative NK cells (242). *In vivo*, two weeks following transfer of Ly-6C negative NK cells, roughly 30% of the cells acquired Ly-6C expression (242). Additionally, NK cells with expression of Ly-6C prior to adoptive transfer, remained Ly-6C positive two weeks post transfer (242). Additionally, since I did not observe a substantial reversion of Ly-6C positive to Ly-6C negative NK cells, it is possible that long-lived Ly-6C^{Neg} NK cells may represent a long-term reservoir for the generation of Ly-6C

positive NK cells. Nonetheless, a small percentage of Ly-6C positive origin NK cell did seem to revert back to the Ly-6C^{Neg} stage. This may be a result of a population of self-renewing contaminating Ly-6C^{Neg} NK cells in the original sorted Ly-6C positive population. Additionally, while Ly-6C expression on NK cells seemed stable, a reversion of Ly-6C positive NK cells to Ly-6C negative NK cells may be accomplished through high levels of IL-15 stimulation *in vivo* and *ex vivo* (242). As my experiments utilized IL-15 competent mice as adoptive transfer recipients, it is also possible that IL-15 stimulation of long-lived Ly-6C positive NK cells resulted in a fraction of NK cells down-regulated Ly-6C expression. Traditionally, NK cells were believed to be short lived innate immune cells, however, these experiments demonstrated NK cell longevity to be much longer than previously expected. Indeed, recent reports have suggested the potential life spans of MCMV specific memory NK cells to be perhaps greater than six months (236).

Furthermore, my results also identified previously unknown stages of NK cell differentiation. While NK cell maturation has been well documented with regards to CD11b, CD27 and KLRG1 expression, the relationship between NK cell maturation and Ly-6C expression had not been well characterized. Six weeks post transfer of Ly-6C^{Neg} NK cells, the vast majority of the cells displayed a CD11b^{+}CD27^{-}KLRG1^{+} phenotype with over 70% of the cells expressing Ly-6C. Following the transfer of Ly-6C$^{AL\text{-}21}$ NK cells, nearly all the cells remained Ly-6C positive and CD11b^{+}CD27^{-}KLRG1^{+}, however, less than half of the cells progressed to become Ly-6C$^{AL\text{-}21/iMAP}$ NK cells. Similarly, six weeks post transfer of Ly-6C$^{AL\text{-}21/iMAP}$ NK cells, over 70% of the NK cells remained Ly-6C$^{AL\text{-}21/iMAP}$ and were almost exclusively CD11b^{+}CD27^{-}KLRG1^{+}. These results suggest that among long-lived NK cells, acquisition of Ly-6C expression, occur on matured CD11b^{+}CD27^{-}KLRG1^{+} NK cells thereby defining a previously undocumented stage of NK cell differentiation. Additionally, co-expression of AL-21 and iMAP epitope Ly-6C molecules further identified NK cells that mature from Ly-6C$^{AL\text{-}21}$CD11b^{+}CD27^{-}KLRG1^{+} NK cells

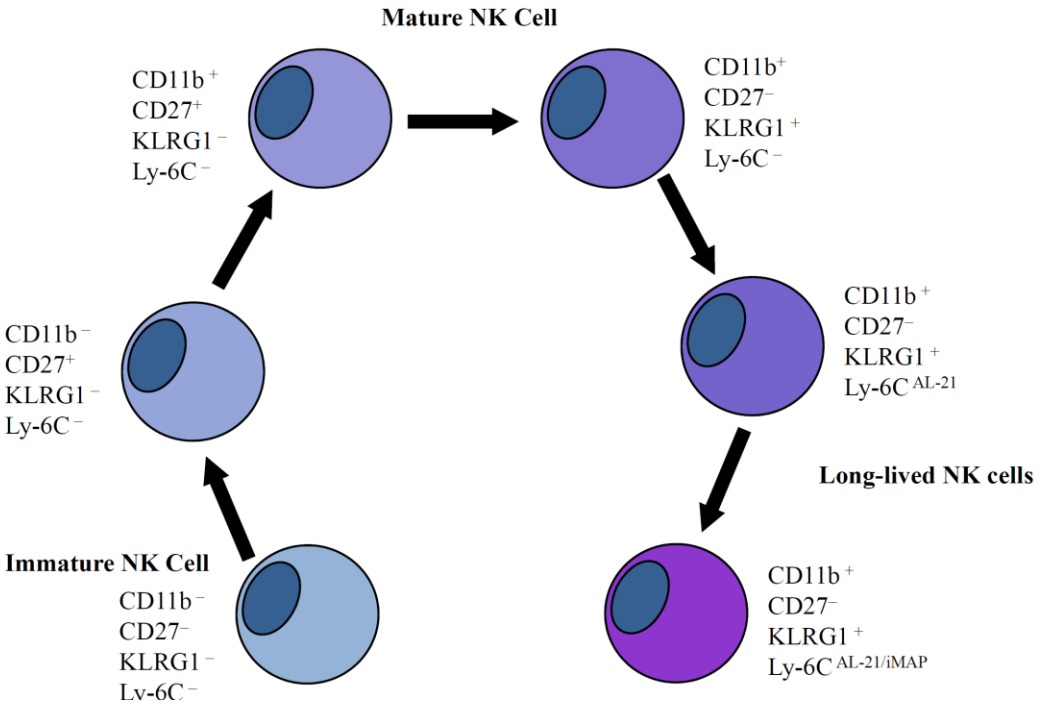

Figure 6-2: NK cell maturation/differentiation markers.

NK cell maturation has long been characterized through surface expression of CD11b, CD27 and KLRG1. In the periphery, immature NK cells are negative for CD11b, CD27, KLRG1 and Ly-6C expression. As the NK cells mature, they gain and lose expression of CD27 as well as acquire expression of CD11b and KLRG1. In long-lived NK cells, matured $CD11b^{+}CD27^{-}KLRG1^{+}$ NK cells acquire Ly-6C expression. In these NK cells, they first acquire Ly-6C molecules expressing the AL-21 epitope followed by Ly-6C molecules expressing both AL-21 and iMAP epitopes. The examination of Ly-6C expression on NK cells suggest a previously undescribed stage of NK cell differentiation and may be utilized as a NK cell longevity marker in future studies.

(Figure 6-2). Collectively, my results describe two additional stages of NK cells differentiation that have not previously been described (Figure 6-2).

Future Directions

FasL expression in low dose acute viral infections

Degranulation has been suggested to be the dominant mechanism for $CD8^+$ T cell clearance of acute infections. However, recently, FasL has been shown to play a role in mediating acute viral infections such as LCMV and influenza (164, 170). A number of studies have also identified an important role for FasL mediated immunity under low TCR stimulation conditions (171, 212). Importantly, *in vivo* studies have also demonstrated a role for FasL during low viral and tumor antigen levels (211, 218). Collectively, these reports and my observations of FasL protein expression in $CD8^+$ T cells suggest that FasL may play a key role in $CD8^+$ T cell response during sub-optimal T cell activation conditions. Therefore, it would of interest to re-examine FasL expression patterns in $CD8^+$ T cells during infection by additional viruses. Particularly, with low infectious doses that would induce a sub-optimum stimulation of antigen-specific $CD8^+$ T cells, similar to that described in this thesis. Such studies may provide further insight into the particular importance of FasL during low viral titer infections compared to high infection titers. Future studies involving low doses of virus infections could also be performed using mice conditionally deficient in FasL expression in parallel.

Co-stimulatory induction of FasL expression

In this thesis, I observed an increase in FasL expression following B7.1 and ICAM-1 co-stimulation *ex vivo*. Interestingly, high levels of B7.1 and ICAM-1 co-stimulation seemed to augment FasL expression in stimulated T cells, however, it did not induce sustained expression of FasL in the stimulated cells. Recent findings have suggested that CD27 co-stimulation may augment FasL expression following antigen

specific stimulation of OVA peptide restricted OT-I $CD8^+$ T cells (244). Wensveen *et al.* found co-stimulation effects on FasL expression with high rather than low levels of peptide stimulation (244). However, in this recent report, FasL expression was determined by cell surface staining, intracellular expression of FasL following CD27 co-stimulation was not examined (244). Therefore, it would be interesting to determine the effects of CD27 on intracellular and surface FasL expression on co-stimulated $CD8^+$ T cells. Additionally, it would be important to further examine additional co-stimulatory molecules for their effect on FasL expression. From results with CD27 co-stimulation, as a member of the TNFR family, other TNFR co-stimulatory molecule members may also augment FasL expression.

iMAP staining on MCMV specific Ly49H$^+$ memory NK cells

My initial experiments regarding memory NK cells was triggered following observations of MCMV and cytokine induced adaptive features in NK cells (73, 142). In their study, long-lived memory Ly-$49H^+$ NK cells generated following MCMV infections were found within the Ly-6C positive population of NK cells (73). However, no distinct long-lived NK cell markers were described following cytokine stimulation (142). From these observations, I sought to examine whether cytokine induced long-lived NK cells also expressed high levels of Ly-6C. With the use of clone AL-21 and iMAP, I demonstrated two subsets of Ly-6C positive splenic NK cell populations. Furthermore, long-lived splenic NK cells, after acquiring Ly-6C expression, can further differentiate from Ly-$6C^{AL\text{-}21}$ NK cells to Ly-$6C^{AL\text{-}21/iMAP}$ NK cells. My results suggest that high level expression of Ly-6C may be a hallmark of long-lived splenic NK cells. Therefore, it would be interesting to re-examine the expression profile of Ly-6C using both clone AL-21 and iMAP antibodies on MCMV memory Ly-$49H^+$ NK cells. From my results, I would suspect that MCMV specific Ly-$49H^+$ memory NK cells may be enriched within the Ly-$6C^{AL\text{-}21/iMAP}$ subset of NK cells, further defining markers for splenic memory NK cells. Furthermore, it would

also be interesting to evaluate the protective potential of Ly-6C$^{AL-21/iMAP}$ MCMV memory Ly-49H^{+} NK cells against a MCMV infection.

Functionality of long-lived memory NK cells

Recent studies have demonstrated enhanced effector functions of memory NK cells *in vivo* and *ex vivo* (73, 151). In separate studies, hapten specific hepatic memory NK cells have been shown to have enhanced cytolytic functions against hapten coated target cells and MCMV specific memory NK cells have been shown to better protect neonatal mice against MCMV infections (73, 151). Recently, a genomic microarray study comparing memory CD8^{+} T cells following VSV and memory NK cells following MCMV infection was conducted. This study found a number of common effector molecule genes that are upregulated in memory CD8^{+} T cells and NK cells, such as GrB and FasL (245). However, in addition to direct protective and cytolytic functions, NK cells have also been demonstrated to augment DC activation (246). Through cell-cell contact mechanisms and IFNγ production, NK cells have been shown to enhance DC maturation and IL-12 production (247, 248). Additionally, NK cells have also been suggested to enhance T cell functions through modulation of DCs (249). Therefore, it would be of interest to examine DC modulatory functions of long-lived memory NK cells. It is possible that memory NK cells, in addition to enhanced effector functions, may also have enhanced DC modulatory properties that augment memory T and B cells responses upon a secondary infection.

REFERENCES

1. Sirisinha, S. 2014. Evolutionary insights into the origin of innate and adaptive immune systems: different shades of grey. *Asian Pacific Journal of Allergy and Immunology* 32: 3-15.
2. Takeuchi, O., and S. Akira. 2009. Innate immunity to virus infection. *Immunological Reviews* 227: 75-86.
3. Hoffmann, J., and S. Akira. 2013. Innate immunity. *Current Opinion in Immunology* 25: 1-3.
4. Kumar, H., T. Kawai, and S. Akira. 2009. Pathogen recognition in the innate immune response. *Biochemical Journal* 420: 1-16.
5. Rouzaire, P., C. Luci, E. Blasco, J. Bienvenu, T. Walzer, J.-F. Nicolas, and A. Hennino. 2012. Natural killer cells and T cells induce different types of skin reactions during recall responses to haptens. *European Journal of Immunology* 42: 80-88.
6. Market, E., and F. N. Papavasiliou. 2003. V(D)J recombination and the evolution of the adaptive immune system. *PLoS Biology* 1: e16.
7. Mombaerts, P., J. Iacomini, R. S. Johnson, K. Herrup, S. Tonegawa, and V. E. Papaioannou. 1992. RAG-1-deficient mice have no mature B and T lymphocytes. *Cell* 68: 869-877.
8. Shinkai, Y., G. Rathbun, K.-P. Lam, E. M. Oltz, V. Stewart, M. Mendelsohn, J. Charron, M. Datta, F. Young, A. M. Stall, and F. W. Alt. 1992. RAG-2-deficient mice lack mature lymphocytes owing to inability to initiate V(D)J rearrangement. *Cell* 68: 855-867.
9. Dörner, T., and A. Radbruch. 2007. Antibodies and B cell memory in viral immunity. *Immunity* 27: 384-392.
10. Kaech, S. M., and E. J. Wherry. 2007. Heterogeneity and cell-fate decisions in effector and memory $CD8^+$ T cell differentiation during viral infection. *Immunity* 27: 393-405.
11. Barry, M., and R. C. Bleackley. 2002. Cytotoxic T lymphocytes: all roads lead to death. *Nat Rev Immunol* 2: 401-409.
12. Schatz, D. G., and Y. Ji. 2011. Recombination centres and the orchestration of V(D)J recombination. *Nature Reviews Immunology* 11: 251-263.
13. Singer, A., S. Adoro, and J.-H. Park. 2008. Lineage fate and intense debate: myths, models and mechanisms of CD4- versus CD8-lineage choice. *Nat Rev Immunol* 8: 788-801.
14. Hogquist, K. A., T. A. Baldwin, and S. C. Jameson. 2005. Central tolerance: learning self-control in the thymus. *Nat Rev Immunol* 5: 772-782.
15. Saito , T., and N. Watanabe. 1998. Positive and Negative Thymocyte Selection. *Critical Reviews in Immunology* 18: 359-370.
16. Mathis, D., and C. Benoist. 2009. Aire. *Annual Review of Immunology* 27: 287-312.
17. Anderson, M. S., E. S. Venanzi, L. Klein, Z. Chen, S. P. Berzins, S. J. Turley, H. von Boehmer, R. Bronson, A. Dierich, C. Benoist, and D. Mathis. 2002.

Projection of an immunological self shadow within the thymus by the Aire protein. *Science* 298: 1395-1401.
18. Weninger, W., N. Manjunath, and U. H. Von Andrian. 2002. Migration and differentiation of $CD8^+$ T cells. *Immunological Reviews* 186: 221-233.
19. Mescher, M. F., J. M. Curtsinger, P. Agarwal, K. A. Casey, M. Gerner, C. D. Hammerbeck, F. Popescu, and Z. Xiao. 2006. Signals required for programming effector and memory development by $CD8^+$ T cells. *Immunological Reviews* 211: 81-92.
20. Hochrein, H., K. Shortman, D. Vremec, B. Scott, P. Hertzog, and M. O'Keeffe. 2001. Differential production of IL-12, IFN-α, and IFN-γ by mouse dendritic cell subsets. *The Journal of Immunology* 166: 5448-5455.
21. Bevan, M. J. 2004. Helping the CD8+ T-cell response. *Nat Rev Immunol* 4: 595-602.
22. Zhang, S., H. Zhang, and J. Zhao. 2009. The role of CD4 T cell help for CD8 CTL activation. *Biochemical and Biophysical Research Communications* 384: 405-408.
23. Williams, M. A., A. J. Tyznik, and M. J. Bevan. 2006. Interleukin-2 signals during priming are required for secondary expansion of CD8+ memory T cells. *Nature* 441: 890-893.
24. Shedlock, D. J., and H. Shen. 2003. Requirement for CD4 T Cell Help in Generating Functional CD8 T Cell Memory. *Science* 300: 337-339.
25. Sun, J. C., and M. J. Bevan. 2003. Defective CD8 T Cell Memory Following Acute Infection Without CD4 T Cell Help. *Science* 300: 339-342.
26. Butz, E. A., and M. J. Bevan. 1998. Massive expansion of antigen-specific CD8+ T cells during an acute virus infection. *Immunity* 8: 167-175.
27. Curtsinger, J. M., D. C. Lins, and M. F. Mescher. 2003. Signal 3 determines tolerance versus full activation of naive CD8 T cells: dissociating proliferation and development of effector function. *The Journal of Experimental Medicine* 197: 1141-1151.
28. Murali-Krishna, K., J. D. Altman, M. Suresh, D. J. D. Sourdive, A. J. Zajac, J. D. Miller, J. Slansky, and R. Ahmed. 1998. Counting antigen-specific CD8 T cells: A reevaluation of bystander activation during viral infection. *Immunity* 8: 177-187.
29. Curtsinger, J. M., D. C. Lins, C. M. Johnson, and M. F. Mescher. 2005. Signal 3 tolerant CD8 T cells degranulate in response to antigen but lack granzyme B to mediate cytolysis. *The Journal of Immunology* 175: 4392-4399.
30. Hernández, J., S. Aung, K. Marquardt, and L. A. Sherman. 2002. Uncoupling of proliferative potential and gain of effector function by $CD8^+$ T cells responding to self-antigens. *The Journal of Experimental Medicine* 196: 323-333.
31. van den Broek, M., M. F. Bachmann, G. Köhler, M. Barner, R. Escher, R. Zinkernagel, and M. Kopf. 2000. IL-4 and IL-10 antagonize IL-12-mediated protection against acute vaccinia virus infection with a limited role of IFN-γ and nitric oxide synthetase 2. *The Journal of Immunology* 164: 371-378.

32. Kolumam, G. A., S. Thomas, L. J. Thompson, J. Sprent, and K. Murali-Krishna. 2005. Type I interferons act directly on CD8 T cells to allow clonal expansion and memory formation in response to viral infection. *The Journal of Experimental Medicine* 202: 637-650.
33. Duttagupta, P. A., A. C. Boesteanu, and P. D. Katsikis. 2009. Costimulation Signals for Memory CD8⁺ T Cells During Viral Infections. 29: 469-486.
34. Bour-Jordan, H., J. H. Esensten, M. Martinez-Llordella, C. Penaranda, M. Stumpf, and J. A. Bluestone. 2011. Intrinsic and extrinsic control of peripheral T-cell tolerance by costimulatory molecules of the CD28/B7 family. *Immunological Reviews* 241: 180-205.
35. Chen, L., and D. B. Flies. 2013. Molecular mechanisms of T cell co-stimulation and co-inhibition. *Nat Rev Immunol* 13: 227-242.
36. Duttagupta, P. A., A. C. Boesteanu, and P. D. Katsikis. 2009. Costimulation signals for memory $CD8^+$ T cells during viral infections. *Critical Reviews in Immunology* 29: 469-486.
37. Croft, M. 2003. Co-stimulatory members of the TNFR family: keys to effective T-cell immunity? *Nat Rev Immunol* 3: 609-620.
38. Maj, T., S. Wei, T. Welling, and W. Zou. 2013. T cells and costimulation in cancer. *The Cancer Journal* 19: 473-482
39. Chattopadhyay, K., E. Lazar-Molnar, Q. Yan, R. Rubinstein, C. Zhan, V. Vigdorovich, U. A. Ramagopal, J. Bonanno, S. G. Nathenson, and S. C. Almo. 2009. Sequence, structure, function, immunity: structural genomics of costimulation. *Immunological Reviews* 229: 356-386.
40. Gross, J. A., E. Callas, and J. P. Allison. 1992. Identification and distribution of the costimulatory receptor CD28 in the mouse. *The Journal of Immunology* 149: 380-388.
41. Shahinian, A., K. Pfeffer, K. P. Lee, T. M. Kündig, K. Kishihara, A. Wakeham, K. Kawai, P. S. Ohashi, C. B. Thompson, and T. W. Mak. 1993. Differential T cell costimulatory requirements in CD28-deficient mice. *Science* 261: 609-612.
42. Suresh, M., J. K. Whitmire, L. E. Harrington, C. P. Larsen, T. C. Pearson, J. D. Altman, and R. Ahmed. 2001. Role of CD28-B7 interactions in generation and maintenance of CD8 T cell memory. *The Journal of Immunology* 167: 5565-5573.
43. Lumsden, J. M., J. M. Roberts, N. L. Harris, R. J. Peach, and F. Ronchese. 2000. Differential requirement for CD80 and CD80/CD86-dependent costimulation in the lung immune response to an influenza virus infection. *The Journal of Immunology* 164: 79-85.
44. Fuse, S., J. J. Obar, S. Bellfy, E. K. Leung, W. Zhang, and E. J. Usherwood. 2006. CD80 and CD86 control antiviral $CD8^+$ T-cell function and immune surveillance of murine gammaherpesvirus 68. *Journal of Virology* 80: 9159-9170.

45. McAdam, A. J., E. A. Farkash, B. E. Gewurz, and A. H. Sharpe. 2000. B7 costimulation is critical for antibody class switching and $CD8^+$ cytotoxic T-lymphocyte generation in the host response to vesicular stomatitis virus. *Journal of Virology* 74: 203-208.
46. Bertram, E. M., A. Tafuri, A. Shahinian, V. S. F. Chan, L. Hunziker, M. Recher, P. S. Ohashi, T. W. Mak, and T. H. Watts. 2002. Role of ICOS versus CD28 in antiviral immunity. *European Journal of Immunology* 32: 3376-3385.
47. Halstead, E. S., Y. M. Mueller, J. D. Altman, and P. D. Katsikis. 2002. In vivo stimulation of CD137 broadens primary antiviral $CD8^+$ T cell responses. *Nat Immunol* 3: 536-541.
48. Chen, W., J. R. Bennink, P. A. Morton, and J. W. Yewdell. 2002. Mice Deficient in Perforin, CD4+ T Cells, or CD28-Mediated Signaling Maintain the Typical Immunodominance Hierarchies of CD8+ T-Cell Responses to Influenza Virus. *Journal of Virology* 76: 10332-10337.
49. Kündig, T. M., A. Shahinian, K. Kawai, H.-W. Mittrücker, E. Sebzda, M. F. Bachmann, T. W. Mak, and P. S. Ohashi. 1996. Duration of TCR stimulation determines costimulatory requirement of T cells. *Immunity* 5: 41-52.
50. Viola, A., and A. Lanzavecchia. 1996. T cell activation determined by T cell receptor number and tunable thresholds. *Science* 273: 104-106.
51. Borowski, A. B., A. C. Boesteanu, Y. M. Mueller, C. Carafides, D. J. Topham, J. D. Altman, S. R. Jennings, and P. D. Katsikis. 2007. Memory $CD8^+$ T cells require CD28 costimulation. *The Journal of Immunology* 179: 6494-6503.
52. Sharpe, A. H., and G. J. Freeman. 2002. The B7-CD28 superfamily. *Nat Rev Immunol* 2: 116-126.
53. Rudd, C. E., A. Taylor, and H. Schneider. 2009. CD28 and CTLA-4 coreceptor expression and signal transduction. *Immunological Reviews* 229: 12-26.
54. Harada, Y., D. Ohgai, R. Watanabe, K. Okano, O. Koiwai, K. Tanabe, H. Toma, A. Altman, and R. Abe. 2003. A single amino acid alteration in cytoplasmic domain determines IL-2 promoter activation by ligation of CD28 but not inducible costimulator (ICOS). *The Journal of Experimental Medicine* 197: 257-262.
55. Davis, D. M. 2009. Mechanisms and functions for the duration of intercellular contacts made by lymphocytes. *Nat Rev Immunol* 9: 543-555.
56. Bianchi, E., S. Denti, A. Granata, G. Bossi, J. Geginat, A. Villa, L. Rogge, and R. Pardi. 2000. Integrin LFA-1 interacts with the transcriptional co-activator JAB1 to modulate AP-1 activity. *Nature* 404: 617-621.
57. Mor, A., G. Campi, G. Du, Y. Zheng, D. A. Foster, M. L. Dustin, and M. R. Philips. 2007. The lymphocyte function-associated antigen-1 receptor costimulates plasma membrane Ras via phospholipase D2. *Nat Cell Biol* 9: 713-719.
58. Ni, H.-T., M. J. Deeths, and M. F. Mescher. 2001. LFA-1-mediated costimulation of $CD8^+$ T cell proliferation requires phosphatidylinositol 3-kinase activity. *The Journal of Immunology* 166: 6523-6529.

59. Li, D., J. J. Molldrem, and Q. Ma. 2009. LFA-1 regulates $CD8^+$ T cell activation via T cell receptor-mediated and LFA-1-mediated Erk1/2 signal pathways. *Journal of Biological Chemistry* 284: 21001-21010.
60. Geginat, J., B. Clissi, M. Moro, P. Dellabona, J. R. Bender, and R. Pardi. 2000. CD28 and LFA-1 contribute to cyclosporin A-resistant T cell growth by stabilizing the IL-2 mRNA through distinct signaling pathways. *European Journal of Immunology* 30: 1136-1144.
61. Chirathaworn, C., J. E. Kohlmeier, S. A. Tibbetts, L. M. Rumsey, M. A. Chan, and S. H. Benedict. 2002. Stimulation through intercellular adhesion molecule-1 provides a second signal for T cell activation. *The Journal of Immunology* 168: 5530-5537.
62. Deeths, M. J., and M. F. Mescher. 1999. ICAM-1 and B7-1 provide similar but distinct costimulation for CD8+ T cells, while CD4+ T cells are poorly costimulated by ICAM-1. *European Journal of Immunology* 29: 45-53.
63. Abraham, C., J. Griffith, and J. Miller. 1999. The dependence for leukocyte function-associated antigen-1/ICAM-1 interactions in T cell activation cannot be overcome by expression of high density TCR ligand. *The Journal of Immunology* 162: 4399-4405.
64. Scholer, A., S. Hugues, A. Boissonnas, L. Fetler, and S. Amigorena. 2008. Intercellular adhesion molecule-1-dependent stable interactions between T cells and dendritic cells determine $CD8^+$ T cell memory. *Immunity* 28: 258-270.
65. Krammer, P. H., R. Arnold, and I. N. Lavrik. 2007. Life and death in peripheral T cells. *Nat Rev Immunol* 7: 532-542.
66. Araki, Y., Z. Wang, C. Zang, W. H. Wood Iii, D. Schones, K. Cui, T.-Y. Roh, B. Lhotsky, R. P. Wersto, W. Peng, K. G. Becker, K. Zhao, and N.-p. Weng. 2009. Genome-wide analysis of histone methylation reveals chromatin state-based regulation of gene transcription and function of memory CD8+ T cells. *Immunity* 30: 912-925.
67. Weng, N.-p., Y. Araki, and K. Subedi. 2012. The molecular basis of the memory T cell response: differential gene expression and its epigenetic regulation. *Nat Rev Immunol* 12: 306-315.
68. Kiessling, R., and E. Klein. 1973. Cytotoxic potential of mouse spleen cells on H-2 antibody-treated target cells. *The Journal of Experimental Medicine* 137: 527-532.
69. Chang, J. T., V. R. Palanivel, I. Kinjyo, F. Schambach, A. M. Intlekofer, A. Banerjee, S. A. Longworth, K. E. Vinup, P. Mrass, J. Oliaro, N. Killeen, J. S. Orange, S. M. Russell, W. Weninger, and S. L. Reiner. 2007. Asymmetric T lymphocyte division in the initiation of adaptive immune responses. *Science* 315: 1687-1691.
70. Kiessling, R., E. Klein, and H. Wigzell. 1975. "Natural" killer cells in the mouse. I. Cytotoxic cells with specificity for mouse Moloney leukemia cells. Specificity and distribution according to genotype. *European Journal of Immunology* 5: 112-117.

71. Kiessling, R., E. Klein, H. Pross, and H. Wigzell. 1975. "Natural" killer cells in the mouse. II. Cytotoxic cells with specificity for mouse Moloney leukemia cells. Characteristics of the killer cell. *European Journal of Immunology* 5: 117-121.
72. Veiga-Fernandes, H., U. Walter, C. Bourgeois, A. McLean, and B. Rocha. 2000. Response of naive and memory $CD8^+$ T cells to antigen stimulation in vivo. *Nat Immunol* 1: 47-53.
73. Sun, J. C., J. N. Beilke, and L. L. Lanier. 2009. Adaptive immune features of natural killer cells. *Nature* 457: 557-561.
74. Lanier, L. L., J. H. Phillips, J. Hackett, M. Tutt, and V. Kumar. 1986. Natural killer cells: definition of a cell type rather than a function. *The Journal of Immunology* 137: 2735-2739.
75. Karre, K., H. G. Ljunggren, G. Piontek, and R. Kiessling. 1986. Selective rejection of H-2-deficient lymphoma variants suggests alternative immune defence strategy. *Nature* 319: 675-678.
76. Bix, M., N.-S. Liao, M. Zijlstra, J. Loring, R. Jaenisch, and D. Raulet. 1991. Rejection of class I MHC-deficient haemopoietic cells by irradiated MHC-matched mice. *Nature* 349: 329-331.
77. Höglund, P., C. Ohlén, E. Carbone, L. Franksson, H. G. Ljunggren, A. Latour, B. Koller, and K. Kärre. 1991. Recognition of beta 2-microglobulin-negative (beta 2m-) T-cell blasts by natural killer cells from normal but not from beta 2m- mice: nonresponsiveness controlled by beta 2m- bone marrow in chimeric mice. *Proceedings of the National Academy of Sciences* 88: 10332-10336.
78. Colucci, F., M. A. Caligiuri, and J. P. Di Santo. 2003. What does it take to make a natural killer? *Nat Rev Immunol* 3: 413-425.
79. Yu, J., A. G. Freud, and M. A. Caligiuri. 2013. Location and cellular stages of natural killer cell development. *Trends in Immunology* 34: 573-582.
80. Kennedy, M. K., M. Glaccum, S. N. Brown, E. A. Butz, J. L. Viney, M. Embers, N. Matsuki, K. Charrier, L. Sedger, C. R. Willis, K. Brasel, P. J. Morrissey, K. Stocking, J. C. L. Schuh, S. Joyce, and J. J. Peschon. 2000. Reversible defects in natural killer and memory CD8 T cell lineages in interleukin 15–deficient mice. *The Journal of Experimental Medicine* 191: 771-780.
81. Fehniger, T. A., K. Suzuki, J. B. VanDeusen, M. A. Cooper, A. G. Freud, and M. A. Caligiuri. 2001. Fatal leukemia in interleukin-15 transgenic mice. *Blood Cells, Molecules, and Diseases* 27: 223-230.
82. Yokoyama, W. M., S. Kim, and A. R. French. 2004. The dynamic life of natural killer cells. *Annual Review of Immunology* 22: 405-429.
83. Yokota, Y., A. Mansouri, S. Mori, S. Sugawara, S. Adachi, S.-I. Nishikawa, and P. Gruss. 1999. Development of peripheral lymphoid organs and natural killer cells depends on the helix-loop-helix inhibitor Id2. *Nature* 397: 702-706.
84. Boos, M. D., Y. Yokota, G. Eberl, and B. L. Kee. 2007. Mature natural killer cell and lymphoid tissue–inducing cell development requires Id2-mediated

suppression of E protein activity. *The Journal of Experimental Medicine* 204: 1119-1130.
85. Boos, M., K. Ramirez, and B. Kee. 2008. Extrinsic and intrinsic regulation of early natural killer cell development. *Immunol Res* 40: 193-207.
86. Hayakawa, Y., N. D. Huntington, S. L. Nutt, and M. J. Smyth. 2006. Functional subsets of mouse natural killer cells. *Immunological Reviews* 214: 47-55.
87. Hayakawa, Y., and M. J. Smyth. 2006. CD27 dissects mature NK cells into two subsets with distinct responsiveness and migratory capacity. *The Journal of Immunology* 176: 1517-1524.
88. Chiossone, L., J. Chaix, N. Fuseri, C. Roth, E. Vivier, and T. Walzer. 2009. Maturation of mouse NK cells is a 4-stage developmental program. *Blood* 113: 5488-5496.
89. Huntington, N. D., H. Tabarias, K. Fairfax, J. Brady, Y. Hayakawa, M. A. Degli-Esposti, M. J. Smyth, D. M. Tarlinton, and S. L. Nutt. 2007. NK cell maturation and peripheral homeostasis is associated with KLRG1 up-regulation. *The Journal of Immunology* 178: 4764-4770.
90. Shifrin, N., D. H. Raulet, and M. Ardolino. 2014. NK cell self tolerance, responsiveness and missing self recognition. *Seminars in Immunology* 26: 138-144.
91. Orr, M. T., and L. L. Lanier. 2010. Natural killer cell education and tolerance. *Cell* 142: 847-856.
92. Vance, R. E., J. R. Kraft, J. D. Altman, P. E. Jensen, and D. H. Raulet. 1998. Mouse CD94/NKG2A Is a Natural Killer Cell Receptor for the Nonclassical Major Histocompatibility Complex (MHC) Class I Molecule Qa-1(b). *The Journal of Experimental Medicine* 188: 1841-1848.
93. Kraft, J. R., R. E. Vance, J. Pohl, A. M. Martin, D. H. Raulet, and P. E. Jensen. 2000. Analysis of Qa-1(b)Peptide Binding Specificity and the Capacity of Cd94/Nkg2a to Discriminate between Qa-1–Peptide Complexes. *The Journal of Experimental Medicine* 192: 613-624.
94. Fernandez, N. C., E. Treiner, R. E. Vance, A. M. Jamieson, S. Lemieux, and D. H. Raulet. 2005. A subset of natural killer cells achieves self-tolerance without expressing inhibitory receptors specific for self-MHC molecules. *Blood* 105: 4416-4423.
95. Joncker, N. T., N. C. Fernandez, E. Treiner, E. Vivier, and D. H. Raulet. 2009. NK cell responsiveness is tuned commensurate with the number of inhibitory receptors for self-MHC class I: the rheostat model. *The Journal of Immunology* 182: 4572-4580.
96. Pegram, H. J., D. M. Andrews, M. J. Smyth, P. K. Darcy, and M. H. Kershaw. 2011. Activating and inhibitory receptors of natural killer cells. *Immunology and Cell Biology* 89: 216-224.
97. Peterson, M. E., and E. O. Long. 2008. Inhibitory receptor signaling via tyrosine phosphorylation of the adaptor Crk. *Immunity* 29: 578-588.

98. Burshtyn, D. N., A. M. Scharenberg, N. Wagtmann, S. Rajagopalan, K. Berrada, T. Yi, J.-P. Kinet, and E. O. Long. 1996. Recruitment of tyrosine phosphatase HCP by the killer cell inhibitory receptor. *Immunity* 4: 77-85.
99. Stebbins, C. C., C. Watzl, D. D. Billadeau, P. J. Leibson, D. N. Burshtyn, and E. O. Long. 2003. Vav1 dephosphorylation by the tyrosine phosphatase SHP-1 as a mechanism for inhibition of cellular cytotoxicity. *Molecular and Cellular Biology* 23: 6291-6299.
100. Bryceson, Y. T., H.-G. Ljunggren, and E. O. Long. 2009. Minimal requirement for induction of natural cytotoxicity and intersection of activation signals by inhibitory receptors. *Blood* 114: 2657-2666.
101. Long, E. O., H. Sik Kim, D. Liu, M. E. Peterson, and S. Rajagopalan. 2013. Controlling natural killer cell responses: integration of signals for activation and inhibition. *Annual Review of Immunology* 31: 227-258.
102. Rahim, M. M. A., M. M. Tu, A. B. Mahmoud, A. Wight, E. Abou-Samra, P. D. A. Lima, and A. P. Makrigiannis. 2014. Ly49 receptors: Innate and adaptive immune paradigms. *Frontiers in Immunology* 5.
103. Tomasello, E., M. Blery, E. Vely, and E. Vivier. 2000. Signaling pathways engaged by NK cell receptors: double concerto for activating receptors, inhibitory receptors and NK cells. *Seminars in Immunology* 12: 139-147.
104. Lanier, L. L., B. C. Corliss, J. Wu, C. Leong, and J. H. Phillips. 1998. Immunoreceptor DAP12 bearing a tyrosine-based activation motif is involved in activating NK cells. *Nature* 391: 703-707.
105. Negishi, I., N. Motoyama, K.-i. Nakayama, K. Nakayama, S. Senju, S. Hatakeyama, Q. Zhang, A. C. Chan, and D. Y. Loh. 1995. Essential role for ZAP-70 in both positive and negative selection of thymocytes. *Nature* 376: 435-438.
106. Colucci, F., M. Turner, E. Schweighoffer, D. Guy-Grand, V. Di Bartolo, M. Salcedo, V. L. J. Tybulewicz, and J. P. Di Santo. 1999. Redundant role of the syk protein tyrosine kinase in mouse NK cell differentiation. *The Journal of Immunology* 163: 1769-1774.
107. Wu, J., Y. Song, A. B. H. Bakker, S. Bauer, T. Spies, L. L. Lanier, and J. H. Phillips. 1999. An activating immunoreceptor complex formed by NKG2D and DAP10. *Science* 285: 730-732.
108. Zompi, S., J. A. Hamerman, K. Ogasawara, E. Schweighoffer, V. L. J. Tybulewicz, J. P. Di Santo, L. L. Lanier, and F. Colucci. 2003. NKG2D triggers cytotoxicity in mouse NK cells lacking DAP12 or Syk family kinases. *Nat Immunol* 4: 565-572.
109. Fogel, L. A., M. M. Sun, T. L. Geurs, L. N. Carayannopoulos, and A. R. French. 2013. Markers of nonselective and specific NK cell activation. *The Journal of Immunology* 190: 6269-6276.
110. Dokun, A. O., S. Kim, H. R. C. Smith, H.-S. P. Kang, D. T. Chu, and W. M. Yokoyama. 2001. Specific and nonspecific NK cell activation during virus infection. *Nat Immunol* 2: 951-956.

111. French, A. R., H. Sjölin, S. Kim, R. Koka, L. Yang, D. A. Young, C. Cerboni, E. Tomasello, A. Ma, E. Vivier, K. Kärre, and W. M. Yokoyama. 2006. DAP12 signaling directly augments proproliferative cytokine stimulation of NK cells during viral infections. *The Journal of Immunology* 177: 4981-4990.
112. Nguyen, K. B., T. P. Salazar-Mather, M. Y. Dalod, J. B. Van Deusen, X.-q. Wei, F. Y. Liew, M. A. Caligiuri, J. E. Durbin, and C. A. Biron. 2002. Coordinated and distinct roles for IFN-αβ, IL-12, and IL-15 regulation of NK cell responses to viral infection. *The Journal of Immunology* 169: 4279-4287.
113. Pien, G. C., A. R. Satoskar, K. Takeda, S. Akira, and C. A. Biron. 2000. Cutting Edge: Selective IL-18 requirements for induction of compartmental IFN-γ responses during viral infection. *The Journal of Immunology* 165: 4787-4791.
114. Lauwerys, B. R., J.-C. Renauld, and F. A. Houssiau. 1999. Synergistic proliferation and activation of natural killer cells by interleukin 12 and interleukin 18. *Cytokine* 11: 822-830.
115. Marçais, A., S. Viel, M. Grau, T. Henry, J. Marvel, and T. Walzer. 2013. Regulation of NK cell development and function by cytokines. *Frontiers in Immunology* 4.
116. Ni, J., M. Miller, A. Stojanovic, N. Garbi, and A. Cerwenka. 2012. Sustained effector function of IL-12/15/18–preactivated NK cells against established tumors. *The Journal of Experimental Medicine* 209: 2351-2365.
117. Cooper, M. A., J. E. Bush, T. A. Fehniger, J. B. VanDeusen, R. E. Waite, Y. Liu, H. L. Aguila, and M. A. Caligiuri. 2002. In vivo evidence for a dependence on interleukin 15 for survival of natural killer cells. *Blood* 100: 3633-3638.
118. Dubois, S., J. Mariner, T. A. Waldmann, and Y. Tagaya. 2002. IL-15Rα recycles and presents IL-15 in trans to neighboring cells. *Immunity* 17: 537-547.
119. Mortier, E., T. Woo, R. Advincula, S. Gozalo, and A. Ma. 2008. IL-15Rα chaperones IL-15 to stable dendritic cell membrane complexes that activate NK cells via trans presentation. *The Journal of Experimental Medicine* 205: 1213-1225.
120. Koka, R., P. R. Burkett, M. Chien, S. Chai, F. Chan, J. P. Lodolce, D. L. Boone, and A. Ma. 2003. Interleukin (IL)-15Rα–deficient natural killer cells survive in normal but not IL-15Rα–deficient mice. *The Journal of Experimental Medicine* 197: 977-984.
121. Burkett, P. R., R. Koka, M. Chien, S. Chai, D. L. Boone, and A. Ma. 2004. Coordinate expression and trans presentation of interleukin (IL)-15Rα and IL-15 supports natural killer cell and memory $CD8^+$ T cell homeostasis. *The Journal of Experimental Medicine* 200: 825-834.
122. Prlic, M., B. R. Blazar, M. A. Farrar, and S. C. Jameson. 2003. In vivo survival and homeostatic proliferation of natural killer cells. *The Journal of Experimental Medicine* 197: 967-976.

123. Koka, R., P. Burkett, M. Chien, S. Chai, D. L. Boone, and A. Ma. 2004. Cutting Edge: Murine dendritic cells require IL-15Rα to prime NK cells. *The Journal of Immunology* 173: 3594-3598.
124. Lucas, M., W. Schachterle, K. Oberle, P. Aichele, and A. Diefenbach. 2007. Dendritic cells prime natural killer cells by trans-presenting interleukin 15. *Immunity* 26: 503-517.
125. Parihar, R., J. Dierksheide, Y. Hu, and W. E. Carson. 2002. IL-12 enhances the natural killer cell cytokine response to Ab-coated tumor cells. *The Journal of Clinical Investigation* 110: 983-992.
126. Kobayashi, M., L. Fitz, M. Ryan, R. M. Hewick, S. C. Clark, S. Chan, R. Loudon, F. Sherman, B. Perussia, and G. Trinchieri. 1989. Identification and purification of natural killer cell stimulatory factor (NKSF), a cytokine with multiple biologic effects on human lymphocytes. *The Journal of Experimental Medicine* 170: 827-845.
127. Orange, J. S., B. Wang, C. Terhorst, and C. A. Biron. 1995. Requirement for natural killer cell-produced interferon gamma in defense against murine cytomegalovirus infection and enhancement of this defense pathway by interleukin 12 administration. *The Journal of Experimental Medicine* 182: 1045-1056.
128. Majewska-Szczepanik, M., S. Paust, U. H. von Andrian, P. W. Askenase, and M. Szczepanik. 2013. Natural killer cell-mediated contact sensitivity develops rapidly and depends on interferon-α, interferon-γ and interleukin-12. *Immunology* 140: 98-110.
129. Sun, J. C., S. Madera, N. A. Bezman, J. N. Beilke, M. H. Kaplan, and L. L. Lanier. 2012. Proinflammatory cytokine signaling required for the generation of natural killer cell memory. *The Journal of Experimental Medicine* 209: 947-954.
130. Orange, J. S., and C. A. Biron. 1996. Characterization of early IL-12, IFN-alphabeta, and TNF effects on antiviral state and NK cell responses during murine cytomegalovirus infection. *The Journal of Immunology* 156: 4746-4756.
131. Cella, M., D. Scheidegger, K. Palmer-Lehmann, P. Lane, A. Lanzavecchia, and G. Alber. 1996. Ligation of CD40 on dendritic cells triggers production of high levels of interleukin-12 and enhances T cell stimulatory capacity: T-T help via APC activation. *The Journal of Experimental Medicine* 184: 747-752.
132. Goldszmid, Romina S., P. Caspar, A. Rivollier, S. White, A. Dzutsev, S. Hieny, B. Kelsall, G. Trinchieri, and A. Sher. 2012. NK cell-derived interferon-γ orchestrates cellular dynamics and the differentiation of monocytes into dendritic cells at the site of infection. *Immunity* 36: 1047-1059.
133. Borg, C., A. Jalil, D. Laderach, K. Maruyama, H. Wakasugi, S. Charrier, B. Ryffel, A. Cambi, C. Figdor, W. Vainchenker, A. Galy, A. Caignard, and L. Zitvogel. 2004. NK cell activation by dendritic cells (DCs) requires the formation of a synapse leading to IL-12 polarization in DCs. *Blood* 104: 3267-3275.

134. Andrews, D. M., A. A. Scalzo, W. M. Yokoyama, M. J. Smyth, and M. A. Degli-Esposti. 2003. Functional interactions between dendritic cells and NK cells during viral infection. *Nat Immunol* 4: 175-181.
135. Sun, J. C., A. Ma, and L. L. Lanier. 2009. Cutting Edge: IL-15-independent NK cell response to mouse cytomegalovirus infection. *The Journal of Immunology* 183: 2911-2914.
136. Haeberlein, S., H. Sebald, C. Bogdan, and U. Schleicher. 2010. IL-18, but not IL-15, contributes to the IL-12-dependent induction of NK-cell effector functions by Leishmania infantum in vivo. *European Journal of Immunology* 40: 1708-1717.
137. Wang, Y., G. Chaudhri, R. J. Jackson, and G. Karupiah. 2009. IL-12p40 and IL-18 play pivotal roles in orchestrating the cell-mediated immune response to a poxvirus infection. *The Journal of Immunology* 183: 3324-3331.
138. Wei, X.-q., B. P. Leung, W. Niedbala, D. Piedrafita, G.-j. Feng, M. Sweet, L. Dobbie, A. J. H. Smith, and F. Y. Liew. 1999. Altered immune responses and susceptibility to leishmania major and staphylococcus aureus infection in IL-18-deficient mice. *The Journal of Immunology* 163: 2821-2828.
139. Gracie, J. A., S. E. Robertson, and I. B. McInnes. 2003. Interleukin-18. *Journal of Leukocyte Biology* 73: 213-224.
140. Humann, J., and L. L. Lenz. 2010. Activation of naive NK cells in response to listeria monocytogenes requires IL-18 and contact with infected dendritic cells. *The Journal of Immunology* 184: 5172-5178.
141. Semino, C., G. Angelini, A. Poggi, and A. Rubartelli. 2005. NK/iDC interaction results in IL-18 secretion by DCs at the synaptic cleft followed by NK cell activation and release of the DC maturation factor HMGB1. *Blood* 106: 609-616.
142. Cooper, M. A., J. M. Elliott, P. A. Keyel, L. Yang, J. A. Carrero, and W. M. Yokoyama. 2009. Cytokine-induced memory-like natural killer cells. *Proceedings of the National Academy of Sciences* 106: 1915-1919.
143. Keppel, M. P., L. Yang, and M. A. Cooper. 2013. Murine NK cell intrinsic cytokine-induced memory-like responses are maintained following homeostatic proliferation. *The Journal of Immunology* 190: 4754-4762.
144. Romee, R., S. E. Schneider, J. W. Leong, J. M. Chase, C. R. Keppel, R. P. Sullivan, M. A. Cooper, and T. A. Fehniger. 2012. Cytokine activation induces human memory-like NK cells. *Blood* 120: 4751-4760.
145. Min-Oo, G., Y. Kamimura, D. W. Hendricks, T. Nabekura, and L. L. Lanier. 2013. Natural killer cells: walking three paths down memory lane. *Trends in Immunology* 34: 251-258.
146. Rölle, A., J. Pollmann, and A. Cerwenka. 2013. Memory of infections: An emerging role for natural killer cells. *PLoS Pathogen* 9: e1003548.
147. Marcus, A., and David H. Raulet. 2013. Evidence for natural killer cell memory. *Current Biology* 23: R817-R820.
148. Nabekura, T., M. Kanaya, A. Shibuya, G. Fu, Nicholas R. J. Gascoigne, and Lewis L. Lanier. 2013. Costimulatory molecule DNAM-1 is essential for

optimal differentiation of memory natural killer cells during mouse cytomegalovirus infection. *Immunity* 40: 225-234.
149. Sun, J. C., and L. L. Lanier. 2011. NK cell development, homeostasis and function: parallels with $CD8^+$ T cells. *Nat Rev Immunol* 11: 645-657.
150. O'Leary, J. G., M. Goodarzi, D. L. Drayton, and U. H. von Andrian. 2006. T cell- and B cell-independent adaptive immunity mediated by natural killer cells. *Nat Immunol* 7: 507-516.
151. Paust, S., H. S. Gill, B.-Z. Wang, M. P. Flynn, E. A. Moseman, B. Senman, M. Szczepanik, A. Telenti, P. W. Askenase, R. W. Compans, and U. H. von Andrian. 2010. Critical role for the chemokine receptor CXCR6 in NK cell-mediated antigen-specific memory of haptens and viruses. *Nat Immunol* 11: 1127-1135.
152. Gillard, G. O., M. Bivas-Benita, A.-H. Hovav, L. E. Grandpre, M. W. Panas, M. S. Seaman, B. F. Haynes, and N. L. Letvin. 2011. $Thy1^+$ Nk Cells from vaccinia virus-primed mice confer protection against vaccinia virus challenge in the absence of adaptive lymphocytes. *PLoS Pathogen* 7: e1002141.
153. Matloubian, M., A. David, S. Engel, J. E. Ryan, and J. G. Cyster. 2000. A transmembrane CXC chemokine is a ligand for HIV-coreceptor Bonzo. *Nat Immunol* 1: 298-304.
154. van der Voort, R., V. Verweij, T. M. de Witte, E. Lasonder, G. J. Adema, and H. Dolstra. 2010. An alternatively spliced CXCL16 isoform expressed by dendritic cells is a secreted chemoattractant for $CXCR6^+$ cells. *Journal of Leukocyte Biology* 87: 1029-1039.
155. Peng, H., X. Jiang, Y. Chen, D. K. Sojka, H. Wei, X. Gao, R. Sun, W. M. Yokoyama, and Z. Tian. 2013. Liver-resident NK cells confer adaptive immunity in skin-contact inflammation. *The Journal of Clinical Investigation* 123: 1444-1456.
156. Kurtulus, S., P. Tripathi, and D. Hildeman. 2013. Protecting and rescuing the effectors: roles of differentiation and survival in the control of memory T cell development. *Frontiers in Immunology* 3.
157. Abdul-Careem, M. F., A. J. Lee, E. A. Pek, N. Gill, A. E. Gillgrass, M. V. Chew, S. Reid, and A. A. Ashkar. 2012. Genital HSV-2 Infection Induces Short-Term NK Cell Memory. *PLoS ONE* 7: e32821.
158. Kagi, D., F. Vignaux, B. Ledermann, K. Burki, V. Depraetere, S. Nagata, H. Hengartner, and P. Golsteiin. 1994. Fas and perforin pathways as major mechanisms of T cell-mediated cytotoxicity. *Science* 265: 528-530.
159. Bossi, G., and G. M. Griffiths. 1999. Degranulation plays an essential part in regulating cell surface expression of Fas ligand in T cells and natural killer cells. *Nat Med* 5: 90-96.
160. Lettau, M., M. Paulsen, H. Schmidt, and O. Janssen. 2011. Insights into the molecular regulation of FasL (CD178) biology. *European Journal of Cell Biology* 90: 456-466.

161. He, J.-S., and H. L. Ostergaard. 2007. CTLs contain and use intracellular stores of FasL distinct from cytolytic granules. *The Journal of Immunology* 179: 2339-2348.
162. Kassahn, D., U. Nachbur, S. Conus, O. Micheau, P. Schneider, H. U. Simon, and T. Brunner. 2008. Distinct requirements for activation-induced cell surface expression of preformed Fas/CD95 ligand and cytolytic granule markers in T cells. *Cell Death and Differentiation* 16: 115-124.
163. Russell, J. H., and T. J. Ley. 2002. Lymphocyte-mediated cytotoxicity. *Annual Review of Immunology* 20: 323-370.
164. Rode, M., S. Balkow, V. Sobek, R. Brehm, P. Martin, A. Kersten, T. Dumrese, T. Stehle, A. Mullbacher, R. Wallich, and M. M. Simon. 2004. Perforin and Fas act together in the induction of apoptosis, and both are critical in the clearance of lymphocytic choriomeningitis virus infection. *Journal of Virology* 78: 12395-12405.
165. Zelinskyy, G., S. Balkow, S. Schimmer, K. Schepers, M. M. Simon, and U. Dittmer. 2004. Independent roles of perforin, granzymes, and Fas in the control of Friend retrovirus infection. *Virology* 330: 365-374.
166. Caldwell, S. A., M. H. Ryan, E. McDuffie, and S. I. Abrams. 2003. The Fas/Fas ligand pathway is important for optimal tumor regression in a mouse model of CTL adoptive immunotherapy of experimental CMS4 lung metastases. *The Journal of Immunology* 171: 2402-2412.
167. Dobrzanski, M. J., J. B. Reome, J. A. Hollenbaugh, and R. W. Dutton. 2004. Tc1 and Tc2 Effector Cell Therapy Elicit Long-Term Tumor Immunity by Contrasting Mechanisms That Result in Complementary Endogenous Type 1 Antitumor Responses. *The Journal of Immunology* 172: 1380-1390.
168. Seki, N., A. D. Brooks, C. R. D. Carter, T. C. Back, E. M. Parsoneault, M. J. Smyth, R. H. Wiltrout, and T. J. Sayers. 2002. Tumor-specific CTL kill murine renal cancer cells using both perforin and Fas ligand-mediated lysis in vitro, but cause tumor regression in vivo in the absence of perforin. *The Journal of Immunology* 168: 3484-3492.
169. Shrestha, B., and M. S. Diamond. 2007. Fas ligand interactions contribute to $CD8^+$ T-cell-mediated control of west nnile virus infection in the central nervous system. *Journal of Virology* 81: 11749-11757.
170. Price, G. E., L. Huang, R. Ou, M. Zhang, and D. Moskophidis. 2005. Perforin and Fas cytolytic pathways coordinately shape the selection and diversity of $CD8^+$ T-cell escape variants of influenza virus. *Journal of Virology* 79: 8545-8559.
171. He, J.-S., D.-E. Gong, and H. L. Ostergaard. 2010. Stored Fas ligand, a mediator of rapid CTL-mediated killing, has a lower threshold for response than degranulation or newly synthesized Fas ligand. *The Journal of Immunology* 184: 555-563.
172. Kagi, D., B. Ledermann, K. Burki, P. Seiler, B. Odermatt, K. J. Olsen, E. R. Podack, R. M. Zinkernagel, and H. Hengartner. 1994. Cytotoxicity mediated

by T cells and natural killer cells is greatly impaired in perforin-deficient mice. *Nature* 369: 31-37.
173. van den Broek, M. E., D. Kägi, F. Ossendorp, R. Toes, S. Vamvakas, W. K. Lutz, C. J. Melief, R. M. Zinkernagel, and H. Hengartner. 1996. Decreased tumor surveillance in perforin-deficient mice. *The Journal of Experimental Medicine* 184: 1781-1790.
174. Rousalova, I., and E. Krepela. 2010. Granzyme B-induced apoptosis in cancer cells and its regulation (Review). *International Journal of Oncology* 37: 1361-1378.
175. Voskoboinik, I., M. J. Smyth, and J. A. Trapani. 2006. Perforin-mediated target-cell death and immune homeostasis. *Nat Rev Immunol* 6: 940-952.
176. Motyka, B., G. Korbutt, M. J. Pinkoski, J. A. Heibein, A. Caputo, M. Hobman, M. Barry, I. Shostak, T. Sawchuk, C. F. B. Holmes, J. Gauldie, and R. C. Bleackley. 2000. Mannose 6-phosphate/insulin-like growth factor II receptor is a death receptor for granzyme B during cytotoxic T cell–induced apoptosis. *Cell* 103: 491-500.
177. Kurschus, F. C., R. Bruno, E. Fellows, C. S. Falk, and D. E. Jenne. 2005. Membrane receptors are not required to deliver granzyme B during killer cell attack. *Blood* 105: 2049-2058.
178. Shi, L., D. Keefe, E. Durand, H. Feng, D. Zhang, and J. Lieberman. 2005. Granzyme B binds to target cells mostly by charge and must be added at the same time as perforin to trigger apoptosis. *The Journal of Immunology* 174: 5456-5461.
179. Strasser, A., P. J. Jost, and S. Nagata. 2009. The many roles of FAS receptor signaling in the immune system. *Immunity* 30: 180-192.
180. Scott, F. L., B. Stec, C. Pop, M. K. Dobaczewska, J. J. Lee, E. Monosov, H. Robinson, G. S. Salvesen, R. Schwarzenbacher, and S. J. Riedl. 2009. The Fas-FADD death domain complex structure unravels signalling by receptor clustering. *Nature* 457: 1019-1022.
181. Peshes-Yaloz, N., D. Rosen, P. M. Sondel, P. H. Krammer, and G. Berke. 2007. Up-regulation of Fas (CD95) expression in tumour cells in vivo. *Immunology* 120: 502-511.
182. Wigginton, J. M., J.-K. Lee, T. A. Wiltrout, W. G. Alvord, J. A. Hixon, J. Subleski, T. C. Back, and R. H. Wiltrout. 2002. Synergistic engagement of an ineffective endogenous anti-tumor immune response and induction of IFN-γ and Fas-ligand-dependent tumor eradication by combined administration of IL-18 and IL-2. *The Journal of Immunology* 169: 4467-4474.
183. Boselli, D., G. Losana, P. Bernabei, D. Bosisio, P. Drysdale, R. Kiessling, J. S. H. Gaston, D. Lammas, J.-L. Casanova, D. S. Kumararatne, and F. Novelli. 2007. IFN-γ regulates Fas ligand expression in human $CD4^+$ T lymphocytes and controls their anti-mycobacterial cytotoxic functions. *European Journal of Immunology* 37: 2196-2204.
184. Medvedev, A. E., A.-C. Johnsen, J. Haux, B. Steinkjer, K. Egeberg, D. H. Lynch, A. Sundan, and T. Espevik. 1997. Regulation of Fas and Fas-ligand

expression in NK cells by cytokines and the involvement of Fas-ligand in NK/LAK cell-mediated cytotoxicity. *Cytokine* 9: 394-404.

185. Medina, M. A., J. Couturier, M. L. Feske, A. E. Mahne, M. Turner, X. Yu, C. A. Kozinetz, A. F. Orozco, A. T. Hutchison, T. C. Savidge, J. R. Rodgers, and D. E. Lewis. 2012. Granzyme B- and Fas ligand-mediated cytotoxic function induced by mitogenic CD28 stimulation of human memory $CD4^+$ T cells. *Journal of Leukocyte Biology* 91: 759-771.
186. Nakano, K., K. Saito, S. Mine, S. Matsushita, and Y. Tanaka. 2007. Engagement of CD44 up-regulates Fas ligand expression on T cells leading to activation-induced cell death. *Apoptosis* 12: 45-54.
187. Aung, S., and B. S. Graham. 2000. IL-4 diminishes perforin-mediated and increases Fas ligand-mediated cytotoxicity in vivo. *The Journal of Immunology* 164: 3487-3493.
188. Xiao, S., K. Matsui, A. Fine, B. Zhu, A. Marshak-Rothstein, R. L. Widom, and S.-T. Ju. 1999. FasL promoter activation by IL-2 through SP1 and NFAT but not Egr-2 and Egr-3. *European Journal of Immunology* 29: 3456-3465.
189. Esser, M. T., R. D. Dinglasan, B. Krishnamurthy, C. A. Gullo, M. B. Graham, and V. L. Braciale. 1997. IL-2 induces Fas ligand/Fas (CD95L/CD95) cytotoxicity in $CD8^+$ and $CD4^+$ T lymphocyte clones. *The Journal of Immunology* 158: 5612-5618.
190. O' Reilly, L. A., L. Tai, L. Lee, E. A. Kruse, S. Grabow, W. D. Fairlie, N. M. Haynes, D. M. Tarlinton, J.-G. Zhang, G. T. Belz, M. J. Smyth, P. Bouillet, L. Robb, and A. Strasser. 2009. Membrane-bound Fas ligand only is essential for Fas-induced apoptosis. *Nature* 461: 659-663.
191. Lee, P. Y., J.-X. Wang, E. Parisini, C. C. Dascher, and P. A. Nigrovic. 2013. Ly6 family proteins in neutrophil biology. *Journal of Leukocyte Biology* 94: 585-594.
192. Bamezai, A. 2004. Mouse Ly-6 proteins and their extended family: markers of cell differentiation and regulators of cell signaling. *Archivum Immunologiae et Therapia Experimentalis* 52: 255-266.
193. Schlueter, A. J., T. R. Malek, C. N. Hostetler, P. A. Smith, P. deVries, and T. J. Waldschmidt. 1997. Distribution of Ly-6C on lymphocyte subsets: I. Influence of allotype on T lymphocyte expression. *The Journal of Immunology* 158: 4211-4222.
194. Mueller, S. N., T. Gebhardt, F. R. Carbone, and W. R. Heath. 2013. Memory T cell subsets, migration patterns, and tissue residence. *Annual Review of Immunology* 31: 137-161.
195. Curtsinger, J. M., D. C. Lins, and M. F. Mescher. 1998. $CD8^+$ memory T cells ($CD44^{high}$, Ly-$6C^+$) are more sensitive than naive cells ($CD44^{low}$, Ly-$6C^-$) to TCR/CD8 signaling in response to antigen. *The Journal of Immunology* 160: 3236-3243.
196. Walunas, T. L., D. S. Bruce, L. Dustin, D. Y. Loh, and J. A. Bluestone. 1995. Ly-6C is a marker of memory $CD8^+$ T cells. *The Journal of Immunology* 155: 1873-1883.

197. Hänninen, A., I. Jaakkola, M. Salmi, O. Simell, and S. Jalkanen. 1997. Ly-6C regulates endothelial adhesion and homing of $CD8^+$ T cells by activating integrin-dependent adhesion pathways. *Proceedings of the National Academy of Sciences* 94: 6898-6903.
198. Hänninen, A., M. Maksimow, C. Alam, D. J. Morgan, and S. Jalkanen. 2011. Ly6C supports preferential homing of central memory $CD8^+$ T cells into lymph nodes. *European Journal of Immunology* 41: 634-644.
199. Jaakkola, I., M. Merinen, S. Jalkanen, and A. Hänninen. 2003. Ly6C induces clustering of LFA-1 (CD11a/CD18) and is involved in subtype-specific adhesion of CD8 T cells. *The Journal of Immunology* 170: 1283-1290.
200. Pflugh, D. L., S. E. Maher, and A. L. M. Bothwell. 2002. Ly-6 superfamily members Ly-6A/E, Ly-6C, and Ly-6I recognize two potential ligands expressed by B lymphocytes. *The Journal of Immunology* 169: 5130-5136.
201. Wrammert, J., E. Källberg, W. W. Agace, and T. Leanderson. 2002. Ly6C expression differentiates plasma cells from other B cell subsets in mice. *European Journal of Immunology* 32: 97-103.
202. Marshall, Heather D., A. Chandele, Yong W. Jung, H. Meng, Amanda C. Poholek, Ian A. Parish, R. Rutishauser, W. Cui, Steven H. Kleinstein, J. Craft, and Susan M. Kaech. 2011. Differential expression of Ly6C and T-bet distinguish effector and memory Th1 $CD4^+$ cell properties during viral infection. *Immunity* 35: 633-646.
203. Blom, K. G., M. Rahman Qazi, J. B. Noronha Matos, B. D. Nelson, J. W. DePierre, and M. Abedi-Valugerdi. 2009. Isolation of murine intrahepatic immune cells employing a modified procedure for mechanical disruption and functional characterization of the B, T and natural killer T cells obtained. *Clinical and Experimental Immunology* 155: 320-329.
204. Chang, C. S., E. T. Silver, and K. P. Kane. 1999. Generation of a monoclonal antibody that recognizes a polymorphic epitope of C57BL/6 Ly-49G2. *Hybridoma* 18: 423-429.
205. Dustin, M. L., and E. O. Long. 2010. Cytotoxic immunological synapses. *Immunological Reviews* 235: 24-34.
206. Li, J., S. K. Figueira, A. C. A. Vrazo, B. F. Binkowski, B. L. Butler, Y. Tabata, A. Filipovich, M. B. Jordan, and K. A. Risma. 2014. Real-time detection of CTL function reveals distinct patterns of caspase activation mediated by Fas versus Granzyme B. *The Journal of Immunology* 193: 519-528.
207. Hassin, D., O. G. Garber, A. Meiraz, Y. S. Schiffenbauer, and G. Berke. 2011. Cytotoxic T lymphocyte perforin and Fas ligand working in concert even when Fas ligand lytic action is still not detectable. *Immunology* 133: 190-196.
208. Ostergaard, H. L., K. P. Kane, M. F. Mescher, and W. R. Clark. 1987. Cytotoxic T lymphocyte mediated lysis without release of serine esterase. *Nature* 330: 71-72.
209. Trenn, G., H. Takayama, and M. V. Sitkovsky. 1987. Exocytosis of cytolytic granules may not be required for target cell lysis by cytotoxic T-lymphocytes. *Nature* 330: 72-74.

210. Shanker, A., A. D. Brooks, K. M. Jacobsen, J. W. Wine, R. H. Wiltrout, H. Yagita, and T. J. Sayers. 2009. Antigen presented by tumors in vivo determines the nature of $CD8^+$ T-cell cytotoxicity. *Cancer Research* 69: 6615-6623.
211. Meiraz, A., O. G. Garber, S. Harari, D. Hassin, and G. Berke. 2009. Switch from perforin-expressing to perforin-deficient $CD8^+$ T cells accounts for two distinct types of effector cytotoxic T lymphocytes in vivo. *Immunology* 128: 69-82.
212. Afshar-Sterle, S., D. Zotos, N. J. Bernard, A. K. Scherger, L. Rodling, A. E. Alsop, J. Walker, F. Masson, G. T. Belz, L. M. Corcoran, L. A. O'Reilly, A. Strasser, M. J. Smyth, R. Johnstone, D. M. Tarlinton, S. L. Nutt, and A. Kallies. 2014. Fas ligand-mediated immune surveillance by T cells is essential for the control of spontaneous B cell lymphomas. *Nat Med* 20: 283-290.
213. Stoll, S., J. Delon, T. M. Brotz, and R. N. Germain. 2002. Dynamic imaging of T cell-dendritic cell interactions in lymph nodes. *Science* 296: 1873-1876.
214. Listopad, J. J., T. Kammertoens, K. Anders, B. Silkenstedt, G. Willimsky, K. Schmidt, A. A. Kuehl, C. Loddenkemper, and T. Blankenstein. 2013. Fas expression by tumor stroma is required for cancer eradication. *Proceedings of the National Academy of Sciences* 110: 2276-2281.
215. Moscovitch-Lopatin, M., R. J. Petrillo, O. G. Pankewycz, E. Hadro, C. R. Bleackley, T. B. Strom, and K. J. Wieder. 1991. Interleukin 2 counteracts the inhibition of cytotoxic T lymphocytes by cholera toxin in vitro and in vivo. *European Journal of Immunology* 21: 1439-1444.
216. Wherry, E. J., and R. Ahmed. 2004. Memory CD8 T-cell differentiation during viral infection. *Journal of Virology* 78: 5535-5545.
217. Liu, L., A. Chahroudi, G. Silvestri, M. E. Wernett, W. J. Kaiser, J. T. Safrit, A. Komoriya, J. D. Altman, B. Z. Packard, and M. B. Feinberg. 2002. Visualization and quantification of T cell-mediated cytotoxicity using cell-permeable fluorogenic caspase substrates. *Nature Medicine* 8: 185-189.
218. Zelinskyy, G., S. Balkow, S. Schimmer, T. Werner, M. M. Simon, and U. Dittmer. 2007. The level of Friend Retrovirus replication determines the cytolytic pathway of $CD8^+$ T-cell-mediated pathogen control. *Journal of Virology* 81: 11881-11890.
219. Leo, O., M. Foo, D. M. Segal, E. Shevach, and J. A. Bluestone. 1987. Activation of murine T lymphocytes with monoclonal antibodies: detection on Lyt-2^+ cells of an antigen not associated with the T cell receptor complex but involved in T cell activation. *The Journal of Immunology* 139: 1214-1222.
220. Herold, K. C., A. G. Montag, S. M. Meyer, C. Wojcikowski, and F. W. Fitch. 1990. Expression of Ly-6C by T lymphocytes of NOD mice after CD3-complex stimulation. Identification of activated cells during insulitis of prediabetic mice. *Diabetes* 39: 815-820.
221. Havran, W. L., D. W. Lancki, R. L. Moldwin, D. P. Dialynas, and F. W. Fitch. 1988. Characterization of an anti-Ly-6 monoclonal antibody which defines

and activates cytolytic T lymphocytes. *The Journal of Immunology* 140: 1034-1042.
222. Cho, B. K., C. Wang, S. Sugawa, H. N. Eisen, and J. Chen. 1999. Functional differences between memory and naive CD8 T cells. *Proceedings of the National Academy of Sciences* 96: 2976-2981.
223. Sato, N., T. Yahata, K. Santa, A. Ohta, Y. Ohmi, S. Habu, and T. Nishimura. 1996. Functional characterization of $NK1.1^{+}$ $Ly\text{-}6C^{+}$ cells. *Immunology Letters* 54: 5-9.
224. Jiang, X., Y. Chen, H. Peng, and Z. Tian. 2013. Memory NK cells: why do they reside in the liver? *Cellular and Molecular Immunology* 10: 196-201.
225. Daniel, M. A., and J. S. Mark. 2009. A potential role for RAG-1 in NK cell development revealed by analysis of NK cells during ontogeny. *Immunology and Cell Biology* 88: 107-116.
226. Herberman, R. B., M. E. Nunn, and D. H. Lavrin. 1975. Natural cytotoxic reactivity of mouse lymphoid cells against syngeneic and allogeneic tumors. I. Distribution of reactivity and specificity. *International Journal of Cancer* 16: 216-229.
227. Grundy, M. A., and C. L. Sentman. 2006. Immunodeficient mice have elevated numbers of NK cells in non-lymphoid tissues. *Experimental Cell Research* 312: 3920-3926.
228. Vivier, E., D. H. Raulet, A. Moretta, M. A. Caligiuri, L. Zitvogel, L. L. Lanier, W. M. Yokoyama, and S. Ugolini. 2011. Innate or adaptive immunity? The example of natural killer cells. *Science* 331: 44-49.
229. Vivier, E., E. Tomasello, M. Baratin, T. Walzer, and S. Ugolini. 2008. Functions of natural killer cells. *Nat Immunol* 9: 503-510.
230. Orange, J. S. 2006. Human natural killer cell deficiencies. *Curr Opin Allergy Clin Immunol* 6: 399-409.
231. Desrosiers, M.-P., A. Kielczewska, J. C. Loredo-Osti, S. G. Adam, A. P. Makrigiannis, S. Lemieux, T. Pham, M. B. Lodoen, K. Morgan, L. L. Lanier, and S. M. Vidal. 2005. Epistasis between mouse Klra and major histocompatibility complex class I loci is associated with a new mechanism of natural killer cell-mediated innate resistance to cytomegalovirus infection. *Nat Genet* 37: 593-599.
232. Arase, H., E. S. Mocarski, A. E. Campbell, A. B. Hill, and L. L. Lanier. 2002. Direct recognition of cytomegalovirus by activating and inhibitory NK cell receptors. *Science* 296: 1323-1326.
233. Kielczewska, A., M. Pyzik, T. Sun, A. Krmpotic, M. B. Lodoen, M. W. Munks, M. Babic, A. B. Hill, U. H. Koszinowski, S. Jonjic, L. L. Lanier, and S. M. Vidal. 2009. Ly49P recognition of cytomegalovirus-infected cells expressing $H2\text{-}D^{k}$ and CMV-encoded m04 correlates with the NK cell antiviral response. *The Journal of Experimental Medicine* 206: 515-523.
234. Chaix, J., M. S. Tessmer, K. Hoebe, N. Fuséri, B. Ryffel, M. Dalod, L. Alexopoulou, B. Beutler, L. Brossay, E. Vivier, and T. Walzer. 2008. Cutting

Edge: Priming of NK cells by IL-18. *The Journal of Immunology* 181: 1627-1631.
235. Brandstadter, J. D., X. Huang, and Y. Yang. 2014. NK cell-extrinsic IL-18 signaling is required for efficient NK-cell activation by vaccinia virus. *European Journal of Immunology* 44: 2659-2666.
236. Sun, J. C., S. Lopez-Verges, C. C. Kim, J. L. DeRisi, and L. L. Lanier. 2011. NK cells and immune "memory". *The Journal of Immunology* 186: 1891-1897.
237. Min-Oo, G., N. A. Bezman, S. Madera, J. C. Sun, and L. L. Lanier. 2014. Proapoptotic Bim regulates antigen-specific NK cell contraction and the generation of the memory NK cell pool after cytomegalovirus infection. *The Journal of Experimental Medicine* 211: 1289-1296.
238. Cho, B. K., V. P. Rao, Q. Ge, H. N. Eisen, and J. Chen. 2000. Homeostasis-stimulated proliferation drives naive T cells to differentiate directly into memory T cells. *The Journal of Experimental Medicine* 192: 549-556.
239. Murali-Krishna, K., and R. Ahmed. 2000. Cutting Edge: Naive T cells masquerading as memory cells. *The Journal of Immunology* 165: 1733-1737.
240. Andrews, D. M., and M. J. Smyth. 2009. A potential role for RAG-1 in NK cell development revealed by analysis of NK cells during ontogeny. *Immunology and Cell Biology* 88: 107-116.
241. Karo, Jenny M., David G. Schatz, and Joseph C. Sun. 2014. The RAG Recombinase Dictates Functional Heterogeneity and Cellular Fitness in Natural Killer Cells. *Cell* 159: 94-107.
242. Omi, A., Y. Enomoto, T. Kiniwa, N. Miyata, and A. Miyajima. 2014. Mature resting Ly6C^{high} natural killer cells can be reactivated by IL-15. *European Journal of Immunology* 44: 2638-2647.
243. Brown, M. G., A. O. Dokun, J. W. Heusel, H. R. C. Smith, D. L. Beckman, E. A. Blattenberger, C. E. Dubbelde, L. R. Stone, A. A. Scalzo, and W. M. Yokoyama. 2001. Vital Involvement of a Natural Killer Cell Activation Receptor in Resistance to Viral Infection. *Science* 292: 934-937.
244. Wensveen, F. M., P.-P. A. Unger, N. A. M. Kragten, I. A. M. Derks, A. ten Brinke, R. Arens, R. A. W. van Lier, E. Eldering, and K. P. J. M. van Gisbergen. 2012. CD70-driven costimulation induces survival or Fas-mediated apoptosis of T cells depending on antigenic load. *The Journal of Immunology* 188: 4256-4267.
245. Bezman, N. A., C. C. Kim, J. C. Sun, G. Min-Oo, D. W. Hendricks, Y. Kamimura, J. A. Best, A. W. Goldrath, and L. L. Lanier. 2012. Molecular definition of the identity and activation of natural killer cells. *Nat Immunol* 13: 1000-1009.
246. Cook, K. D., S. N. Waggoner, and J. K. Whitmire. 2014. NK cells and their ability to modulate T cells during virus infections. *Critical Reviews in Immunology* 34: 359-388.
247. Jiao, L., X. Gao, A. G. Joyee, L. Zhao, H. Qiu, M. Yang, Y. Fan, S. Wang, and X. Yang. 2011. NK cells promote type 1 T cell immunity through

modulating the function of dendritic cells during intracellular bacterial infection. *The Journal of Immunology* 187: 401-411.
248. Gerosa, F., B. Baldani-Guerra, C. Nisii, V. Marchesini, G. Carra, and G. Trinchieri. 2002. Reciprocal activating interaction between natural killer cells and dendritic cells. *The Journal of Experimental Medicine* 195: 327-333.
249. Adam, C., S. King, T. Allgeier, H. Braumüller, C. Lüking, J. Mysliwietz, A. Kriegeskorte, D. H. Busch, M. Röcken, and R. Mocikat. 2005. DC-NK cell cross talk as a novel $CD4^+$ T-cell–independent pathway for antitumor CTL induction. *Blood* 106: 338-344.